



Publicly Accessible Penn Dissertations


1-1-2015

The Biochemical and Biophysical Mechanisms of Macrophage Migration

Laurel Erin Hind

University of Pennsylvania, lmoses@seas.upenn.edu

Follow this and additional works at: <http://repository.upenn.edu/edissertations>

 Part of the [Allergy and Immunology Commons](#), [Biomedical Commons](#), [Immunology and Infectious Disease Commons](#), and the [Medical Immunology Commons](#)

Recommended Citation

Hind, Laurel Erin, "The Biochemical and Biophysical Mechanisms of Macrophage Migration" (2015). *Publicly Accessible Penn Dissertations*. 1062.

<http://repository.upenn.edu/edissertations/1062>

This paper is posted at Scholarly Commons. <http://repository.upenn.edu/edissertations/1062>

For more information, please contact libraryrepository@pobox.upenn.edu.

The Biochemical and Biophysical Mechanisms of Macrophage Migration

Abstract

The ability of macrophages to migrate is critical for a proper immune response. During an innate immune response, macrophages migrate to sites of infection or inflammation where they clear pathogens through phagocytosis and activate an adaptive immune response by releasing cytokines and acting as antigen-presenting cells. Unfortunately, improper regulation of macrophage migration is associated with a variety of diseases including cancer, atherosclerosis, wound-healing, and rheumatoid arthritis. In this thesis, engineered substrates were used to study the chemical and physical mechanisms of macrophage migration. We first used microcontact printing to generate surfaces specifically functionalized with fibronectin and functionally blocked against cell adhesion to study the migration of RAW/LR5 murine macrophages. Using these surfaces we found that macrophage migration is biphasic with respect to increasing surface ligand or soluble chemokine concentration, and that RAW/LR5 migration is dependent on PI3K and ROCK signaling. We then used traction force microscopy to measure the force generation capabilities of primary human macrophages and found that these cells generate strong forces at their leading edge in a stiffness-dependent manner. Through the use of chemical inhibitors we showed that force generation is dependent on myosin II contraction, PI3K signaling, and Rac signaling downstream of the GEF Vav1, but not the GEF Tiam1. Finally, we investigated the motility and force generation of M1 and M2 polarized primary human macrophages. We found that M1 macrophages are less motile and generate less force than M0 or M2 macrophages, and that M2 macrophages are more motile but do not have any change in force generation compared to M0 macrophages. We have been able to show that both chemical signals and mechanical mechanisms contribute to macrophage migration. This work contributes to the growing understanding of the mechanisms that govern macrophage migration and demonstrates the importance of mechanics when studying leukocyte migration.

Degree Type

Dissertation

Degree Name

Doctor of Philosophy (PhD)

Graduate Group

Bioengineering

First Advisor

Daniel A. Hammer

Keywords

Macrophage, Migration, Traction Force

Subject Categories

Allergy and Immunology | Biomedical | Immunology and Infectious Disease | Medical Immunology

THE BIOCHEMICAL AND BIOPHYSICAL MECHANISMS OF
MACROPHAGE MIGRATION

Laurel Erin Hind

A DISSERTATION

in

Bioengineering

Presented to the Faculties of the University of Pennsylvania

in

Partial Fulfillment of the Requirements for the

Degree of Doctor of Philosophy

2015

Supervisor of Dissertation

Daniel A. Hammer

Alfred G. and Meta A. Ennis Professor of Bioengineering and Chemical and
Biomolecular Engineering

Graduate Group Chairperson

Jason A. Burdick, Professor of Bioengineering

Dissertation Committee

Jason A. Burdick (chair), Professor of Bioengineering

Beth A. Winkelstein, Professor of Bioengineering

Dianne Cox, Professor of Anatomy and Structural Biology, Albert Einstein College of
Medicine

THE BIOCHEMICAL AND BIOPHYSICAL MECHANISMS OF
MACROPHAGE MIGRATION

COPYRIGHT

2015

Laurel Erin Hind

This thesis is dedicated to my parents:

Gregory and Sharon Moses

ACKNOWLEDGEMENTS

I would first like to thank my advisor, Daniel A. Hammer. Dan has been a wonderful mentor who has challenged me and allowed me to grow into an independent researcher. His encouragement and guidance have made my time at Penn more productive and rewarding than I could have imagined. I would also like to thank my thesis committee, Jason Burdick, Beth Winkelstein, and Dianne Cox as well as our collaborators Chris Chen and Micah Dembo for their helpful discussions, input, and interest in my project.

I am extremely grateful to the members of the Hammer Lab, both past and present, for being great colleagues and friends. It was truly a joy to come into lab every day because of the amazing people I was fortunate enough to work with. Randi Saunders, Olga Shebanova, Brendon Ricart, Dooyoung Lee, and Aaron Dominguez welcomed me into the lab as part of the cell group and taught me innumerable skills and techniques that provided the foundation for my dissertation research. The other lab members when I joined including Dalia Levine, Greg Robins, Neha Kamat, Nimil Sood, and Josh Katz were also very welcoming and made lab a fun place to work. Everyone who has joined with me and since I arrived including Steven Henry, Kevin Vargo, Amy Chevalier, Nick Anderson, Joanna MacKay, Chen Gao, Woo-Sik Jang, Seung Chul Park, and Ben Schuster, you have continued to teach me new things and offered many helpful discussions over the years. I would also like to thank Eric Johnston for all of his technical expertise, without your support on the microscopes none of this work would have been possible. Some of my best friends in Philadelphia are part of the Hammer Lab,

especially Neha Kamat, Aaron Dominguez, and Randi Saunders and I want to thank you all for making lab a second home.

To all of my amazing friends outside of the lab, especially Iris Marklein, Neha Kamat, Aaron Dominguez, and Rob Warden-Rothman, thank you for all the happy hours, dinners, talks, and amazing memories we have made. I did not know coming into graduate school that I would meet such wonderful people but I have been so blessed to know you and I am sure our friendships will last a lifetime.

I would like to thank everyone else in the Penn engineering community who have been such great friends over the years. I would especially like to thank members of the Advancing Women in Engineering board and Michele Grab. This board is made up of extraordinary women in the Penn engineering community and I have made great friends in all departments through our meetings and events. I cannot express how much it has meant to me to be part of a group focused on promoting women in engineering and how important it has been to have a group of friends to talk to about the stresses and joys of pursuing a graduate degree. You have all made the challenging journey through graduate school seem a little easier and a lot more fun.

Lastly, I would like to thank my family. To my parents, thank you for constantly loving me and encouraging me, without your support I would not be who I am today. You inspired me to become an engineer, to always do my best work, and to strive for greatness. I also want to thank my sister Lindsey, a fun, loving, and truly caring person. You amaze me every day with your own achievements and push me to be a better scientist and person. For the past ten years I have also had a wonderful second family of in-laws (and out-laws) who have loved me and celebrated my achievements with me.

And finally, to my husband Justin, thank you for being my best friend over the past decade. Your strength and patience has helped me achieve so much. Thank you for always encouraging me and acting as my strongest supporter throughout college and graduate school, I would not be where I am today without you.

ABSTRACT

THE BIOCHEMICAL AND BIOPHYSICAL MECHANISMS OF MACROPHAGE MIGRATION

Laurel E. Hind

Daniel A. Hammer

The ability of macrophages to migrate is critical for a proper immune response. During an innate immune response, macrophages migrate to sites of infection or inflammation where they clear pathogens through phagocytosis and activate an adaptive immune response by releasing cytokines and acting as antigen-presenting cells. Unfortunately, improper regulation of macrophage migration is associated with a variety of diseases including cancer, atherosclerosis, wound-healing, and rheumatoid arthritis. In this thesis, engineered substrates were used to study the chemical and physical mechanisms of macrophage migration. We first used microcontact printing to generate surfaces specifically functionalized with fibronectin and functionally blocked against cell adhesion to study the migration of RAW/LR5 murine macrophages. Using these surfaces we found that macrophage migration is biphasic with respect to increasing surface ligand or soluble chemokine concentration, and that RAW/LR5 migration is dependent on PI3K and ROCK signaling. We then used traction force microscopy to measure the force generation capabilities of primary human macrophages and found that these cells generate strong forces at their leading edge in a stiffness-dependent manner. Through the use of chemical inhibitors we showed that force generation is dependent on myosin II

contraction, PI3K signaling, and Rac signaling downstream of the GEF Vav1, but not the GEF Tiam1. Finally, we investigated the motility and force generation of M1 and M2 polarized primary human macrophages. We found that M1 macrophages are less motile and generate less force than M0 or M2 macrophages, and that M2 macrophages are more motile but do not have any change in force generation compared to M0 macrophages. We have been able to show that both chemical signals and mechanical mechanisms contribute to macrophage migration. This work contributes to the growing understanding of the mechanisms that govern macrophage migration and demonstrates the importance of mechanics when studying leukocyte migration.

TABLE OF CONTENTS

ACKNOWLEDGEMENTS	IV
ABSTRACT.....	VII
LIST OF TABLES	XII
LIST OF FIGURES	XIII
CHAPTER 1: INTRODUCTION	1
MOTIVATION	1
Specific Aim 1: Macrophage Chemokinesis on Microcontact Printed PDMS Substrates	3
Specific Aim 2: Traction Force Generation by Primary Human Macrophages	3
Specific Aim 3: Traction Force Generation by M1 and M2 Polarized Primary Human Macrophages	4
REFERENCES	5
CHAPTER 2: BACKGROUND	7
IMMUNITY.....	7
MACROPHAGE BIOLOGY	8
MACROPHAGE MIGRATION	15
CHEMOKINESIS.....	19
ENGINEERED PLATFORMS FOR STUDYING CELL MIGRATION	22
SUBSTRATE ELASTICITY AND CELLULAR BEHAVIOR	26
MEASURING TRACTION FORCES	30
REFERENCES	49
CHAPTER 3: MACROPHAGE CHEMOKINESIS ON MICROCONTACT PRINTED PDMS SUBSTRATES.....	59

ABSTRACT	59
INTRODUCTION	61
MATERIALS AND METHODS	64
RESULTS	68
DISCUSSION	90
CONCLUSIONS	96
REFERENCES	97
CHAPTER 4: FORCE GENERATION BY MOTILE PRIMARY HUMAN MACROPHAGES.....	101
ABSTRACT	101
INTRODUCTION	102
MATERIALS AND METHODS	106
RESULTS	111
DISCUSSION	120
CONCLUSIONS	124
REFERENCES	125
CHAPTER 5: MOTILITY AND FORCE GENERATION OF M1 AND M2 POLARIZED MACROPHAGES.....	129
ABSTRACT	129
INTRODUCTION	131
MATERIALS AND METHODS	134
RESULTS	140
DISCUSSION	146
CONCLUSIONS	149
REFERENCES	150
CHAPTER 6: CONCLUSIONS AND FUTURE WORK.....	153

SPECIFIC AIMS	153
SPECIFIC FINDINGS	153
FUTURE WORK.....	157
FINAL THOUGHTS	162
ACKNOWLEDGEMENTS	163
REFERENCES	164

LIST OF TABLES

Table 3.1: Alpha values for RAW/LR5 macrophages on varying concentration of fibronectin.....	78
---	----

LIST OF FIGURES

Figure 2.1: Macrophage differentiation as described by the Mononuclear Phagocyte System.....	10
Figure 2.2: Macrophage polarization.....	14
Figure 2.3: Macrophage motility signaling.....	17
Figure 3.1: Microcontact-printing of fibronectin on PDMS.....	69
Figure 3.2: Adhesion staining of RAW/LR5 macrophages on PDMS surfaces coated with fibronectin.....	71
Figure 3.3: Biphasic motility of RAW/LR5 macrophages.....	73
Figure 3.4: Biphasic motility of murine bone-marrow derived macrophages (BMMs).....	75
Figure 3.5: RAW/LR5 macrophage motility on PDMS surfaces coated with fibronectin.....	76
Figure 3.6: Motility of RAW/LR5 cells with reduced endogenous Cdc42 and chemically inhibited PI3K.....	79
Figure 3.7: Migration of RAW/LR5 macrophages with inhibited ROCK signaling.....	83

Figure 3.8: Quantitative analysis of RAW/LR5 migration.....	87
Figure 4.1: Primary human macrophages on polyacrylamide gels of increasing stiffness.....	112
Figure 4.2: Traction contour maps of migrating macrophage.....	114
Figure 4.3: Macrophage force generation with rear contraction inhibition.....	116
Figure 4.4: Macrophage force generation with leading edge inhibition.....	117
Figure 5.1: Motility of polarized macrophages.....	141
Figure 5.2: Traction force generation by polarized macrophages.....	143
Figure 5.3: Traction force generation by polarized macrophages under ROCK inhibition.....	145
Figure 6.1: Primary human macrophage transfected with LifeAct-GFP.....	161

CHAPTER 1: INTRODUCTION

MOTIVATION

An effective immune response is necessary for maintaining homeostasis and health in the human body. In order to protect against disease and persistent inflammation, cells of the immune system must be able to migrate efficiently to sites of infection and injury [1]. Macrophages are members of the innate immune response and act as first responders, migrating to sites of infection wherein they phagocytose pathogens and act as antigen presenting cells to activate the adaptive immune response through cytokine release. Improper macrophage migration has been linked to several auto-immune diseases [2]. Migrating macrophages have been associated with the egress of tumor cells away from primary tumors and into blood vessels, and are often linked to metastasis [3, 4]. Macrophages also migrate to and become primary components of atherosclerotic plaques [5]. Like other leukocytes, macrophages migrate in response to gradients and uniform fields of chemokines released by pathogens and inflamed tissues [6]. In order to migrate to sites of infection, macrophages bind the extracellular matrix through cell surface adhesion receptors known as integrins [7]. Overall macrophage function is dependent on the integration of the signals generated by chemokine engagement and integrin – ligand binding to ensure proper directional migration. It is therefore critical that we understand how these signals contribute to macrophage

migration and how defects in these signaling events can lead to the various pathologies that impair immune function and contribute to disease.

In addition to cytokine activation and integrin – ligand binding, cells must be able to generate traction force against their underlying substrate in order to migrate efficiently. Traction forces have been studied in anchorage-dependent cells such as endothelial cells and fibroblasts for over a decade [8-10], but only recently has the measurement of traction forces extended to cells of the immune system, or amoeboid cells, such as neutrophils and dendritic cells [11, 12]. The type of motility employed by these two classes of cells is very different, and the traction forces they exert were found to vary in both magnitude and location. Anchorage-dependent cells are slow-moving cells that create focal adhesions and have strong forces at their leading edge. Amoeboid cells are generally faster moving cells that do not create focal adhesions and produce much weaker forces than anchorage-dependent cells. Interestingly, amoeboid cells do not all share a common force distribution pattern. Neutrophils have their strongest forces in the rear of the cell and use a squeezing mechanism to move [11], whereas dendritic cells concentrate their forces at the leading edge of the cell pulling them forward [12]. The magnitude and distribution of forces may correlate to the mechanisms that cells use to migrate, and because there is consistency for how forces are distributed it is important to investigate the force generation of each cell type. It is critical that we develop a complete model of macrophage migration to better understand the role of macrophages in both healthy and diseased tissues. Thus, the objective of this thesis, outlined in the specific aims below, is to use engineered platforms to determine the biochemical and biophysical cues involved in macrophage migration.

Specific Aim 1: Macrophage Chemokinesis on Microcontact Printed PDMS

Substrates

We first hypothesize that the chemokinesis of macrophages can be quantified with respect to surface ligand concentration using engineered substrates. In this aim we will create PDMS surfaces microcontact printed with fibronectin at increasing concentrations to observe the migration of immortalized murine macrophages of the RAW/LR5 line in a uniform field of the chemokine CSF-1. A variety of inhibitors and knockdown cell lines will be used to determine which signaling molecules are required for macrophage migration. Macrophages will be seeded on microcontact printed fibronectin, and their displacements will be tracked over time to calculate their random motility coefficients as a function of ligand concentration.

Specific Aim 2: Traction Force Generation by Primary Human Macrophages

We next hypothesize that macrophages will generate strong traction forces at their leading edges due to the highly protrusive nature of their migration. Force generation by cells on their substrates has been shown to affect many cellular processes, including migration. The traction forces of mesenchymal cells as well as neutrophils and dendritic cells have been studied at length, but to date the tractions generated by macrophages have not been determined. In this aim, we will characterize the magnitude and distribution of forces generated by primary human macrophages; we will also determine which molecules are necessary for force generation. Primary human macrophages, with or

without a chemical inhibitor against signaling molecules, will be seeded on compliant polyacrylamide gels and their forces will be measured using traction force microscopy.

Specific Aim 3: Traction Force Generation by M1 and M2 Polarized Primary Human Macrophages

Finally, it is now known that macrophages encompass a heterogeneous population of cells that have been polarized down either a classical, pro-inflammatory (M1) pathway or an alternative, anti-inflammatory (M2) pathway. These polarized macrophages display different surface molecules, secrete different cytokines, and play different roles in the immune response. We hypothesize that macrophages polarized down an M1 pathway will generate significantly lower forces than macrophages polarized down an M2 pathway because it has been previously shown that M1 macrophages have reduced migratory capabilities compared to M2 macrophages [13]. In this aim, we will compare and contrast the forces generated by M1 polarized macrophages and M2 macrophages. Primary human macrophages will be seeded on compliant polyacrylamide gels and then polarized down either an M1 pathway using LPS and $\text{INF}\gamma$ or an M2 pathway using IL-4 for 24 hours. The traction forces of these macrophages will then be measured using traction force microscopy.

REFERENCES

1. Pollard, J.W., *Trophic macrophages in development and disease*. Nat Rev Immunol, 2009. **9**(4): p. 259-70.
2. Bischof, R.J., et al., *Exacerbation of acute inflammatory arthritis by the colony-stimulating factors CSF-1 and granulocyte macrophage (GM)-CSF: evidence of macrophage infiltration and local proliferation*. Clin Exp Immunol, 2000. **119**(2): p. 361-7.
3. Green, C.E., et al., *Chemoattractant signaling between tumor cells and macrophages regulates cancer cell migration, metastasis and neovascularization*. PLoS One, 2009. **4**(8): p. e6713.
4. Mantovani, A. and A. Sica, *Macrophages, innate immunity and cancer: balance, tolerance, and diversity*. Curr Opin Immunol, 2010. **22**(2): p. 231-7.
5. Gui, T., et al., *Diverse roles of macrophages in atherosclerosis: from inflammatory biology to biomarker discovery*. Mediators Inflamm. **2012**: p. 693083.
6. Pixley, F.J., *Macrophage Migration and Its Regulation by CSF-1*. Int J Cell Biol, 2012. **2012**: p. 501962.
7. Boocock, C.A., et al., *Colony-stimulating factor-1 induces rapid behavioural responses in the mouse macrophage cell line, BAC1.2F5*. J Cell Sci, 1989. **93** (Pt 3): p. 447-56.
8. Dembo, M. and Y.L. Wang, *Stresses at the cell-to-substrate interface during locomotion of fibroblasts*. Biophys J, 1999. **76**(4): p. 2307-16.

9. Pelham, R.J., Jr. and Y. Wang, *Cell locomotion and focal adhesions are regulated by substrate flexibility*. Proc Natl Acad Sci U S A, 1997. **94**(25): p. 13661-5.
10. Reinhart-King, C.A., M. Dembo, and D.A. Hammer, *The dynamics and mechanics of endothelial cell spreading*. Biophys J, 2005. **89**(1): p. 676-89.
11. Jannat, R.A., M. Dembo, and D.A. Hammer, *Traction forces of neutrophils migrating on compliant substrates*. Biophys J, 2011. **101**(3): p. 575-84.
12. Ricart, B.G., et al., *Measuring traction forces of motile dendritic cells on micropost arrays*. Biophys J, 2011. **101**(11): p. 2620-8.
13. Cougoule, C., et al., *Blood leukocytes and macrophages of various phenotypes have distinct abilities to form podosomes and to migrate in 3D environments*. Eur J Cell Biol, 2012. **91**(11-12): p. 938-49.

CHAPTER 2: BACKGROUND

IMMUNITY

The immune system is designed to protect the human body from infection and assist in injury resolution. It is comprised of two interacting responses: the innate immune response and the adaptive immune response. The innate immune response is the body's first line of defense against infection. Cells of the innate immune system recognize and destroy pathogens in a generic way without lasting or protective immunity. Innate immune cells also release chemical signals and present antigens on their surface to activate an adaptive immune response. In contrast to the innate response, the adaptive immune response is highly specific to an individual pathogen and provides immunological memory, protecting the body against a subsequent attack by the same pathogen.

Both the innate and adaptive immune responses are carried out by specialized blood cells known as leukocytes. This diverse group of cells is tasked with recognizing and destroying foreign pathogens, resolving inflammation, targeting cells for destruction, and protecting against a variety of diseases. In order to properly carry out these functions, leukocytes must be able to quickly and effectively migrate to sites of infection and areas of the body in which they are needed. Improper migration of leukocytes can cause a breakdown in the immune response and is associated with many disease pathologies, increased infections, and risk of death.

MACROPHAGE BIOLOGY

The Discovery and History of Macrophages

Macrophages were discovered in the 1880's by a Russian scientist named Elie Metchnikoff. Metchnikoff is considered one of the founders of immunology and for his discovery of macrophages, along with his other contributions to the field, he was awarded the Nobel Prize for Medicine in 1908 along with another immunologist, Paul Ehrlich [1].

Metchnikoff was originally interested in how simple organisms engulfed nutrients without a fully developed digestive system. While studying the cellular uptake of food particulates in transparent starfish larvae, he observed cells engulfing microbes and hypothesized that this process was the mechanism by which the host was protected against infection [2]. He theorized that there were specialized cells within the organism that attack and ingest foreign bodies and he named these cells phagocytes, from the Greek words "phage" meaning "to eat" and "cite" meaning "cell" [1]. To test his hypothesis, he challenged *Daphnia*, a type of water flea, with spores of an infectious fungus and observed phagocytes within the fleas surrounding and engulfing the spores [3]. He identified two types of phagocytes: microphages, smaller cells with polymorphic nuclei, and macrophages, large cells with single nuclei [2]. He further tested his theory of phagocytic protection against foreign bodies on higher species including mammals confirming the role of phagocytes in natural immunity at all levels of life [3].

It was not until the 1960's that it became clear that macrophages are ultimately derived from bone marrow precursors. This "Mononuclear-Phagocyte System" (or MPS) as reported by van Furth *et al.* [4] grouped highly phagocytic cells together, separating

them from other lymphocytes, by their origin, life span, and function within the body.

Van Furth had previously determined that both inflammatory and tissue macrophages are derived from blood monocytes that ultimately originate in the bone marrow [5]. The MPS explained the differentiation path from precursor cells found in the bone marrow (now known as hematopoietic stem cells), to promonocytes in the bone marrow (now termed common myeloid progenitors), to circulating monocytes in the blood, to fully differentiated macrophages found in most tissues within the body [4]. This differentiation path laid out by van Furth and colleagues is still largely what we know to be true today (Figure 1.1).

The most recent advance in macrophage biology has been the discovery that macrophages are not only diverse in function but can be activated along different paths by exposure to different chemical signals. It has long been known that macrophages can be activated by microbial signals such as interferon- γ or lipopolysaccharide, but only recently has it been discovered that macrophages can also be alternatively activated by anti-inflammatory signals such as IL-4, IL-10, and IL-13 [6, 7]. These “polarized” macrophages, classified M1 or “classically activated” and M2 or “alternatively activated” macrophages, were found to differ in surface receptor expression, cytokine and chemokine production, as well as effector function [8]. Finally, in the last decade it has been determined that the set of macrophages previously designated M2 is actually a collection of several subsets of distinct macrophage populations, termed M2a, M2b, M2c,

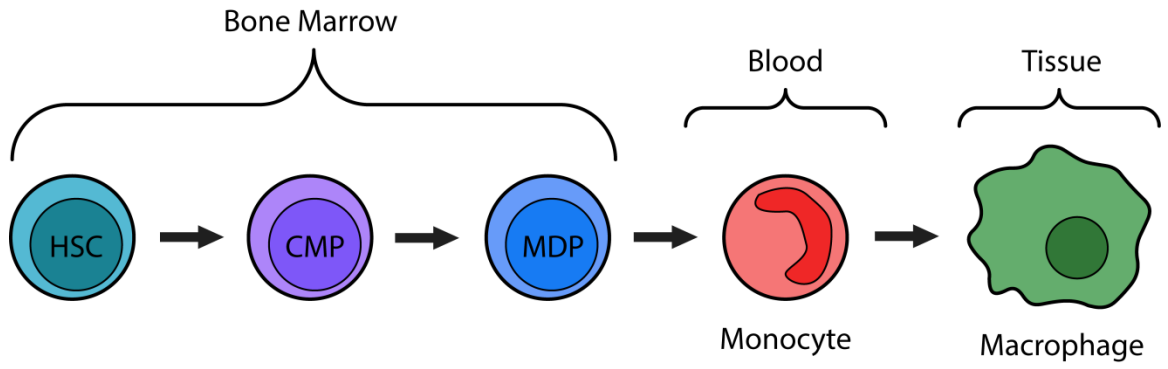


Figure 1.1: Macrophage differentiation as described by the Mononuclear Phagocyte System. HSC: hematopoietic stem cell. CMP: common myeloid progenitor. MDP: Macrophage-Dendritic Cell Progenitor. Adapted from [9].

and M2d [10, 11]. It is clear that the full spectrum of macrophage diversity has not yet been determined and new subsets of cells with diverse functions and properties will continue to emerge.

The Lifetime and Role of Macrophages

Macrophages are large, terminally differentiated, phagocytic cells that reside in almost all tissues in the human body. Macrophages arise primarily from circulating monocytes in the blood. Like all blood cells, monocytes begin as multipotent hematopoietic stem cells in the bone marrow. In the bone marrow, these stem cells go through a series of sequential differentiation steps: first becoming a common myeloid progenitor, then a granulocyte/macrophage precursor, then a monoblast, and finally a pro-monocyte [12]. Pro-monocytes then become monocytes which are released by the bone marrow into circulation. In response to a signal, such as colony-stimulating factor-1 or CSF-1 (also known as macrophage colony-stimulating factor or M-CSF), monocytes enter tissues and differentiate into macrophages.

Macrophages have two main roles in maintaining homeostasis. Mature, tissue-resident macrophages are located throughout the body and provide immune surveillance, monitoring their immediate surroundings for signs of tissue damage or infection. They phagocytose damaged or necrotic tissue and are primed to activate an immune reaction in response to danger signals [13]. Macrophages are often among the first cells to encounter a pathogen, and upon phagocytosing the intruder they become activated, killing the

pathogen itself and releasing cytokines to recruit other immune cells to the site of the infection [14].

Macrophage Polarization

Macrophages are a heterogeneous group of cells. They reside in different tissues throughout the body and perform a variety of functions based on stimuli from their environment. Two main macrophage phenotypes have emerged to categorize the functional diversity of macrophages in the body (Figure 1.2). “Classically activated” or M1 macrophages are pro-inflammatory cells that release cytokines to recruit other immune cells to sites of infection. In contrast, “alternatively activated” or M2 macrophages are involved in the resolution of inflammation and are considered anti-inflammatory. They release cytokines and function to clear inflammation and promote tissue repair and remodeling [15]. In reality, these subtypes simply categorize a spectrum of functional phenotypes present *in vivo* into two extremes. Some researchers have further classified the M2 macrophages into subsets: M2a, M2b, and M2c [16] and others have proposed a color wheel of activation [11] pointing to the diversity of signals and phenotypes found within the body. These phenotypic distinctions are clearly important to consider when studying the behavior of macrophages.

Macrophages in Disease

In addition to their healing roles as members of the innate immune system, macrophages are also associated with a variety of disease pathologies including autoimmune diseases, cancer, and atherosclerosis.

Many autoimmune diseases are caused or worsened by macrophage activity. In rheumatoid arthritis, synovial fibroblasts produce large quantities of the macrophage chemokine CSF-1, which recruits monocytes and macrophages into the inflamed joints. Monocyte differentiation into osteoclasts then causes loss of bone, and uncontrolled macrophage tissue-remodeling results in severe tissue damage [19]. It has also recently been shown that impaired macrophage migration contributes to pyogenic sterile arthritis pyoderma gangrenosum and acne (PAPA) syndrome, which is a disorder characterized by destructive inflammation of the skin [20].

Macrophages are also associated with progression and metastasis of several types of cancer. Tumor-associated macrophages (TAMs) have been correlated with a poor prognosis in breast, prostate, bladder, kidney, esophageal, and other types of cancer [21]. This poor prognosis is a result of several processes in which macrophages are thought to assist growing tumors by supporting tumor invasion, growth, and angiogenesis [21]. Macrophages are also thought to play a role in metastasis of tumors. It has been shown that macrophages and tumor cells communicate with each other through an EGF-1/CSF-1 paracrine signaling loop [22] and that this signaling increases the migration of both cell

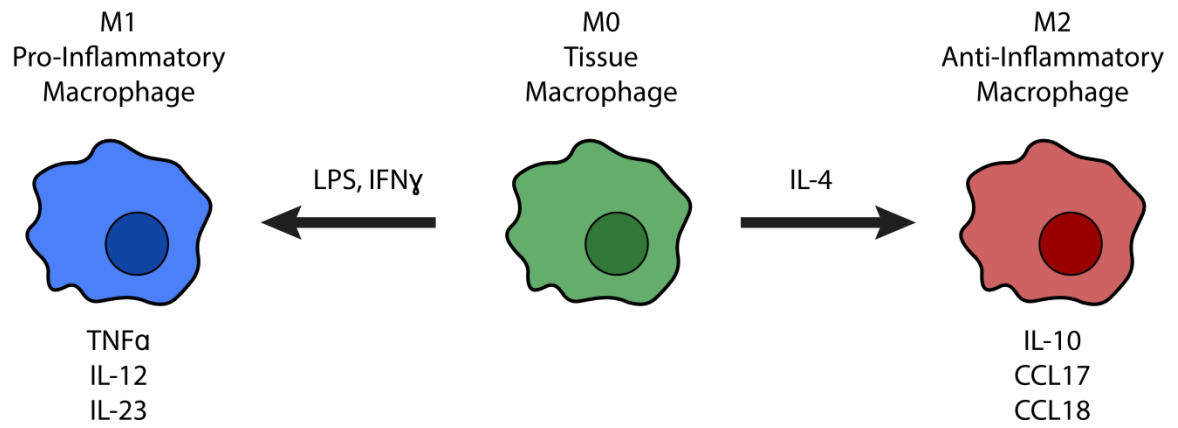


Figure 1.2: Macrophage polarization. Macrophages can be polarized into pro-inflammatory M1 macrophages or anti-inflammatory M2 macrophages. These polarized macrophages release different cytokines and express different surface receptors.

Redrawn from data presented in [15, 17, 18].

types. Macrophages and tumor cells have also been observed co-migrating away from tumors and into the vasculature, further indicating a role for macrophages in metastasis [23]. Finally, macrophages in the tumor environment play an immunosuppressive role, limiting the effectiveness of other immune cell responses [21].

Macrophages also play a major role in atherosclerosis. Macrophages are the first leukocytes to invade atherosclerotic plaques. Within the plaques, macrophages phagocytose low-density lipoproteins, or LDL, and become large foam cells. A buildup of these cells can lead to vascular occlusion. The level of cell death present in these plaques can also cause inflammation and further infiltration of monocytes and macrophages [24].

MACROPHAGE MIGRATION

Macrophage Polarity

An effective immune response depends on the ability of leukocytes to migrate through the vasculature and tissues to sites of infection and inflammation. Macrophages, in particular, must be able to migrate while monitoring their surroundings as well as in response to a pathogenic signal. In order to efficiently migrate, all cells must polarize and reorganize their cytoskeleton [25]. This polarization is generally considered to split the cell into two main regions: the “front” and the “rear” of the cell. The front leading edge, or pseudopod, consists of lamellipodia or filopodia, two types of F-actin-rich protrusions. Lamellipodia are broad, flat protrusions whereas filopodia are long, thin

projections. Both types of protrusions are seen in macrophage migration downstream of different signaling pathways [26]. These frontal protrusions drive the cell forward through actin polymerization and the formation of nascent adhesions to the substratum. The rear trailing edge, or uropod, is characterized by myosin II contraction and the detachment of old adhesions from the substratum, allowing translocation of the cell. It is thought that the two poles of a cell are governed by specific and distinct signaling pathways (Figure 1.3). Actin polymerization molecules such as Arp2/3 and WASp/WAVE as well as PI3K, Rac, and Cdc42 are found at the leading edge of cells. In macrophages, WASp signaling at the leading edge is specifically thought to lead to filopodial protrusions, whereas WAVE signaling leads to lamellipodial protrusions. The trailing edge of macrophages contains molecules associated with myosin II contraction such as RhoA and ROCK [26]. The specific localization of these molecules is still a hotly contested topic and new findings may lead to a revision in thinking on the driving force behind cell polarity.

Macrophage Motility

Almost all cells are capable of migration but the types and properties of migration vary greatly. Cell migration has generally been described as a cyclic process that can be broken down into five distinct steps: (1) cell polarization creates a leading edge, (2) the leading edge protrudes due to actin polymerization, (3) nascent adhesions form under the extended protrusion connecting the cell to the underlying extracellular matrix, (4) the cell

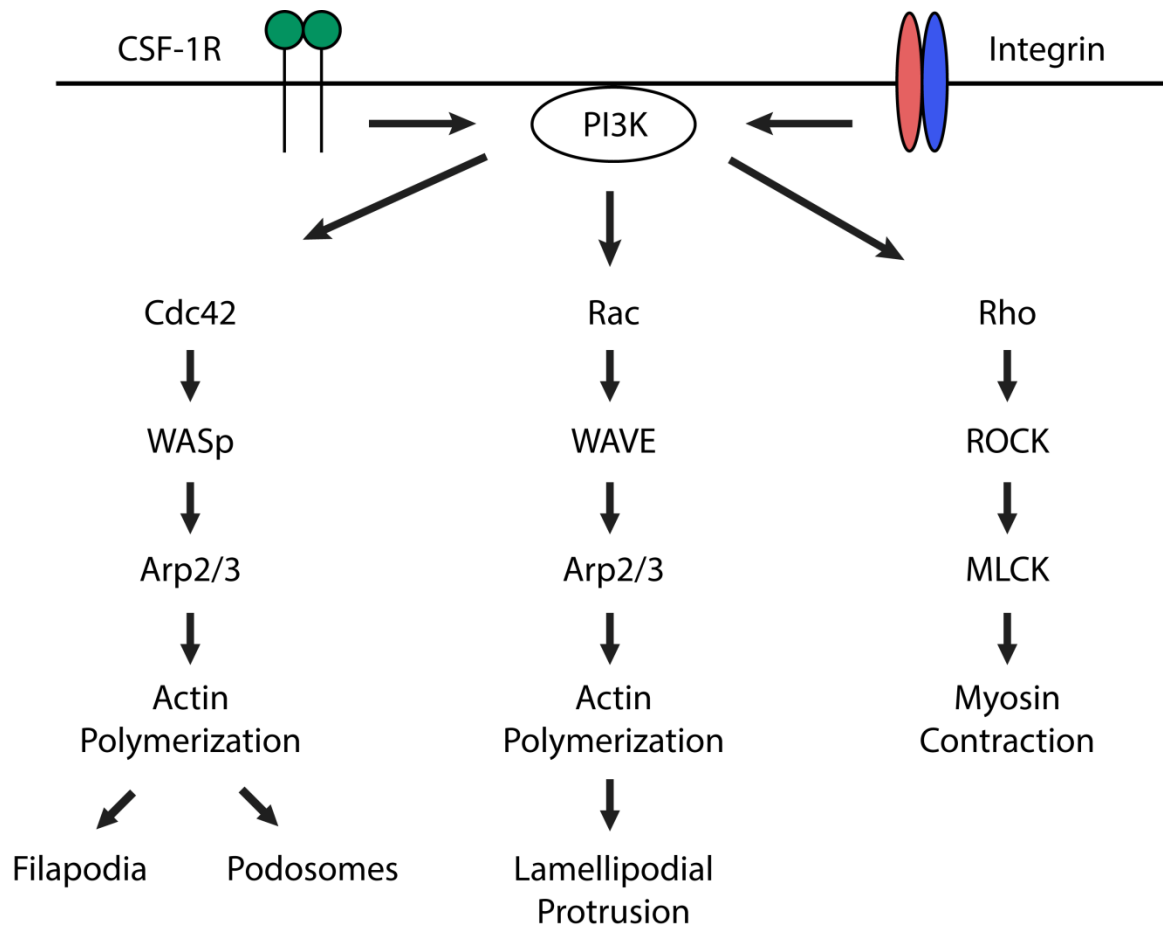


Figure 1.3: Macrophage motility signaling. A schematic of the signaling pathways activated by the CSF-1 receptor and integrins downstream of PI3K. Rho GTPases are activated downstream of both signaling receptors and their outcomes in the actin-myosin pathways are shown. Adapted from data presented in [26, 27].

body is translocated forward due to actomyosin-contraction, (5) old adhesions in the rear of the cell detach. This process most correctly describes the migration of large, slow mesenchymal cells such as endothelial cells and fibroblasts. Leukocytes are required to move much more quickly throughout the body and therefore more commonly use a form of migration known as amoeboid migration. Cells undergoing amoeboid migration do not create classical adhesion structures seen in mesenchymal cells such as stress fibers or focal adhesions. They instead create weak, short-lived adhesions and use squeezing mechanisms to move through small spaces such as tight junctions. Their migration is also much faster and more highly dynamic. Recent work even suggests that dendritic cells do not require any adhesions for interstitial migration [28]. Neutrophils and dendritic cells both display classical amoeboid motility and their migration has been intensely studied [29, 30].

Macrophages migrate more slowly than other leukocytes such as neutrophils or T cells, but they are considerably faster than mesenchymal cells such as epithelial cells or fibroblasts [26, 31]. Consistent with their intermediate migration speed, macrophages have been found to be capable of migrating using either amoeboid or mesenchymal migration, depending on the structure of the surrounding matrix [32]. Human macrophages were found to use the mesenchymal mode to migrate through dense 3D gels, and the amoeboid mode to migrate when in more porous fibrillar gels. Their mesenchymal migration was dependent on protease mediated matrix remodeling [32].

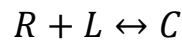
Unlike large mesenchymal cells, macrophages do not form large focal adhesions to their underlying substratum. Instead, they form small punctate adhesions called

podosomes. Podosomes are F-actin-rich structures that contain a number of adhesion proteins commonly found in focal adhesions such as FAK, paxillin, and vinculin. Podosomes are regularly found under the leading edge of migrating cells and have been linked to macrophage chemotaxis and matrix degradation [33].

CHEMOKINESIS

Receptor – Ligand Binding Kinetics

Receptor–ligand kinetics can be used to predict how cells will respond to a free chemokine in solution by modeling the interaction between the chemokine and its cell-surface receptor. The equilibrium binding between a free receptor R and a free ligand L to form a receptor/ligand complex C in a simple reversible reaction can be written as



where the relevant rate constants are the association rate constant k_f and the dissociation rate constant k_r . Using mass action kinetics, we can solve for the time rate of change for the receptor/ligand complex C as a function of the free receptor R and ligand concentration L

$$\frac{dC}{dt} = k_f RL - k_r C$$

Under steady–state conditions, the rate of change of the complex becomes zero and the receptor–ligand binding equation can be solved for the complex concentration

$$C = \frac{RL}{K_D}$$

where $K_D = \frac{k_r}{k_f}$ and is known as the equilibrium dissociation constant. The values of K_D span a wide range from 10^{-12} M for high affinity interactions to 10^{-6} M for low affinity binding. If we assume that the ligand concentration is nearly constant and the number of receptors on the cell surface is not changing, we can solve for the number of receptor/ligand complexes at equilibrium, C_{eq} ,

$$C_{eq} = \frac{R_T L}{K_D + L}$$

where R_T represents the total number of receptors on the cell surface [34].

Differential receptor occupancy theory tells us that there are an ideal number of bound receptor/ligand complexes on a cell that will lead to optimal chemokinesis [35]. If the concentration of ligand in the system is much lower than the K_D ($[L] \ll K_D$) then $C_{eq} \approx 0$ and the cell will not sense the presence of the chemokine. Conversely, if the concentration of the ligand is much higher than the K_D ($[L] \gg K_D$) then $C_{eq} \approx R_T$ meaning all available receptors will be bound, causing receptor saturation. However, when the concentration of the chemokine is near the K_D then $C_{eq} \approx 0.5R_T$ and only half of the receptors are bound, causing a differential in the receptor occupancy around the cell, allowing for intercellular signaling to drive migration.

The theory of receptor occupancy predicts the observed result that cells undergoing chemokinesis have a biphasic response to increasing chemokine or surface ligand concentration [30, 31, 36, 37].

Quantifying Chemokinesis

The most basic form of migration in a uniform environment lacking any directional cues is called random motility and is well described by a persistent random walk model [38]. Over short periods of time, cells will seem to move in a straight path while over long periods of time, the cells movement resembles Brownian motion. Each cell type has characteristic properties that describe its movement. The first property of migration is the speed of the cell, defined as the displacement of the cell body over time. The second property of migration is the persistence time of the cell, defined as the average time between significant changes in the cell's direction of motion. Among all cell types, these two properties are roughly inversely correlated with each other. It is intuitive to consider this fact. Fast cells must constantly survey their surroundings or risk going too far in the wrong direction, whereas slow cells must make small adjustments but continuously move in a single direction or risk traversing the same area.

The average speed and persistence time for a cell population can be quantitatively determined by tracking the cell path over time and fitting the data to the Dunn equation for mean-squared-displacement [38]

$$\langle d^2 \rangle = nS^2 \left[Pt - P^2 \left(1 - e^{-t/P} \right) \right]$$

The values of speed and persistence time can then be used to determine the random motility coefficient (μ) for the population of cells

$$\mu = \frac{1}{n} S^2 P$$

where n is the dimensionality of the system; $n = 2$ for two-dimensional motility and $n = 3$ for three-dimensional motility. The random motility coefficient for cell migration is analogous to a diffusion coefficient for gas particles, it characterizes the dispersion of the cell population in space [39].

ENGINEERED PLATFORMS FOR STUDYING CELL MIGRATION

The ability to engineer cellular microenvironments for studying cell migration in the laboratory has allowed a greater number of physiological features to be brought into *in vitro* work, increasing the relevance and impact of new discoveries. The use of soft lithography in the creation of polymer-based devices, stamps, and molds with features on the micron and nanometer scale has allowed for the creation of many of these newly engineered environments [40, 41].

Polydimethylsiloxane (PDMS)

Polydimethylsiloxane (PDMS) is widely used in the creation of engineered cellular devices. PDMS is a member of the family of organic silicon polymers known as silicones. For a number of reasons, PDMS is the most commonly used silicone in biological applications. The rheological properties of PDMS make it suitable for casting complex structures and maintaining these features after curing. After curing, PDMS is stiff enough to withstand large amounts of pressure, allowing its use in microfluidics. It is also optically clear, making it ideal for imaging purposes [42]. The shear modulus of PDMS can also be varied from 100 kPa to 10 MPa by altering the ratio of the elastomer to the curing agent [43]. While not fully bio-compatible, PDMS is considered to be inert and non-toxic. After polymerization, the surface of PDMS is hydrophobic and the Si surface chemistry makes it difficult for polar solvents to wet the surface, creating an attractive binding field for hydrophobic compounds such as proteins. Plasma or UV ozone treatment can be used to oxidize the surface, creating silanol (Si-OH) groups at the surface temporarily rendering the surface hydrophilic before hydrophobic recovery can occur. Finally, PDMS can be functionally blocked against cell attachment through chemical interaction with the family of co-polymers known as pluronics [29]. This presents a major advantage over typical surfaces used for cell motility experiments such as glass and tissue culture plastic because it guarantees specificity of cell-surface interactions.

Photolithography and Soft Lithography

Photolithography was developed in the 1950's to aid in the manufacture of semiconductors and involves the etching of complex patterns into very flat surfaces. Spin coating is used to deposit a very thin layer of photoresist onto a perfectly flat silicon wafer. There are two types of photoresist; negative photoresists cure when exposed to light and positive photoresists degrade upon exposure to light [44]. Separately, the desired pattern is turned into a high-resolution photomask, considering the type of photoresist being used. The pattern is transferred to the photoresist by shining co-illuminated light through the mask creating a master. A negative replica can be cast with PDMS by pouring uncured PDMS over the master and then allowing the polymer to fully crosslink.

Soft lithography, invented by George Whitesides in the 1990's [41], builds upon this process and uses photomasks, polymer stamps, and molds to fabricate and replicate patterns. The term "soft" comes from the use of elastomeric substrates such as PDMS in the process. The process of soft lithography is comprised of two steps. First, a master is created by fabricating a pattern onto a substrate and second, that pattern is used to produce a negative of the pattern's relief structure in an elastomeric substrate. The master can be created in a number of ways but is often fabricated using photolithography techniques. Many elastomeric replicates can be created from a single master and often these replicates can be used to generate a copy of the original master [41, 44].

Microcontact Printing

Two-dimensional motility assays are often performed on glass or tissue culture plastic that has been incubated with an adhesive ligand and blocked with a solution of bovine serum albumin (BSA). The BSA is intended to cover or “block” regions of the surface not otherwise functionalized with ligand to discourage non-specific cell-substrate interactions. Unfortunately, it has been shown that leukocytes are capable of interacting with BSA-blocked surfaces; specifically it was discovered that human neutrophils bind BSA directly through the integrin $\alpha_M\beta_2$ [29]. Microcontact printing allows for the creation of surfaces specifically functionalized with adhesive regions surrounded by non-adhesive regions, allowing greater control over the cellular microenvironment.

Microcontact printing, developed by George Whitesides [41], involves the transfer of “inked” protein from a flat PDMS stamp onto a substrate. Surfaces specifically functionalized and completely blocked against cell-substrate interactions can be created by microcontact printing proteins onto a substrate of spin-coated PDMS followed by functional blocking of the PDMS with pluronics. These surfaces are an ideal platform for motility assays, allowing for the investigation of cell-protein interactions without confounding cell-substrate adhesions. The combination of microcontact printing and soft lithography has also allowed for the creation of surfaces specifically patterned with protein lines and islands of precise width and area [23, 45].

SUBSTRATE ELASTICITY AND CELLULAR BEHAVIOR

Many cells in the body are anchorage dependent and must attach to a surface in order to survive. Even cells that do not require attachment, like many leukocytes, often create attachments to their surrounding environment. These attachments between the cell and the substrate can generate ‘outside-in’ signals, including mechanical signals pertaining to the stiffness of the substrate and chemical signals pertaining to the type of ligand and adhesiveness of the substrate. Cells are constantly probing their surroundings using these attachments and changing their behavior based on mechanical cues from their environment. It is especially important to understand how cells respond to changes in the mechanics of their environment because many disease pathologies, such as the development of solid tumors in cancer or the formation of caps in atherosclerotic plaques, are associated with a change in tissue stiffness [46-48].

Substrate stiffness is a proven regulator of many cell behaviors. It has been shown that the stiffness of their underlying substrate regulates the adhesion and spreading of 3T3 fibroblasts [49]. Smooth muscle cells have also been shown to correlate spreading with substrate stiffness [50]. Cells can also undergo durotaxis, migrating up or down a gradient of changing stiffness. Fibroblasts have been shown to preferentially migrate from a softer substrate to a stiffer substrate. They will also choose to turn around and continue migrating on a stiffer substrate if they encounter a softer substrate in their path [51]. Smooth muscle cells have also been shown to exhibit durotaxis, accumulating in the stiffer regions of a substrate with a compliance gradient. It has further been shown

that they migrate with increased speed on the compliance gradient when compared to a gel of consistent stiffness, further indicating a preference for the stiffer surface [52].

It has also been shown that cells can communicate through the substrate via the traction stresses they exert, and this communication is substrate stiffness dependent [53]. The distance a cell could pull on the substrate was measured by plating cells on compliant polyacrylamide gels with embedded fluorescent beads and measuring the furthest bead movement from the cell. The stiffer the substrate, the less the cell was able to pull on it up to a threshold stiffness where the cell cannot exert enough traction stress to pull the substrate at all. Any cells within the area of the gel that could be pulled by the cell would feel those traction stresses through the substrate and communicate through their generated forces. In addition to affecting how cells communicate with each other, substrate stiffness can also alter the interaction of cells [53]. On soft substrates, cells will come into contact with each other frequently and stay within close proximity of each other over time. On much stiffer gels, cells only briefly interact and then immediately separate and migrate away from each other. Consistent with these extremes, cells on intermediate stiffness will come in and out of contact with each other, staying near each other but not as close together as cells on soft gels [53]. These results show that substrate stiffness not only affects the behavior of individual cells but also drives cellular interactions.

Substrate elasticity has also been shown to influence the cell cycle. Multiple types of cells including mammary epithelial cells, vascular smooth muscle cells, and osteoblasts, were shown to rarely enter the G1 phase and progress to the S phase of the

cell cycle when plated on soft hydrogels. The number of cells entering G1 from both quiescence and cycling from G2/M phase, however, increased with the stiffness of the underlying substrate [53].

Substrate elasticity has been shown to play a major role in the differentiation of stem cells and provides sufficient signaling to drive the commitment of stem cells without the addition of growth factors [54]. Mesenchymal stem cells (MSCs) plated and maintained in identical growth media were found to exhibit cell morphologies, RNA profiles, transcription factors, and cytoskeletal markers consistent with neuronal differentiation when plated on substrates with an elasticity comparable to brain tissue ($E \sim 0.1-1$ kPa), myoblast differentiation when plated on substrates with the elasticity of muscle ($E \sim 8-17$ kPa), and osteoblast differentiation when plated on substrates with the elasticity similar to bone ($E \sim 25-40$ kPa). The MSCs grown on lineage specific matrices were found to be less plastic and more resistant to induction by lineage specific induction media. All of the compliance-directed differentiation can be abrogated by eliminating the cell's ability to detect the stiffness of the substrate through inhibition of actin-myosin contraction, with blebbistatin to block myosin II activity or ML7 to block myosin light chain kinase activity.

It has been further suggested that the ability of cells to generate tension on their substrate is the driving factor behind this stiffness-driven differentiation as cell spreading has also been shown to direct stem cell fate [55]. MSCs that are allowed to spread over a large area and generate traction stresses differentiate into osteoblasts, whereas MSCs restricted to small islands undergo adipogenesis. This cell area-driven differentiation was

also reduced without actin-myosin contraction through inhibition of the RhoA kinase ROCK or myosin II.

It has been shown that substrate stiffness can promote or inhibit cellular invasiveness [48]. When non-tumorigenic cells are grown on substrates with an elasticity near that of normal breast tissue, they display normal acini with a central lumen. On a stiffer substrate, these cells lose their organization and polarity and display a malignant phenotype. The increased stiffness leads to integrin clustering and induces the formation of focal adhesions resulting in contractility within the cell. Furthermore, without Rho activity, tumorigenic cells on stiff substrates lose their malignant phenotype. These results indicate that substrate stiffness can drive non-tumorigenic cells to become malignant and induce tumorigenic cells to become non-invasive.

Substrate stiffness has been shown to regulate cell behavior in neutrophils in many of the same ways as it does in mesenchymal cells. Substrate stiffness has been shown to affect the spreading of neutrophils with cells plated on stiff polyacrylamide gels ($E \sim 12$ kPa) spreading over a much larger area than cells on soft polyacrylamide gels ($E \sim 2$ kPa) [56]. The stiffness of the underlying substrate also has a significant effect on the chemotactic migration of neutrophils. Increasing the stiffness of the substrate led to a significant increase in the chemotactic index of the neutrophils over a range of chemotactic gradients. In addition to the increase in chemotactic index, it was found that neutrophils were able to generate higher traction stresses on stiffer gels in either a chemotactic or chemokinetic system [56, 57]. It was further shown that the ability of the neutrophils to organize these traction stresses in response to the chemokine gradient was

dependent on the stiffness of the substrate. Neutrophils on stiff gels generated strong tractions in the rear of their cell body relative to the gradient, whereas cells on soft gels were unable to organize their forces during chemotaxis [57]. Finally, it was shown that the increase in traction force generation and organization was dependent on cell-substrate adhesion through the β_2 integrin, and actin-myosin contraction through RhoA activity.

Substrate stiffness clearly has an important impact on cellular behavior, but much of the study in this field has focused on the effect of elasticity on mesenchymal cells. Some of the effects of substrate stiffness on cell behavior are conserved among all cell types, but most are likely not universal. The differences in the adhesion structures formed by mesenchymal cells versus leukocytes as well as the presence or lack of stress fiber formation has a large impact on the types and magnitude of traction stresses generated by cells. These differences in cell structures and traction stresses might lead to differences in the ways cells sense and respond to the mechanics of their environment. Thus, while much is known about the effect of substrate stiffness on mesenchymal cell behavior, there is significant work left to do on the effect of matrix elasticity on leukocytes.

MEASURING TRACTION FORCES

Measuring cellular traction forces is a non-trivial undertaking and there is still no agreed-upon optimal technique for making force measurements. There are several ways to approach the problem, each with its own advantages and drawbacks.

Silicone Films

One of the first observations of cells exerting forces on their substrate was made in 1959 by Paul Weiss using fibroblasts seeded on thin films [58]. Weiss developed a technique for studying blood clot cell masses on fibrin networks and noticed that fibrin fibers became compressed and wrinkled radially around the mass of cells. Furthermore, when two cell masses were plated on the same fibrin network, the fibers between the masses became aligned. Interestingly, Weiss believed that the wrinkles were due to dehydration of the protein networks and not produced by the cells themselves. In the same set of experiments, Weiss noted that the cells would reorient themselves along these fibers and move along the fibers providing the first observation of the now well-known principle of contact guidance [59].

The next development in visualizing cellular traction forces came from Harris and colleagues in 1980. Harris was able to directly observe wrinkles forming underneath cells using a new type of substratum: silicone films [60]. These silicone films were transparent, elastic, non-toxic, and inert allowing for the direct observation of a cell's traction forces. The substrate stiffness of the silicone films could also be altered by varying the initial viscosity of the silicone and the time allowed for crosslinking. Various cell types were plated on these thin films including embryonic heart fibroblasts, liver parenchyma cells, liver macrophages, pigmented retina cells, as well as sensory and sympathetic neurons and glia. Interestingly, the macrophages and neurons did not wrinkle the film, leading to the conclusion that their tractions were too weak to be detected. Individual cells wrinkled and compressed the silicone into an accordion pattern

beneath the cell, and the same alignment of wrinkles seen by Weiss was observed between two cells on the films. Harris concluded that the wrinkles were due to a rearward-directed traction force produced by the cells since the system could not dehydrate, and removal of the cells resulted in a reversal of the wrinkles [60].

The use of silicone thin films to detect traction forces represented a breakthrough in the field because it allowed for direct observation of cellular forces. Although qualitative, the results were able to provide information about the location and magnitude of forces generated by different cell types. There were still several drawbacks to this technique, most significantly the limited tunability of the substrate and the difficulty of quantifying the traction forces. Although the substrate stiffness could be altered by changing the curing time, it was very difficult to accurately and reproducibly make substrates of the same stiffness. It was also very difficult to quantitatively measure the magnitude of the forces. The authors did attempt to quantify the forces using a calibrated glass microneedle to produce wrinkles similar to those generated by the cell; however, these measurements are correlative at best.

There have been some improvements in the use of silicone sheets. Lee *et al.* were able to improve the reproducibility of fabrication for the silicone sheets and generated softer substrates using a glow discharge chamber to cure the silicone [61]. These softer silicone sheets allowed for the measurement of weaker tractions such as those generated by fish keratocytes. Lee was also able to better quantify tractions on the silicone sheets. They were able to do this by embedding beads into the silicone substrate and using a microneedle to reproduce the bead displacements seen under cells rather than trying to

reproduce wrinkles. Using this method they were able to determine the keratocytes generated their largest traction forces at the rear of locomoting cells. Unfortunately, problems with this technique still remained. The softer silicone sheets exhibited both plastic and viscoelastic behavior so the silicone movement was not directly proportional to the traction forces exerted on the substrate; therefore, bead displacement could not be accurately correlated to traction force [61].

The final improvements made to the silicone sheet technology came from Burton *et al.* during their study of force generation by fibroblasts and keratocytes [62]. Burton used a new production technique for generating the films that improved the mechanical resolution of the sheets. They used a heated tungsten wire to crosslink the polymer, reducing the gradients caused by the Bunsen burner flame Harris used. Furthermore, they used phenylmethyl polymer rather than dimethyl polymer because the phenyl groups were able to absorb UV light reducing the strength of the rubber and creating a more compliant substrate. Burton again used a calibrated microneedle to correlate the magnitude of the forces generated to the length of the wrinkles formed in the substrate. Burton also included marker beads to correlate the direction of force with the wrinkles. This combination of marker beads with wrinkles in the substrate allowed for a clearer understanding of force generation, but the non-linearity of the substrate wrinkles prevented true quantitative analysis of the traction forces.

Polyacrylamide Gels with Fluorescent Marker Beads

Motivated by the difficulty in controlling the stiffness of silicone films in a reproducible manner, Pelham and Wang developed a non-wrinkling polyacrylamide (PA) substrate to study cellular traction forces [49]. The PA gels did not wrinkle because they were covalently attached to a glass coverslip using glutaraldehyde. By altering the ratio of pre-polymer (acrylamide) to the crosslinker (bis-acrylamide), the elasticity of the substrate could be systematically and reproducibly changed; the possible combinations lead to a range of gel stiffness that could be produced from 250 Pa to over 70,000 kPa [48]. PA gels are also advantageous because they are thin and optically clear which makes them ideal for microscopy, and they are inert to cells so cell attachment can be controlled. Finally, PA gels are elastic and this elasticity simplifies force measurements because measured strains are linearly related to imposed stresses.

Polyacrylamide gels are non-adhesive to cells and proteins; therefore, the gel surface must be activated with either a chemical or linker so that it can be functionalized with proteins or peptides. Pelham and Wang used Sulfo-SANPAH, a UV photoactivatable linker, to functionalize their gel surfaces [49]. Another option is the use of a protein-adhesive group, such as the N6 linker, that is copolymerized with the polyacrylamide during gel fabrication [63]. Also, the surface can be activated by chemically treating the gel with hydrazine hydrate to change inert amide groups into reactive hydrazide groups [64]. Each of these activation techniques aims to alter the gel so it can be functionalized by covalently binding extracellular matrix proteins or peptides to the surface to allow for cell adhesion.

The elastic properties of the PA gels allowing for precise quantification of traction forces prompted Micah Dembo to collaborate with Pelham and Wang on modifying the gels to quantify traction stresses [65]. Latex fluorescent beads were embedded in the PA gel and by measuring the displacement of these beads Dembo created a novel computational algorithm for determining the cellular forces exerted on the gel. Mapping the forces to bead displacements is still a complex problem despite the elastic properties of the PA gels to force. Dembo breaks the problem down into several small, overlapping strain fields acting in a single plane. His theory defines the displacement field of the elastic substrate as an integral over the traction field [66]. To ensure that this integral exists for all traction fields, the traction field must have bounded support and comply with a global force balance. The Green's functions that are contained within the solution integral provide the substrate displacement induced by a concentrated force, and these are derived from Boussinesq theory for an elastic solid. This theory predicts that any coupling between in-plane and out-of-plane tractions are negligible [65]. Since an arbitrary number of displacement fields can produce the same traction field, the equation does not have an analytic solution and must be solved numerically using statistics.

First, the domain of the traction field is defined by tessellating the image with a quadrilateral mesh. They found that their system has a spatial resolution of $\sim 5\mu\text{m}$ by shrinking the mesh size until the results are no longer dependent on the size of the mesh. A chi-squared statistic is then used to determine the likelihood of a particular traction image to explain a set of bead displacements. The Bayesian likelihood of the tractions is determined by minimizing the chi-squared statistic and the intrinsic complexity to choose

the simplest tractions consistent with a given field of bead displacements. Finally, a bootstrap analysis, where random noise is added to the maximum likelihood displacements and then the tractions are reanalyzed with this error, is used to determine if the tractions are statistically significant [65]. This method of calculating traction forces developed by Dembo is referred to as traction force microscopy.

In traction force microscopy, a phase contrast image of the cell and a fluorescent image of the marker beads are taken concurrently. The cell is then removed and another fluorescent image is taken of the unstressed fluorescent markers. The phase contrast image is used to create an outline of the cell, which is used as the boundary condition within which the forces must occur. By comparing the bead locations in the stressed and unstressed fluorescent images, the bead displacements are calculated. The most likely set of traction forces vectors that describe the bead displacements is then calculated as described above.

Recent work done with micropipette aspiration has shown that polyacrylamide gels are not in fact perfectly elastic and can exhibit nonlinear behavior. The computational analysis developed by Dembo relies on the assumption that the cells are exerting force on a linearly elastic substrate. This nonlinear elastic behavior, however, is only present at very high levels of stress (exceeding 10 kPa) and this error is reduced by using sufficiently thick gels; therefore, the assumption of a semi-infinite medium holds [67]. Furthermore, the stresses exerted by the cells used in this study are sufficiently lower than the non-elastic limit.

The advent of traction force microscopy has led to the study and quantification of force generation by a wide range of cell types including fibroblasts [51, 68], endothelial cells [69], and neutrophils [56, 57, 70]. The first study of traction force microscopy was performed by Dembo and Wang on 3T3 fibroblasts [51]. The fibroblasts were found to exhibit larger traction stresses on stiff substrates than on soft substrates, with the average traction magnitude being ~ 1.1 kPa on 30 kPa gels and ~ 0.6 kPa on 14 kPa gels [51]. Traction force microscopy was further applied to migrating 3T3 fibroblasts and it was shown that a strong band of traction stresses are generated at the leading edge of the cell. It was also observed that when the cell changed polarity to alter its direction of migration, the original leading edge lost its ability to generate strong tractions and strong tractions began to appear at the new leading edge of the cell. When using an H-ras transformed clone of the 3T3 cells, the fibroblasts lose the ability to polarize and display faster, more disorganized migration. The traction stresses in these cells were found to be smaller than in normal fibroblasts and more unorganized, occurring under multiple transient protrusions. These observations led to the frontal towing model as an explanation for the migration of fibroblasts and more generally, mesenchymal cells [68]. The frontal towing model suggests that the cell possesses several transient towing units under its leading edge that adhere to the substrate and transmit strong traction stresses. Directly behind these towing units is an elastic transition zone that transmits contractile force through the cell body, pulling the cell forward. New towing units must be continuously formed at the leading edge of the cell while old towing units are detached at the cell's rear in order for the cell to move forward [68].

Traction forces of endothelial cells have also been reported and were found to be similar in magnitude to those produced by fibroblasts [69]. These forces were shown to be concentrated at the ends of pseudopodia, similar to fibroblasts, with negligible force found under the nucleus, reaffirming the frontal towing model of migration. Forces in the endothelial cells were also found to increase linearly with cell area [69].

Traction force microscopy has also been used to measure the tractions generated by migrating neutrophils. Contrary to what was seen in mesenchymal cells, neutrophils were shown to exert forces primarily in the rear of migrating cells. These forces were found to quickly reorient themselves setting the direction of motion [70]. The traction forces generated by neutrophils were found to be significantly weaker than those generated by mesenchymal cells. Interestingly, neutrophil traction stresses were found to depend not only on the stiffness of the underlying substrate but also on the chemotactic migration of the neutrophils. Neutrophils in an optimal gradient of the chemoattractant fMLP exerted stronger forces than those undergoing random migration or in gradients that were too shallow or too steep for efficient chemotaxis [56]. The orientation of traction forces in neutrophils suggested that their migration might not be governed by the frontal towing model of migration but rather by a rearward squeezing model. It was proposed that in the rearward squeezing model of migration, neutrophils used strong forces at their rear to push the contents of the cell forward, much like squeezing toothpaste out of a tube, and generate forward migration [70].

The measurement of traction stresses has also extended past the evaluation of normal tissue cells and into diseased cells. Casey Kraning-Rush and colleagues have

shown that the metastatic potential of several cancer cell lines is positively correlated with the traction forces generated by the cells [71]. They found that metastatic breast, prostate, and lung cancer lines generated significantly higher forces than their non-metastatic counterparts. Furthermore, they found that this increase in force was more pronounced on higher stiffness substrates; at 1 kPa only the metastatic lung cancer cells generated significantly higher forces than the non-metastatic cells, whereas at 5 and 10 kPa all three metastatic cells generated significantly higher forces. This is especially relevant because of the increase in tissue stiffness that occurs during tumor formation and its possible effect on the metastatic behavior of the cancer cells [48]. Finally, the correlation between metastatic potential and force generation was confirmed using a set of cell lines, derived from MCF10A breast cancer cells, that display increasing metastatic potential [71].

The computational and experimental methods for improving traction force microscopy are continually being updated by Dembo and others. Dembo has added functions to the analysis software that correct for the finite thickness of the gel and that improve the error analysis by including a far-field method and hybrid analysis method [72]. The far-field approximation assumes that bead displacements rapidly die with distance from the cell, which allows for a comparison between real disruptions caused by the cell and erroneous apparent disruptions far from the cell. The hybrid analysis method accounts for the fact that in cases of high magnification, the far-field beads may be out of the viewing window; therefore, it is assumed that the bead movement in an elastic substrate should vary smoothly with position, so large divergences in movement between

nearest neighbor beads is the result of an error [72]. Sabass and colleagues have found that by tracking two sets of differently colored beads using confocal microscopy, the spatial resolution of traction force microscopy can be improved to $\sim 1\mu\text{m}$ [73].

Advances to traction force microscopy are continually being made and it is still considered one of the premiere methods for measuring cellular traction force.

Micropatterned Elastomer Substrates

Traction force microscopy, as developed by Dembo and Wang, allows for high resolution of traction forces due to the large number of beads embedded in the polyacrylamide gels. Unfortunately, the random distribution of beads and the background fluorescence generated by out-of-plane beads makes the bead tracking and numerical methods computationally complex. Balaban *et al.* were able to directly address this problem by micropatterning the fluorescent beads onto a substrate and correlating the traction stresses to fluorescently-labeled focal adhesions [74]. They fabricated the patterned substrates by first curing a thin PDMS layer of a known stiffness onto a glass coverslip. Then either a Si-resist mold or a GaAs-resist was brought into contact with the PDMS and cured. When the resist was peeled away, either a shallow topographical pattern was left in the PDMS (in the case of the Si-resist) or fluorescent beads were left in the PDMS (in the case of the GaAs-resist). It was found using this system of substrate fabrication that using thin films resulted in greater variation in the spatial force distribution than had previously been seen on thicker substrates. This is due to the fact

that the deformation field in an elastic film of finite thickness, caused by localized applied force decays on the length scale of twice the film thickness, results in better spatial resolution of the force [75].

Micropatterning PDMS substrates might allow for better correlation of traction forces to discrete regions within the cell such as focal adhesions; however, the surface topography generated by the resists may affect cell behavior [74]. The analysis may be more computationally robust, but it has also been shown that thin substrates no longer behave elastically which could negatively affect the computational solution [67]. Finally, it has been shown that as the thickness of the substrate decreases there is a corresponding increase in the elastic modulus [76].

One solution to the problems associated with PDMS substrates is to instead micropattern polyacrylamide gels. Stricker and colleagues used a PDMS stamp to pattern discrete islands of fibronectin onto activated polyacrylamide gels [77]. They found that traction stresses were only produced at the islands of fibronectin, allowing traction force analysis using Fourier transforms. Unfortunately this restriction of adhesive ligand again could change the adhesions and forces generated by the cells, limiting the usefulness of this technology.

The micropatterning of polyacrylamide gels with adhesive ligands has been used in combination with traditional traction force microscopy to determine the effect of cell size and shape on force generation and distribution[78]. Rape and colleagues fabricated polyacrylamide gels embedded with fluorescent beads; separately, they created PDMS

stamps with specific patterned features using soft lithography. The stamps were functionalized and brought into contact with the polyacrylamide gels, creating gels with adhesive islands of known geometry. Using this method, they were able to determine that traction force is not determined by the cell area but rather by the distance from the cell center to the cell perimeter [78].

Micromachined Cantilevers

All of the previously described methods for measuring traction forces use substrates that provide a continuous surface for cell migration. Continuous substrates are beneficial because they describe the magnitude and organization of forces across the entire cell. In addition to these continuous surface techniques there exist techniques with discrete surfaces that allow the measurement of subcellular tractions without the influence of tractions generated elsewhere in the cell. The initial study in the use of discrete surfaces was presented by Galbraith and Sheetz using micromachined cantilevers [79]. In this method, cells move over a field of calibrated micro-cantilevers that can dynamically measure the subcellular traction forces generated in non-coupled regions of the cell. The force on each cantilever can be calculated as the cell migrates across a densely packed field yielding highly specific information about local force generation. Using these cantilevers it was determined that the front of a moving cell generates weak forces against the direction of motion. Under the nucleus, forces are strong but unevenly directed, and forces in the rear are stronger and directed with motion. The cantilevers can

only bend in one direction, meaning the measured force will be reduced if the cell crosses the cantilever beam at an angle.

In a similar technique, Prass and colleagues used an atomic force microscopy cantilever directly in the path of migrating keratocytes to directly measure the force generated by the lamellipodia [80]. They were able to measure the deflection versus time and calculate the force using Hooke's law; however, they noticed that the cell protrusion slowed just before reaching the cantilever, indicating that the cell may mechanically sense the cantilever being used to measure force, possibly altering the cell behavior. In addition to the possibility for mechanically altering cell behavior the micro-cantilever fields are technically challenging to produce, making this technique less widely used and far less popular than the continuous surface methods.

Microfabricated Post Array Detectors

Realizing the advantages offered by micromachined cantilevers, Chen and colleagues improved upon the discrete method of measuring traction forces by developing microfabricated post array detectors or mPADs [81]. The microfabricated post array detectors consist of a bed of compliant PDMS microneedles that can simultaneously measure discrete traction forces at many locations underneath a cell. The mPADs are made from a PDMS mold which is created by casting PDMS against an array of SU-8 posts made using photolithography techniques. The PDMS posts can then be printed with adhesive ligand using the microcontact printing technique and blocked with

pluronics so that cells only attach to the tips of the posts. The force at each post can be easily calculated, without the assumptions necessary for standard traction force methods, by measuring the deflection of each post tip and multiplying by the spring constant of the post. The stiffness of the mPAD posts is easily modified by altering the height and diameter of the posts. The stiffness of posts with known height and diameter was determined using calibrated glass pipettes to deflect the posts by a known distance. Each post deflects independently of its neighbors; therefore, each deflection can be linked to individual areas of the cell such as focal adhesions.

The micropost technique has been used to study the forces of subconfluent monolayers of MDCK cells [82]. They improved upon the spatial resolution used by Chen and colleagues by decreasing the post-to-post spacing. They showed that the micropost array did not affect the ability of the cells to adhere, proliferate, or migrate when compared to flat PDMS surfaces. The maximal stresses exerted by cells within the subconfluent epithelium were found to be at the edges of the monolayer and were on the order of $12.7 \pm 0.3 \text{ nN/m}^2$. This value is significantly higher than the maximal stresses in an individual migrating cell.

The Chen lab further developed this technology by improving the spatial resolution of the post technique by using deep reactive ion etching to etch silicone posts rather than etching holes. They then generated positive replicas by double casting PDMS to create the nanopost arrays [83]. This improved technique generated nanopost arrays with post stiffnesses from 7-231 $\text{nN}/\mu\text{m}^2$. Using these arrays they were able to determine

that the array geometries did not affect the cell speed or F-actin polymerization compared to flat PDMS surfaces [83].

Micropost force detectors have also been generated using silicone rather than PDMS for the pillars. In this system, trenches were added within the array to observe the effect of topographical features on the cell behavior [84]. Endothelial cells were found to respond to the trenches with cells approaching the posts parallel to the trenches exhibiting extreme contact guidance, and cells approaching perpendicular exhibiting some contact guidance but to a lesser degree. It was shown that fibroblasts on these arrays altered their force generation while spreading, initially showing an outward force generation followed by an inward force generation against the direction of spreading.

Another advantage of the mPAD system is its sensitivity in measuring weak forces not detectable using traditional traction force microscopy. Ricart and colleagues found that the forces generated by dendritic cells were too weak to resolve using traction force microscopy but could be detected using the mPAD system [85]. They found that dendritic cells generated traction forces on the order of 18 ± 1.4 nN/cell for chemotaxing cells and 16 ± 1.3 nN/cell for cells undergoing chemokinesis. These traction stresses were short-lived with the largest stresses located at the leading edge of migrating cells. The ability of the microposts to resolve very weak forces has also been used to measure the force exerted by neutrophils undergoing transendothelial migration [86]. The forces exerted by different densities of endothelial cells were first measured to determine the background level of post displacement of the monolayer. The neutrophils were then plated on a TNF- α activated endothelial cell monolayer. Neutrophils penetrated between

endothelial cells, creating a gap in VE-cadherin staining that was correlated with micropillar displacement as the neutrophil transmigrated. The average maximum force per posts for neutrophils migrating on top of the monolayer was 4.8 ± 1 nN/pillar, and that force increased to 14 ± 4 nN/pillar when the cell transmigrated. The average force was also found to depend on the rigidity of the micropillars.

The micropost systems offer a number of advantages. It is mathematically simpler to calculate the forces exerted on the posts than it is in a continuous substrate system. The stiffness of the posts can also be easily altered by simply changing their geometry. The discrete nature of the posts allows for a direct correlation of forces with specific areas of the cell or fluorescently labeled proteins within the cell. Finally, the microneedles are sensitive enough to measure the very weak forces produced by dendritic and other amoeboid cells that would not be detectable with traditional traction force systems [85]. The discrete nature of the posts also has some drawbacks when compared to continuous surface systems. Micropillars must be anchored to an elastic substrate of the same material, often PDMS. When force is applied to the pillars, the substrate underneath can also warp, resulting in an additional displacement of the post and an overestimate of the force by as much as 40%. A scaling factor that scales with the dimensionless pillar aspect ratio was determined to account for this additional bending [87]. This result detracts from the mPAD system's force-calculation advantage over traditional traction force systems. The resolution of the continuous systems is also much greater because it is only limited by the number of beads within the substrate. The density of the microposts limits the resolution possible in the mPAD system.

Improvements have increased the post density and resolution [83] but there is a limit to how close the posts can stand until the bending of the posts causes collisions, eliminating the discrete nature of the system. Finally, in vivo cells migrate on continuous surfaces and the topography of the posts might affect how the cells behave in an mPAD system, as has been shown with trenches for endothelial cells [84].

Three-Dimensional Traction Force Microscopy

All of the methods described above measure the traction forces of cells in 2D; however, cells in the body are most commonly surrounded in 3D environments. A method for measuring traction forces in three dimensions using confocal microscopy was developed and reported by Hur *et al.* [88]. In this initial study, bovine aortic endothelial cells (BAECs) were seeded on a 2D polyacrylamide gel and confocal microscopy was used to show that even in a 2D system cells exert tractions on the gel in three dimensions. The forces measured in the XY plane were similar to those measured in 2D traction force microscopy with large forces at the edge of the cells and little force in the center. The tractions exerted in the Z plane were upward at the cell edges and downward under the cell nucleus. This technology was also used to measure forces in migrating cells [89]. It was shown that the front of a migrating cell pushes the matrix down while the rear of the cell pulls the matrix up (in the Z plane). It was also shown that forces in the normal direction and forces in the in-plane direction were coupled [89].

It has been documented that cells in 3D environments exhibit differing morphologies, cytoskeletal structures, adhesions, and signaling than cells on 2D surfaces [90-92]; therefore, it is not unreasonable to hypothesize that cells generate different tractions in 3D environments than they do on 2D surfaces. The 3D traction forces of fibroblasts encapsulated within a PEG hydrogel were determined by measuring the bead displacements with the 3D gel by surrounding the cells with a finite element mesh and imaging with confocal microscopy [93]. The largest tractions were exerted by cell extensions at both the leading tip and from small extensions on the side opposite from the leading edge, indicating force polarity even by cells in 3D environments.

Additional improvements to 3D traction microscopy have been made by using laser scanning confocal microscopy to image the cell and beads simultaneously [94]. A digital volume correlation to track the displacement of particles within the gel in three dimensions was also used. This technique allowed for direct calculation of traction forces along any plane rather than relying on complex numerical methods. This method also found that migrating cells in 3D generated pushing forces at the leading edge and pulling forces at the trailing edge.

While 3D traction force microscopy is the most physiologically relevant technique, it is by far the most technically and computationally challenging. Absolute values of force and stress are hard to determine because it is not possible to take an unstressed image of the marker beads without destroying the structure of the 3D gel. Further advances in this field will likely allow for the most impactful measurements of cellular traction.

REFERENCES

1. Ellis, T.M., S.S. Sutherland, and G. Davies, *Strain variation in Dermatophilus congolensis demonstrated by cross-protection studies*. Vet Microbiol, 1991. **28**(4): p. 377-83.
2. Kaufmann, S.H., *Elie Metchnikoff's and Paul Ehrlich's impact on infection biology*. Microbes Infect, 2008. **10**(14-15): p. 1417-9.
3. Gordon, S., *Elie Metchnikoff: father of natural immunity*. Eur J Immunol, 2008. **38**(12): p. 3257-64.
4. van Furth, R., et al., *The mononuclear phagocyte system: a new classification of macrophages, monocytes, and their precursor cells*. Bull World Health Organ, 1972. **46**(6): p. 845-52.
5. van Furth, R. and Z.A. Cohn, *The origin and kinetics of mononuclear phagocytes*. J Exp Med, 1968. **128**(3): p. 415-35.
6. Goerdts, S. and C.E. Orfanos, *Other functions, other genes: alternative activation of antigen-presenting cells*. Immunity, 1999. **10**(2): p. 137-42.
7. Stein, M., et al., *Interleukin 4 potently enhances murine macrophage mannose receptor activity: a marker of alternative immunologic macrophage activation*. J Exp Med, 1992. **176**(1): p. 287-92.
8. Mantovani, A., et al., *Macrophage polarization: tumor-associated macrophages as a paradigm for polarized M2 mononuclear phagocytes*. Trends Immunol, 2002. **23**(11): p. 549-55.

9. Chow, A., B.D. Brown, and M. Merad, *Studying the mononuclear phagocyte system in the molecular age*. Nat Rev Immunol, 2011. **11**(11): p. 788-98.
10. Colin, S., G. Chinetti-Gbaguidi, and B. Staels, *Macrophage phenotypes in atherosclerosis*. Immunol Rev, 2014. **262**(1): p. 153-66.
11. Mosser, D.M. and J.P. Edwards, *Exploring the full spectrum of macrophage activation*. Nat Rev Immunol, 2008. **8**(12): p. 958-69.
12. Italiani, P. and D. Boraschi, *From Monocytes to M1/M2 Macrophages: Phenotypical vs. Functional Differentiation*. Front Immunol, 2014. **5**: p. 514.
13. Murray, P.J. and T.A. Wynn, *Protective and pathogenic functions of macrophage subsets*. Nat Rev Immunol, 2011. **11**(11): p. 723-37.
14. Bruce Alberts, A.J., Julian Lewis, Martin Ruff, Keith Roberts, and Peter Walter, *Molecular Biology of the Cell, 4th edition*. 2002, New York: Garland Science.
15. Biswas, S.K., et al., *Macrophage polarization and plasticity in health and disease*. Immunol Res, 2012. **53**(1-3): p. 11-24.
16. Martinez, F.O., et al., *Macrophage activation and polarization*. Front Biosci, 2008. **13**: p. 453-61.
17. Hao, N.B., et al., *Macrophages in tumor microenvironments and the progression of tumors*. Clin Dev Immunol, 2012. **2012**: p. 948098.
18. Murray, P.J., et al., *Macrophage activation and polarization: nomenclature and experimental guidelines*. Immunity, 2014. **41**(1): p. 14-20.
19. Pollard, J.W., *Trophic macrophages in development and disease*. Nat Rev Immunol, 2009. **9**(4): p. 259-70.

20. Cortesio, C.L., et al., *Impaired podosome formation and invasive migration of macrophages from patients with a PSTPIP1 mutation and PAPA syndrome*. *Arthritis Rheum*, 2010. **62**(8): p. 2556-8.
21. Lewis, C.E. and J.W. Pollard, *Distinct role of macrophages in different tumor microenvironments*. *Cancer Res*, 2006. **66**(2): p. 605-12.
22. Goswami, S., et al., *Macrophages promote the invasion of breast carcinoma cells via a colony-stimulating factor-1/epidermal growth factor paracrine loop*. *Cancer Res*, 2005. **65**(12): p. 5278-83.
23. Sharma, V.P., et al., *Reconstitution of in vivo macrophage-tumor cell pairing and streaming motility on one-dimensional micro-patterned substrates*. *Intravital*, 2012. **1**(1): p. 77-85.
24. Gui, T., et al., *Diverse roles of macrophages in atherosclerosis: from inflammatory biology to biomarker discovery*. *Mediators Inflamm*. **2012**: p. 693083.
25. Meili, R. and R.A. Firtel, *Two poles and a compass*. *Cell*, 2003. **114**(2): p. 153-6.
26. Pixley, F.J., *Macrophage Migration and Its Regulation by CSF-1*. *Int J Cell Biol*, 2012. **2012**: p. 501962.
27. Pixley, F.J. and E.R. Stanley, *CSF-1 regulation of the wandering macrophage: complexity in action*. *Trends Cell Biol*, 2004. **14**(11): p. 628-38.
28. Lammermann, T., et al., *Rapid leukocyte migration by integrin-independent flowing and squeezing*. *Nature*, 2008. **453**(7191): p. 51-5.
29. Henry, S.J., J.C. Crocker, and D.A. Hammer, *Ligand density elicits a phenotypic switch in human neutrophils*. *Integr Biol (Camb)*, 2014.

30. Ricart, B.G., et al., *Dendritic cells distinguish individual chemokine signals through CCR7 and CXCR4*. J Immunol, 2011. **186**(1): p. 53-61.
31. Hind, L.E., et al., *Two-dimensional motility of a macrophage cell line on microcontact-printed fibronectin*. Cytoskeleton (Hoboken), 2014. **71**(9): p. 542-54.
32. Van Goethem, E., et al., *Matrix architecture dictates three-dimensional migration modes of human macrophages: differential involvement of proteases and podosome-like structures*. J Immunol, 2010. **184**(2): p. 1049-61.
33. Dovas, A., et al., *Regulation of podosome dynamics by WASp phosphorylation: implication in matrix degradation and chemotaxis in macrophages*. J Cell Sci, 2009. **122**(Pt 21): p. 3873-82.
34. Douglas A. Lauffenburger, J.J.L., *Receptors: Modeling for Binding, Trafficking, and Signaling*. 1996, New York: Oxford University Press.
35. Campbell, J.J., et al., *Biology of chemokine and classical chemoattractant receptors: differential requirements for adhesion-triggering versus chemotactic responses in lymphoid cells*. J Cell Biol, 1996. **134**(1): p. 255-66.
36. Dominguez, G.A. and D.A. Hammer, *Effect of adhesion and chemokine presentation on T-lymphocyte haptokinesis*. Integr Biol (Camb), 2014. **6**(9): p. 862-73.
37. Farrell, B.E., R.P. Daniele, and D.A. Lauffenburger, *Quantitative relationships between single-cell and cell-population model parameters for chemosensory migration responses of alveolar macrophages to C5a*. Cell Motil Cytoskeleton, 1990. **16**(4): p. 279-93.

38. Dunn, G.A., *Characterising a kinesis response: time averaged measures of cell speed and directional persistence*. Agents Actions Suppl, 1983. **12**: p. 14-33.
39. Lauffenberger, D.A. and J.J. Linderman, *Receptors: Models for Binding, Trafficking, and Signaling*. 1993: Oxford University Press.
40. Quake, S.R. and A. Scherer, *From micro- to nanofabrication with soft materials*. Science, 2000. **290**(5496): p. 1536-40.
41. Xia, Y.N. and G.M. Whitesides, *Soft lithography*. Angewandte Chemie-International Edition, 1998. **37**(5): p. 550-575.
42. Regehr, K.J., et al., *Biological implications of polydimethylsiloxane-based microfluidic cell culture*. Lab Chip, 2009. **9**(15): p. 2132-9.
43. Ye, H., Z. Gu, and D.H. Gracias, *Kinetics of ultraviolet and plasma surface modification of poly(dimethylsiloxane) probed by sum frequency vibrational spectroscopy*. Langmuir, 2006. **22**(4): p. 1863-8.
44. Rogers, J.A. and R.G. Nuzzo, *Recent progress in soft lithography*. Materials Today, 2005. **8**(2): p. 50-56.
45. Desai, R.A., et al., *Subcellular spatial segregation of integrin subtypes by patterned multicomponent surfaces*. Integr Biol (Camb), 2011. **3**(5): p. 560-7.
46. Bussy, C., et al., *Intrinsic stiffness of the carotid arterial wall material in essential hypertensives*. Hypertension, 2000. **35**(5): p. 1049-54.
47. Kothapalli, D., et al., *Cardiovascular protection by ApoE and ApoE-HDL linked to suppression of ECM gene expression and arterial stiffening*. Cell Rep, 2012. **2**(5): p. 1259-71.

48. Paszek, M.J., et al., *Tensional homeostasis and the malignant phenotype*. *Cancer Cell*, 2005. **8**(3): p. 241-54.
49. Pelham, R.J., Jr. and Y. Wang, *Cell locomotion and focal adhesions are regulated by substrate flexibility*. *Proc Natl Acad Sci U S A*, 1997. **94**(25): p. 13661-5.
50. Engler, A.J., et al., *Surface probe measurements of the elasticity of sectioned tissue, thin gels and polyelectrolyte multilayer films: Correlations between substrate stiffness and cell adhesion*. *Surface Science*, 2004. **570**(1-2): p. 142-154.
51. Lo, C.M., et al., *Cell movement is guided by the rigidity of the substrate*. *Biophys J*, 2000. **79**(1): p. 144-52.
52. Wong, J.Y., et al., *Directed movement of vascular smooth muscle cells on gradient-compliant hydrogels*. *Langmuir*, 2003. **19**(5): p. 1908-1913.
53. Reinhart-King, C.A., M. Dembo, and D.A. Hammer, *Cell-cell mechanical communication through compliant substrates*. *Biophys J*, 2008. **95**(12): p. 6044-51.
54. Engler, A.J., et al., *Matrix elasticity directs stem cell lineage specification*. *Cell*, 2006. **126**(4): p. 677-89.
55. McBeath, R., et al., *Cell shape, cytoskeletal tension, and RhoA regulate stem cell lineage commitment*. *Dev Cell*, 2004. **6**(4): p. 483-95.
56. Jannat, R.A., et al., *Neutrophil adhesion and chemotaxis depend on substrate mechanics*. *J Phys Condens Matter*, 2010. **22**(19): p. 194117.
57. Jannat, R.A., M. Dembo, and D.A. Hammer, *Traction forces of neutrophils migrating on compliant substrates*. *Biophys J*, 2011. **101**(3): p. 575-84.
58. Weiss, P., *Cellular Dynamics*. *Reviews of Modern Physics*, 1959. **31**(1): p. 11-20.

59. Mudera, V.C., et al., *Molecular responses of human dermal fibroblasts to dual cues: contact guidance and mechanical load*. Cell Motil Cytoskeleton, 2000. **45**(1): p. 1-9.
60. Harris, A.K., P. Wild, and D. Stopak, *Silicone-Rubber Substrata - New Wrinkle in the Study of Cell Locomotion*. Science, 1980. **208**(4440): p. 177-179.
61. Lee, J., et al., *Traction forces generated by locomoting keratocytes*. J Cell Biol, 1994. **127**(6 Pt 2): p. 1957-64.
62. Burton, K., J.H. Park, and D.L. Taylor, *Keratocytes generate traction forces in two phases*. Mol Biol Cell, 1999. **10**(11): p. 3745-69.
63. Pless, D.D., et al., *Specific cell adhesion to immobilized glycoproteins demonstrated using new reagents for protein and glycoprotein immobilization*. J Biol Chem, 1983. **258**(4): p. 2340-9.
64. Damljjanovic, V., B.C. Lagerholm, and K. Jacobson, *Bulk and micropatterned conjugation of extracellular matrix proteins to characterized polyacrylamide substrates for cell mechanotransduction assays*. Biotechniques, 2005. **39**(6): p. 847-51.
65. Dembo, M. and Y.L. Wang, *Stresses at the cell-to-substrate interface during locomotion of fibroblasts*. Biophys J, 1999. **76**(4): p. 2307-16.
66. Dembo, M., et al., *Imaging the traction stresses exerted by locomoting cells with the elastic substratum method*. Biophys J, 1996. **70**(4): p. 2008-22.
67. Boudou, T., et al., *Nonlinear elastic properties of polyacrylamide gels: implications for quantification of cellular forces*. Biorheology, 2009. **46**(3): p. 191-205.

68. Munevar, S., Y. Wang, and M. Dembo, *Traction force microscopy of migrating normal and H-ras transformed 3T3 fibroblasts*. Biophys J, 2001. **80**(4): p. 1744-57.
69. Reinhart-King, C.A., M. Dembo, and D.A. Hammer, *The dynamics and mechanics of endothelial cell spreading*. Biophys J, 2005. **89**(1): p. 676-89.
70. Smith, L.A., et al., *Neutrophil traction stresses are concentrated in the uropod during migration*. Biophys J, 2007. **92**(7): p. L58-60.
71. Kraning-Rush, C.M., J.P. Califano, and C.A. Reinhart-King, *Cellular traction stresses increase with increasing metastatic potential*. PLoS One, 2012. **7**(2): p. e32572.
72. Dembo, M., *The LIBTRC User's Guide for Version 2.4*. 2010, Boston.
73. Sabass, B., et al., *High resolution traction force microscopy based on experimental and computational advances*. Biophys J, 2008. **94**(1): p. 207-20.
74. Balaban, N.Q., et al., *Force and focal adhesion assembly: a close relationship studied using elastic micropatterned substrates*. Nat Cell Biol, 2001. **3**(5): p. 466-72.
75. Merkel, R., et al., *Cell force microscopy on elastic layers of finite thickness*. Biophys J, 2007. **93**(9): p. 3314-23.
76. Long, R., et al., *Effects of gel thickness on microscopic indentation measurements of gel modulus*. Biophys J, 2011. **101**(3): p. 643-50.
77. Stricker, J., et al., *Optimization of traction force microscopy for micron-sized focal adhesions*. J Phys Condens Matter, 2010. **22**(19): p. 194104.

78. Rape, A.D., W.H. Guo, and Y.L. Wang, *The regulation of traction force in relation to cell shape and focal adhesions*. *Biomaterials*, 2011. **32**(8): p. 2043-51.
79. Galbraith, C.G. and M.P. Sheetz, *A micromachined device provides a new bend on fibroblast traction forces*. *Proc Natl Acad Sci U S A*, 1997. **94**(17): p. 9114-8.
80. Prass, M., et al., *Direct measurement of the lamellipodial protrusive force in a migrating cell*. *J Cell Biol*, 2006. **174**(6): p. 767-72.
81. Tan, J.L., et al., *Cells lying on a bed of microneedles: an approach to isolate mechanical force*. *Proc Natl Acad Sci U S A*, 2003. **100**(4): p. 1484-9.
82. du Roure, O., et al., *Force mapping in epithelial cell migration*. *Proc Natl Acad Sci U S A*, 2005. **102**(7): p. 2390-5.
83. Yang, M.T., et al., *Assaying stem cell mechanobiology on microfabricated elastomeric substrates with geometrically modulated rigidity*. *Nat Protoc*, 2011. **6**(2): p. 187-213.
84. Tymchenko, N., et al., *A novel cell force sensor for quantification of traction during cell spreading and contact guidance*. *Biophys J*, 2007. **93**(1): p. 335-45.
85. Ricart, B.G., et al., *Measuring traction forces of motile dendritic cells on micropost arrays*. *Biophys J*, 2011. **101**(11): p. 2620-8.
86. Rabodzey, A., et al., *Mechanical forces induced by the transendothelial migration of human neutrophils*. *Biophys J*, 2008. **95**(3): p. 1428-38.
87. Cass, A.S. and M. Luxenberg, *Testicular injuries*. *Urology*, 1991. **37**(6): p. 528-30.
88. Hur, S.S., et al., *Live Cells Exert 3-Dimensional Traction Forces on Their Substrata*. *Cell Mol Bioeng*, 2009. **2**(3): p. 425-436.

89. Maskarinec, S.A., et al., *Quantifying cellular traction forces in three dimensions*. Proc Natl Acad Sci U S A, 2009. **106**(52): p. 22108-13.
90. Cukierman, E., R. Pankov, and K.M. Yamada, *Cell interactions with three-dimensional matrices*. Curr Opin Cell Biol, 2002. **14**(5): p. 633-9.
91. Cukierman, E., et al., *Taking cell-matrix adhesions to the third dimension*. Science, 2001. **294**(5547): p. 1708-12.
92. Van Goethem, E., et al., *Macrophage podosomes go 3D*. Eur J Cell Biol, 2011. **90**(2-3): p. 224-36.
93. Legant, W.R., et al., *Measurement of mechanical tractions exerted by cells in three-dimensional matrices*. Nat Methods, 2010. **7**(12): p. 969-71.
94. Franck, C., et al., *Three-dimensional traction force microscopy: a new tool for quantifying cell-matrix interactions*. PLoS One, 2011. **6**(3): p. e17833.

CHAPTER 3: MACROPHAGE CHEMOKINESIS ON MICROCONTACT PRINTED PDMS SUBSTRATES

Adapted from: Hind LE, MacKay JL, Cox D, and Hammer DA “Two-dimensional motility of a macrophage cell line on microcontact-printed fibronectin.” *Cytoskeleton* (Hoboken). 2014 Sep; 71 (9): 542-54. Reproduced by permission of John Wiley and Sons.

ABSTRACT

The ability of macrophages to migrate to sites of infection and inflammation is critical for their role in the innate immune response. Macrophage cell lines have made it possible to study the roles of individual proteins responsible for migration using molecular biology, but it has not been possible to reliably elicit the motility of macrophage cell lines in two-dimensions. In the past, measurements of the motility of macrophage cell lines have been largely limited to transwell assays which provide limited quantitative information on motility and limited ability to visualize cell morphology. We used microcontact printing to create polydimethylsiloxane (PDMS) surfaces functionalized with fibronectin that otherwise support little macrophage adhesion. We used these surfaces to measure macrophage migration in two-dimensions and found that

these cells migrate efficiently in a uniform field of colony-stimulating factor-1, CSF-1. Knockdown of Cdc42 led to a non-statistically significant reduction in motility, whereas chemical inhibition of PI3K activity led to a complete loss of motility. Inhibition of the RhoA kinase, ROCK, did not abolish the motility of these cells but caused a quantitative change in motility, reducing motility significantly on high concentrations of fibronectin but not on low concentrations. This study illustrates the importance of studying cell motility on well controlled materials to better understand the exact roles of specific proteins on macrophage migration.

INTRODUCTION

Macrophages are highly motile cells of the monocytic lineage and are important in a variety of biological processes including innate immunity, development, and disease [1]. During the innate immune response, macrophages must move quickly and efficiently to sites of infection or inflammation in order to clear the site of pathogens and release cytokines [2]. In order to do this, macrophages move towards cytokine signals released by inflamed tissue, such as macrophage colony stimulating factor-1 (CSF-1 also known as M-CSF1). M-CSF1 signals the cell through the CSF-1 receptor, a tyrosine kinase receptor, which dimerizes and autophosphorylates upon ligand-binding [3]. In addition to cytokine signals, macrophage migration is regulated by proteins of the extracellular matrix (ECM) such as fibronectin and collagen through integrin-binding interactions. Signaling downstream of both the M-CSF1 receptor and integrins is controlled by a variety of proteins including several members of the Rho GTPase family as well as cytoskeletal proteins [4-6]. When properly regulated, macrophage motility is critical to maintain homeostasis, but improper regulation of this migration can lead to a progression of diseases such as cancer, rheumatoid arthritis, and atherosclerosis [1]. For example, tumor associated macrophages have been associated with a poor prognosis in several types of cancer and are often associated with high levels of metastasis and solid tumor angiogenesis [7].

Macrophages, like other leukocytes, employ amoeboid migration. Macrophages do not form strong focal contacts to the substratum but rather create short-lived weak adhesions that allow them to move quickly through their environment [2]. These

adhesions may involve the formation of podosomes, which are comprised of actin-rich cores surrounded by rings of adhesion proteins such as vinculin [8]. Podosomes are known to function in matrix remodeling and degradation, and many of the same proteins found in functional podosomes are critical for macrophage migration; however, no direct link has been found between podosomes and macrophage migration [9]. It is crucial that we understand how macrophages move through their environments and how this movement is coordinated.

Immortalized macrophage cell lines, such as the subline of RAW264.7 (RAW/LR5) cell line, are invaluable tools for studying the specific role of various proteins because of the ability to change their proteomics through molecular biology. In the past, the motility of these cells has been investigated using transwell chambers [9] and ruffling assays [10], but analysis of their 2D migration on specific extracellular matrix (ECM) proteins has not been possible. On most surfaces normally employed to study 2D motility, such as tissue culture plastic and glass, the cells polarize but do not crawl, making studies of directional motility in 2D impossible on those materials. Given the numerous mutants of RAW/LR5 cells that have been created, a means to effectively elicit and measure the 2D motility of these cells would allow us to better understand how motility in macrophages is controlled molecularly.

We used microcontact printing to prepare surfaces specifically coated with fibronectin and quantified the motility of RAW/LR5 macrophages undergoing chemokinesis. Previously, our laboratory showed that microcontact printing fibronectin allowed elucidation of the mechanisms of neutrophil motility [11]. With RAW/LR5 cells, we found that these materials elicit robust migration, which we attribute to the effective

blocking of non-specific adhesion on these materials. We then used these surfaces to compare the migration of wild-type RAW/LR5 cells to the migration of RAW/LR5 cells with chemically inhibited ROCK or PI3K and of RAW/LR5 cells with reduced endogenous levels of the GTPase Cdc42. Cells without PI3K activity lost their ability to polarize and showed no migratory capabilities. Cells with reduced Cdc42 levels showed no significant change in motility compared to wild type RAW/LR5 macrophages, but showed increased ruffling behavior. Finally, cells in which ROCK signaling was inhibited were highly sensitive to fibronectin concentration showing two different motile phenotypes with correspondingly different random motility coefficients on high versus low concentrations of fibronectin, with motility most significantly reduced on high concentrations of fibronectin. These results illustrate the importance of studying cell motility on well defined surfaces and allow us to realize the potential of these modified cell lines for the study of the molecular mechanisms of macrophage migration.

MATERIALS AND METHODS

Reagents

Bovine fibronectin was obtained from Sigma (St. Louis, MO) and recombinant murine CSF-1 was obtained from PeproTech (Rocky Hill, NJ). We used the inhibitors LY294002 at 50 μ M from Cell Signaling (Boston, MA), Wortmannin at 10 μ M from Sigma (St. Louis, MO), and Y27632 at 10 μ M from Millipore (Billerica, MA).

Cell Culture

The RAW/LR5 and RAW/LR5 shCdc42 cell lines have been previously characterized and were obtained from Dianne Cox's lab (Albert Einstein College of Medicine, Bronx, NY) [12, 13]. Murine bone marrow derived macrophages (BMMs) were isolated and prepared according to [13]. The RAW/LR5 LifeAct-mCherry cell line was created by retroviral transduction using the vector pTK93_Lifeact-mCherry (Addgene plasmid 46357), which was generously deposited by Dr. Iain Cheeseman. Retrovirus was packaged using 293T cells, purified by ultracentrifugation, and tittered by flow cytometry as previously described [14]. RAW/LR5 cells were infected at a multiplicity of infection of 0.25 and treated with 3 μ g/ml puromycin for 6 days to select for transduced cells. All cells were cultured in supplemented RPMI medium containing 10% heat-inactivated fetal bovine serum (Sigma, St. Louis, MO) and 1% penicillin-streptomycin (MediaTech, Manassas, VA). All cells were maintained at 37°C and 5% CO₂.

PDMS Microcontact Printing of Fibronectin

Poly(dimethyl siloxane) (Dow Corning, Midland, MI) or PDMS was made at a 10:1 ratio of polymer to cross-linker. Round glass 25 mm coverslips were cleaned in 0.2N hydrochloric acid and then rinsed twice with Milli-Q water and once with 99% ethanol. Coverslips were dried with pressurized N₂. The coverslips were then spincoated with PDMS using the Laurell Spinner (4000 rpm, 1 minute). Coverslips were allowed to cure for 1 hour in a 62°C oven. To generate stamps, flat PDMS was cured against a silicon wafer to ensure a uniform topology. Small 1cm² cubes were then cut from the PDMS block. The stamps were inked with fibronectin (Sigma, St. Louis, MO). The PDMS spincoated coverslips to be stamped were then treated with UV ozone for 7 minutes to create a hydrophilic surface for optimal protein transfer. The stamps were washed with water and carefully dried with pressurized N₂. The stamps were then placed on coverslips prepared under UV ozone, and protein transfer occurred almost immediately. The stamps were then removed, and the stamped coverslips were blocked with 0.2% Pluronic-F127 (Sigma, St. Louis, MO) for 30 minutes. The coverslips were rinsed 3x with 1xPBS and incubated in PBS overnight [15].

Chemokinesis Assay

Stamped coverslips were attached to a 6-well plate for chemokinesis experiments. Cells were plated in each well at 4.2x10⁴ cells/mL. Cells were incubated overnight in RPMI supplemented with 1% fetal bovine serum (Sigma, St. Louis, MO) and 1% penicillin-streptomycin. After incubation, the cells were washed with RPMI to remove any unattached cells. Chemokinesis media consisted of serum-free RPMI supplemented

with the indicated concentration of CSF-1 (PeproTech, Rocky Hill, NJ). Using a custom-built LabView (Texas Instruments, Austin, TX) software, 24 fields of view were imaged at 20x magnification by phase microscopy on a Nikon Eclipse TE300 (Nikon, Melville, NY). Images were captured every two minutes for four hours using time-lapse microscopy. Cell trajectories were captured using the ImageJ Manual Tracking plugin. Chemokinesis parameters were calculated using a custom written MATLAB (Mathworks, Natick, MA) script which fits the speed (S) and persistence time (P) to the Dunn Equation:[16] $\langle d^2 \rangle = nS^2[Pt - P^2(1 - e^{-t/P})]$. The random motility coefficient is a relative diffusion coefficient for the cells in a uniform chemokine field. The random motility coefficient, μ , is calculated using the fit parameters in the following equation, $\mu = \frac{1}{n}S^2P$.

Chemical Inhibition

Pharmacological inhibition of cells, if any, was performed by pre-incubation of cells with inhibitor for 1 hour at the designated concentration before the experiment and continued incubation at the same concentration during the experiment.

Immunofluorescence

Cells were fixed for 7 minutes in 3.7% paraformaldehyde and permeabilized for 4 minutes in 0.1% Triton X-100. Actin was detected using Phalloidin coupled to Alexa-Fluor 568 (Invitrogen, Carlsbad, CA). Vinculin was detected using the monoclonal antibody hVIN1 (ab11194, Abcam, Cambridge, UK). The secondary antibody used was

Alexa-Fluor-488-labeled goat anti-mouse (Invitrogen, Carlsbad, CA). Coverslips were mounted using Fluoromount G (SouthernBiotech, Birmingham, AL) as an anti-fading reagent.

Images of fixed samples were acquired with a confocal microscope (Leica SP5) equipped with a 63x oil objective. Images were processed using the Leica Application Suite (Leica, Wetzlar, Germany) and ImageJ software.

RESULTS

Microcontact Printing of Fibronectin

Microcontact printing was used to prepare the surfaces for all experiments described in this chapter. A schematic overview of the printing technique is shown in Figure 3.1. A flat 1 cm² polydimethylsiloxane (PDMS) stamp was incubated with a specific concentration of the ECM protein fibronectin. Separately, a glass coverslip was spin-coated with a thin layer of PDMS. This PDMS-coated coverslip was then treated with UV ozone to render the surface hydrophilic. Excess protein was removed from the stamp by carefully washing it with water and the stamp was dried with pressurized nitrogen gas. The dry, hydrophobic stamp was then brought into contact with the hydrophilic surface and the protein preferentially transferred to the surface. Finally, the surface was blocked with the polymer Pluronic-F127, which binds to unreacted groups on the PDMS, functionally blocking the surface. Stamping PDMS offers many advantages over traditional techniques for creating molecularly coated surfaces for imaging cell motility in two dimensions. First, the stamping method allows for precise spatial control of a protein ligand, as illustrated with fluorescently-tagged fibronectin in Figure 3.1B. The ligand is also allowed to bind uniformly across the surface because it is transferred from a hydrophobic inked surface to a hydrophilic surface [15]. PDMS is also convenient for imaging because it is transparent to optical wavelengths [17].

We first stamped PDMS with fluorescently labeled fibronectin and then blocked the surfaces with either 0.2% Pluronic-F127 (Figure 3.1D) or 1% bovine serum albumin (Figure 3.1C) to illustrate the fidelity of the stamping method and the importance of

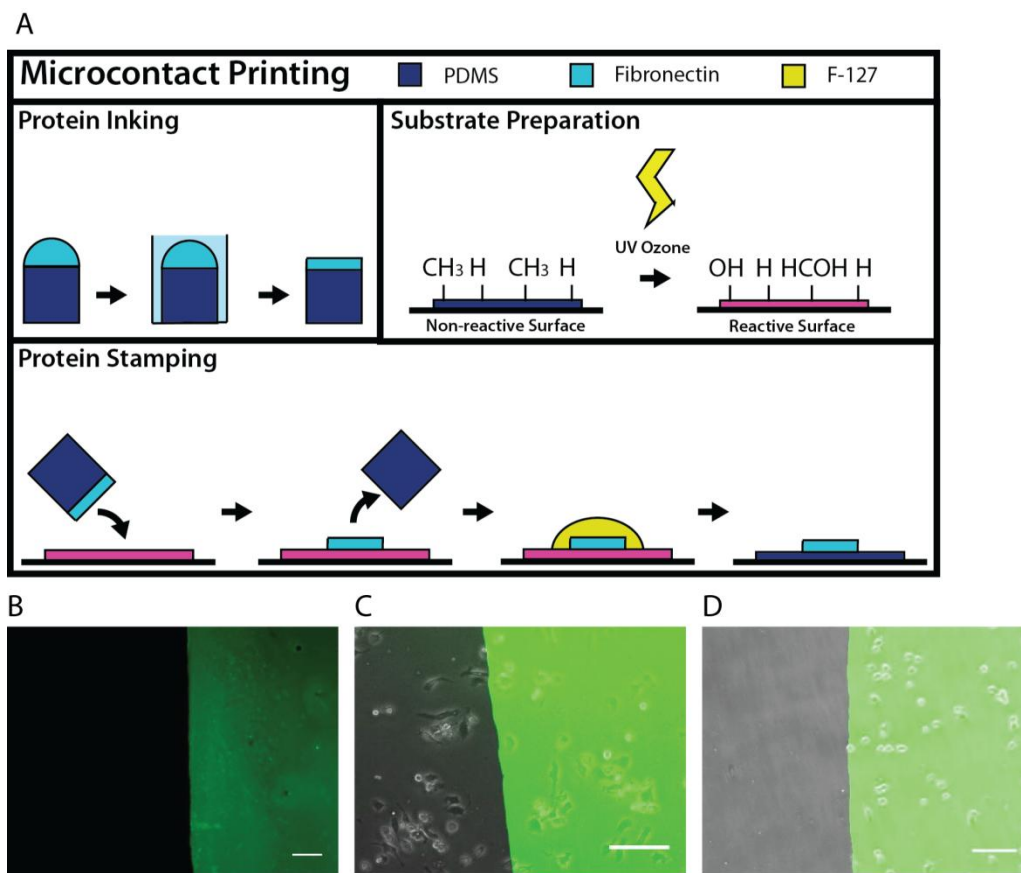


Figure 3.1. Microcontact-printing of fibronectin on PDMS. (A) Schematic representation of stamping process used to prepare surfaces for motility experiments. (B) PDMS surface stamped with fluorescently-tagged fibronectin. (C) PDMS surface stamped with FITC-tagged fibronectin and blocked with BSA. (D) PDMS surface stamped with FITC-fibronectin and blocked with Pluronic-F127. In (C) and (D) cells were allowed to adhere to stamped and blocked surfaces for 2 hours prior to imaging. Scale bar indicates 50 μm .

functionally blocking the surface. In Figure 3.1D, the cells only adhere to the surface on the fibronectin-patterned area, indicated by the fluorescent signal associated with fibronectin. The cells did not interact with the surface blocked solely with pluronics, indicating that cells do not bind to the polymer; therefore, all RAW/LR5 motility is due to binding interactions with fibronectin. Conversely, in Figure 3.1C, when surfaces are blocked with BSA, cells adhere to the surface on both the patterned and unpatterned regions indicating that the cells are interacting with the blocking protein (BSA), and the motile behaviors seen by these cells are not specific to their interaction with the fibronectin ligand. This result is consistent with our recently published observations on the motility of neutrophils on PDMS substrates which showed that BSA, normally thought of as a blocking protein, acts as a ligand for Mac-1 [11]. Our ability to functionally block the PDMS surface offers a distinct advantage over glass or tissue culture plastic, to which pluronics does not bind [18], because it ensures that cell response is due to cell-ligand interactions and not unintended or non-specific cell-surface interactions.

We assessed if RAW/LR5 macrophages would form structures such as podosomes on the microcontact printed surfaces. To visualize molecular organization at the cell-substrate interface, RAW/LR5 macrophages cells were seeded on fibronectin-printed PDMS surfaces blocked with Pluronic-F127, then fixed and stained for F-actin (Figure 3.2B) and vinculin (Figure 3.2C). The RAW/LR5 macrophages showed small punctate F-actin clusters surrounded by vinculin rings, indicative of podosomes. When these stained images are overlaid (Figure 3.2A), typical podosome structures are easily

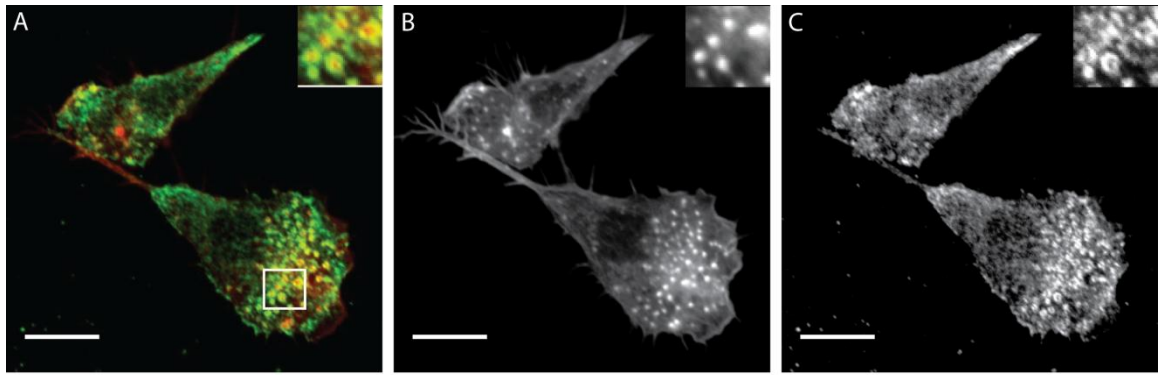


Figure 3.2. Adhesion staining of RAW/LR5 macrophages on PDMS surfaces coated with fibronectin. (A) Merged image of actin and vinculin stains show podosomes. Area of inlay indicated by white box at leading edge of cells. (B) Phalloidin staining shows punctate actin. (C) hVIN1 staining shows rings of vinculin.

recognizable at the leading edge of polarized cells. We further investigated podosome dynamics in motile macrophages using live imaging of the RAW/LR5 mCherry-LifeAct cell line. Cells were imaged in phase to confirm normal motility and in fluorescence to observe actin dynamics. Podosomes are highly active at the leading edge of motile macrophages. When a bifurcation of the leading pseudopod occurs, podosomes appear in both extensions until the leading edge is re-established and podosomes in the rear of the cell are disassembled. This indicates that podosomes are only stable at the leading edge of the cell, suggesting that they are involved in the directional sensing of the cell. We concluded that this method of preparing surfaces is optimal for analyzing two-dimensional migration of RAW/LR5 macrophages. Because cell-substrate interactions are clearly defined, cells retained their ability to form podosomes, and cells were motile.

RAW/LR5 Chemokinesis on Fibronectin-Printed PDMS

Two-dimensional migration of RAW/LR5 macrophages on a clearly defined surface has not been previously described; therefore, migration parameters such as speed, persistence time, and the random motility coefficients for this cell line have not previously been elucidated. Analysis of two-dimensional migration would allow us to determine the type of migration used by RAW/LR5 macrophages and how their migration compares to other ameboid and mesenchymal cells. In one experiment, RAW/LR5 macrophages were seeded on PDMS printed with various concentrations of fibronectin and exposed to a uniform concentration, 20 ng/mL, of the chemokine CSF-1. In a second experiment, cells were seeded on PDMS printed with a uniform concentration

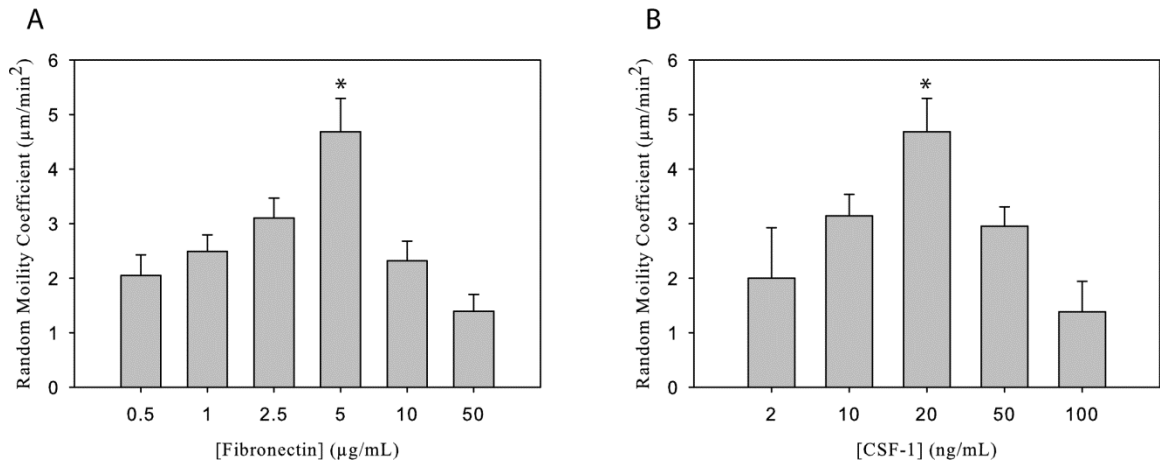


Figure 3.3. Biphastic motility of RAW/LR5 macrophages. (A) Random motility coefficient versus fibronectin concentration shows biphastic motility of macrophages with increasing surface ligand density. (n = 7 experiments; an average of 447±39 cells per condition). (B) Random motility coefficient as a function of CSF-1 concentration shows biphastic motility of macrophages with increasing soluble chemokine. (n = 4 experiments; an average of 246±97 cells per condition). Error bars are standard error, * indicates p < 0.05.

of fibronectin, 5 $\mu\text{g}/\text{mL}$, and exposed to various concentrations of the soluble chemokine CSF-1. RAW/LR5 cells were able to efficiently migrate on fibronectin stamped PDMS, and the random motility coefficient, a relative diffusion coefficient of migrating cells, showed biphasic motility as a function of the concentration of fibronectin (Figure 3.3A), and the concentration of soluble chemokine, CSF-1 (Figure 3.3B). Murine bone marrow derived macrophages (BMMs) were also able to migrate efficiently on PDMS printed with fibronectin and their motility was biphasic as a function of fibronectin concentration with peak motility at 2.5 $\mu\text{g}/\text{mL}$ (Figure 3.4). This result proves that 2D migration of both macrophage cell lines and primary cells is supported by the PDMS printing technique outlined in this chapter. The effect of ligand density on cell migration is commonly seen, because a low concentration of ligand does not provide sufficient traction and a high concentration of ligand makes cells too adhesive [19]. The effect of soluble chemoattractant concentration on migration is also expected to be biphasic, since low concentrations of ligand do not provide sufficient signal and high ligand concentrations overwhelm the cell's signaling pathway, leading to lower response to the signal [20]. The peak concentration of CSF-1 for motility is consistent with the values reported previously for these cells [12]. Plots showing the dispersion of cells were created (Figure 3.5A) for all conditions by tracking each cell and moving the start of each cell track to the origin of the axis. These plots show qualitatively that at high and low concentrations of fibronectin, the RAW/LR5 macrophages migrate to a lesser extent than they do on a moderate fibronectin concentration. The plots also confirm that migration of these cells was random with no bias in one direction. The mean-squared displacement of the cells

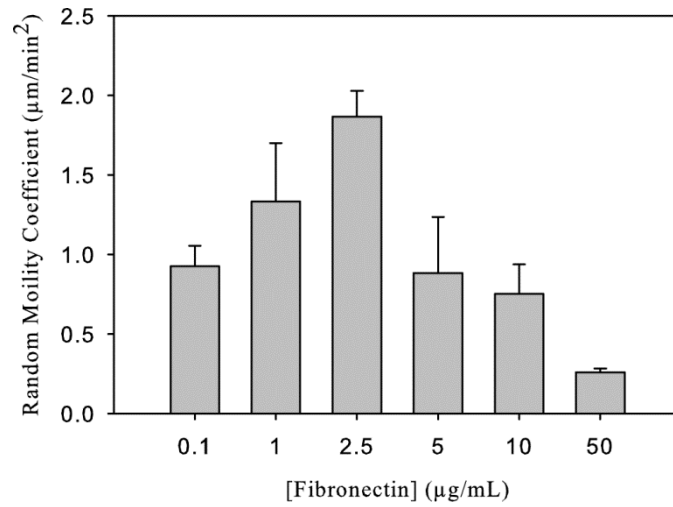


Figure 3.4. Biphasic motility of murine bone-marrow derived macrophages (BMMs).

Random motility versus fibronectin concentration shows biphasic motility of BMMs with increasing surface ligand density.

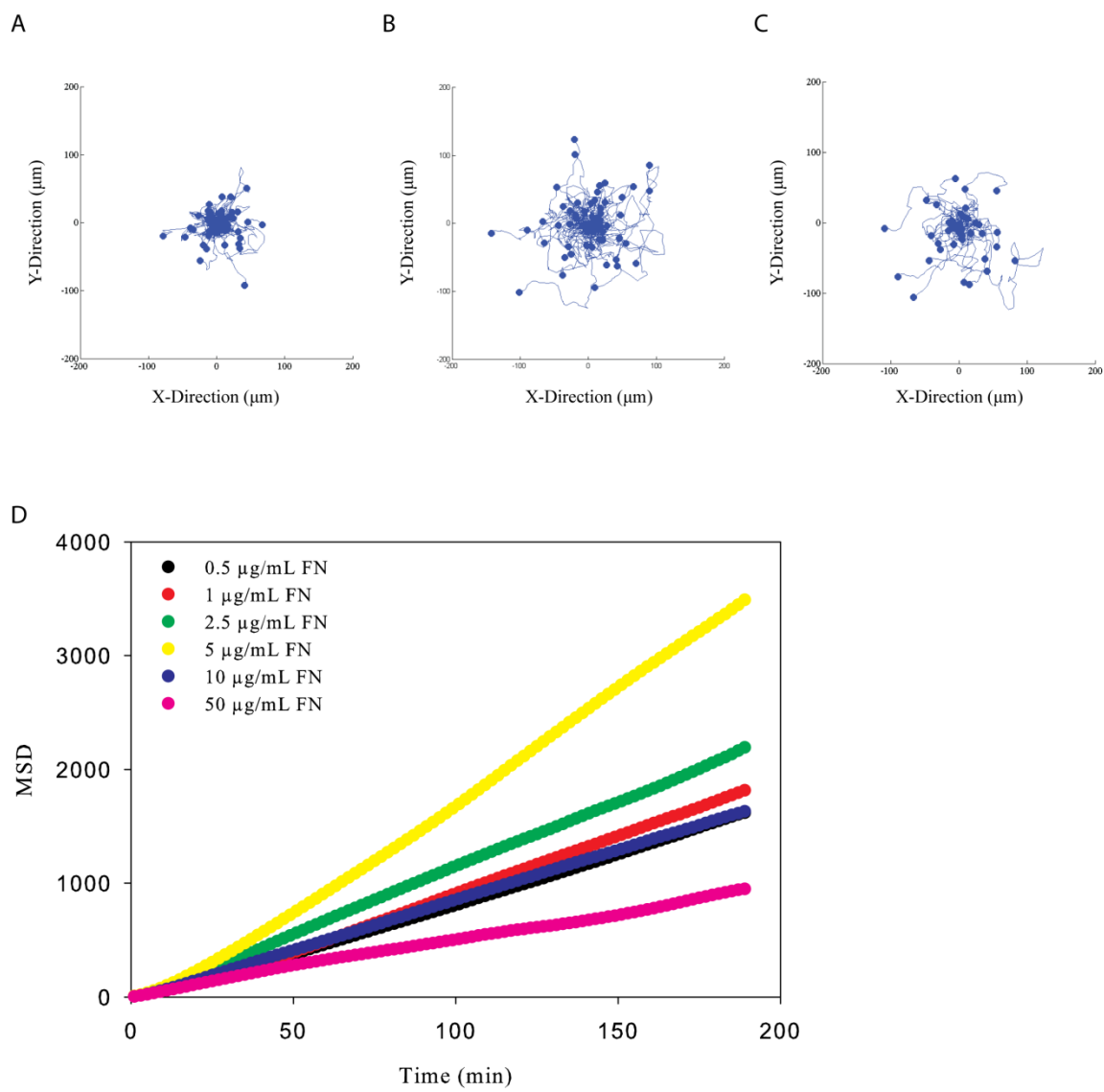


Figure 3.5. RAW/LR5 macrophage motility on PDMS surfaces coated with fibronectin. (A) Dispersion of RAW/LR5 macrophages migrating on 0.5 µg/mL fibronectin. (B) Dispersion of RAW/LR5 macrophages migrating on 5 µg/mL fibronectin shows increased total migration. (C) Dispersion of RAW/LR5 macrophages migrating on 50 µg/mL fibronectin. (D) Mean Squared Displacement versus time on all concentrations of fibronectin.

on each fibronectin concentration was plotted versus time (Figure 3.5B) and this plot was used to fit the speed and persistence time of the cells using the Dunn equation. At all fibronectin concentrations α was found to be nearly one, indicating that RAW/LR5 macrophage chemokinesis is well-defined by the random walk model (Table 3.1).

RAW/LR5 Chemokinesis with Leading Edge Inhibition

Several proteins are known to be important in the migration of cells, and the RAW/LR5 cells provide a unique opportunity to study how these molecules might affect macrophage motility on surfaces that have been printed with fibronectin. Many of these proteins locate specifically to the leading edge of the cell during migration and are responsible for actin polymerization, as well as maintenance of cell polarity and signaling downstream of integrin-fibronectin and chemokine-receptor signaling. We measured the motility of a RAW/LR5 derived cell line with reduced endogenous levels of the GTPase Cdc42. These cells were created using short-hairpin RNAi which led to a greater than 65% reduction in Cdc42 levels [13]. The shCdc42 cells qualitatively showed biphasic motility as a function of fibronectin concentration, much like the wild type RAW/LR5 cells, but there was no significant difference seen in the random motility at any fibronectin concentration (Figure 3.6A). The shCdc42 cells showed a non-statistically significant reduction in motility at each fibronectin concentration compared to the wild type cells but they were still able to efficiently migrate on the printed surfaces. These results indicate that Cdc42 is not required for efficient migration of RAW/LR5 macrophages but might have some contribution downstream of integrin-fibronectin

Table 3.1: Alpha Values for RAW/LR5 Macrophages on Varying Concentrations of Fibronectin.

[Fibronectin] ($\mu\text{g/mL}$)	α
50	0.9831
10	1.1089
5	1.2295
2.5	1.1096
1	1.1848
0.5	1.1264

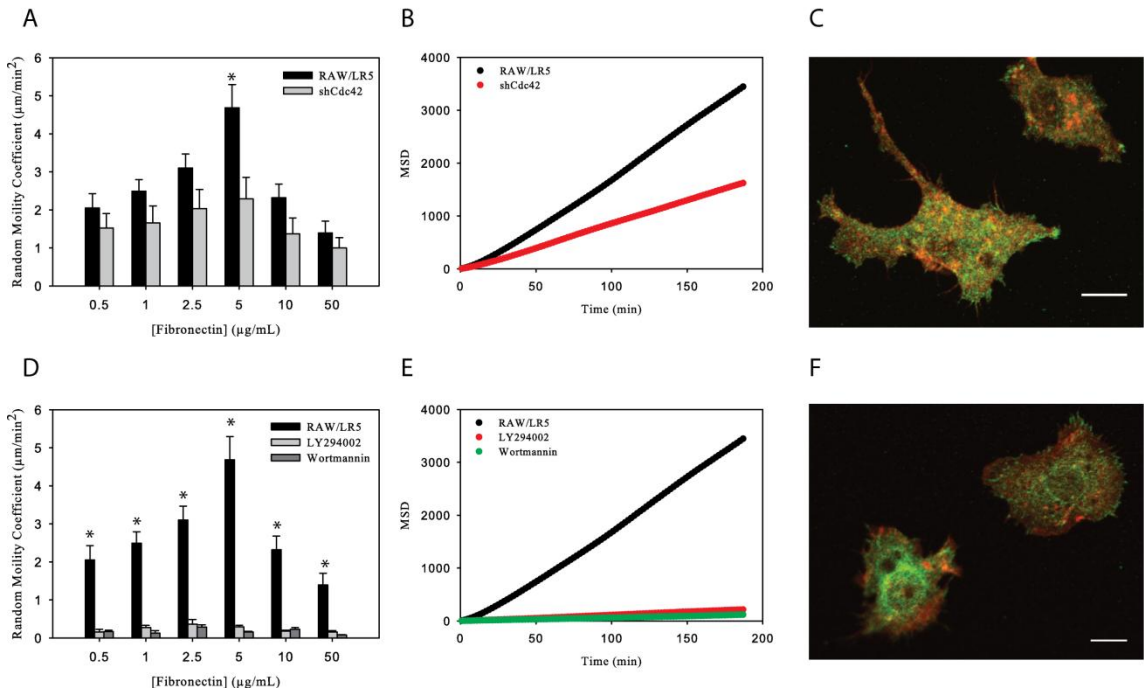


Figure 3.6. Motility of RAW/LR5 cells with reduced endogenous Cdc42 and chemically inhibited PI3K. (A) Random motility coefficients of wild type RAW/LR5 macrophages and shCdc42 cells on increasing concentrations of fibronectin. (n = 11 experiments; an average of 588 ± 53 cells per condition). (B) Mean Squared Displacement versus time for RAW/LR5 and shCdc42 cells. (C) Staining of shCdc42 cells plated on $5 \mu\text{g/mL}$ fibronectin; actin (red) and vinculin (green). (D) Random motility coefficients of wild type RAW/LR5 macrophages and macrophages chemically inhibited with LY294002 and Wortmannin to reduce PI3K signaling. (n = 5 experiments; an average of 237 ± 30 cells per condition). (E) Mean squared displacement versus time for RAW/LR5 cells and cells chemically inhibited with LY294002 and Wortmannin. (F) Staining of RAW/LR5

macrophages plated on 5 μ g/mL fibronectin and chemically inhibited with LY294002; actin (red) and vinculin (green). Error bars are standard error, * indicates $p < 0.05$.

binding. It is possible that the remaining Cdc42 in the knockdown cells provides sufficient signaling to maintain motility; however, it has been previously shown that the same cell line has reduced motility to the chemokine, CX3CL1 [10]. The mean squared displacement was plotted as a function of time (Figure 3.6B), and the speed and persistence time for shCdc42 cells using the Dunn equation. The fit of the mean squared displacement yielded an α of 1.14, so the random migration is well-modeled as a persistent random walk. These cells were also stained for adhesion structures to determine if podosomes were present (Figure 3.6C). Consistent with previously published results [9], the shCdc42 cells have actin-mediated protrusion, but do not show any of the hallmark structures of podosomes such as punctate actin bundles or vinculin rings. This data suggests that in the RAW/LR5 cells, Cdc42 is required for podosome formation but that podosomes are not necessary for efficient random migration.

We further investigated the effect of leading edge inhibition by targeting another protein, phosphoinositide 3-kinase (PI3K), which acts upstream in the signaling pathway from Cdc42. We inhibited this protein using two different chemical inhibitors, LY294002 and Wortmannin, and studied the migratory capacity of inhibited cells. We found that the use of either chemical inhibitor led to the complete loss of cell motility (Figure 3.6D). Under inhibition of PI3K, cells did not polarize to the same degree as uninhibited cells or migrate efficiently. The plot of mean squared displacement versus time (Figure 3.6E) further illustrates that these cells show minimal displacement over time for cells inhibited with either chemical inhibitor. Loss of PI3K activity also led to a disorganized cytoskeleton and the loss of podosomal structures seen in wild type cells (Figure 3.6F). In the inhibited cells, actin and vinculin remain cytoplasmic with no

polarized distribution or organization. These data together indicate that PI3K is necessary for migration of RAW/LR5 macrophages and formation of podosome adhesion structures.

RAW/LR5 Chemokinesis with Cell Contraction Inhibition

The trailing edges of migrating cells rely on myosin II contraction to release the rear of the cell from the substratum and allow the cell to advance forward. Several proteins are important in myosin contraction. RhoA is the Rho family protein primarily involved in myosin contractility and it stimulates this contractility through the RhoA kinase, ROCK. ROCK has been linked to the motility of many different cell types [21] and we wanted to determine its role in RAW/LR5 migration. The ROCK inhibitor Y-27632 was used at 10 μ M to abolish ROCK activity and myosin II contraction in migrating RAW/LR5 macrophages. In contrast to the biphasic motility seen in uninhibited macrophages, RAW/LR5 cells treated with the ROCK inhibitor showed a switch-like change in their random motility coefficient over a range of fibronectin concentrations (Figure 3.7A). At high concentrations of fibronectin, 50 μ g/mL and 10 μ g/mL, cells inhibited with Y-27632 had a low but constant random motility coefficient. However, at fibronectin concentrations lower than 10 μ g/mL, cells inhibited with Y-27632 had a higher and constant random motility coefficient similar to control treated cells. Under inhibition, the random motility coefficients at lower concentrations of fibronectin were not significantly different than each other but they were all significantly higher than the random motility coefficients at higher concentrations of fibronectin. This

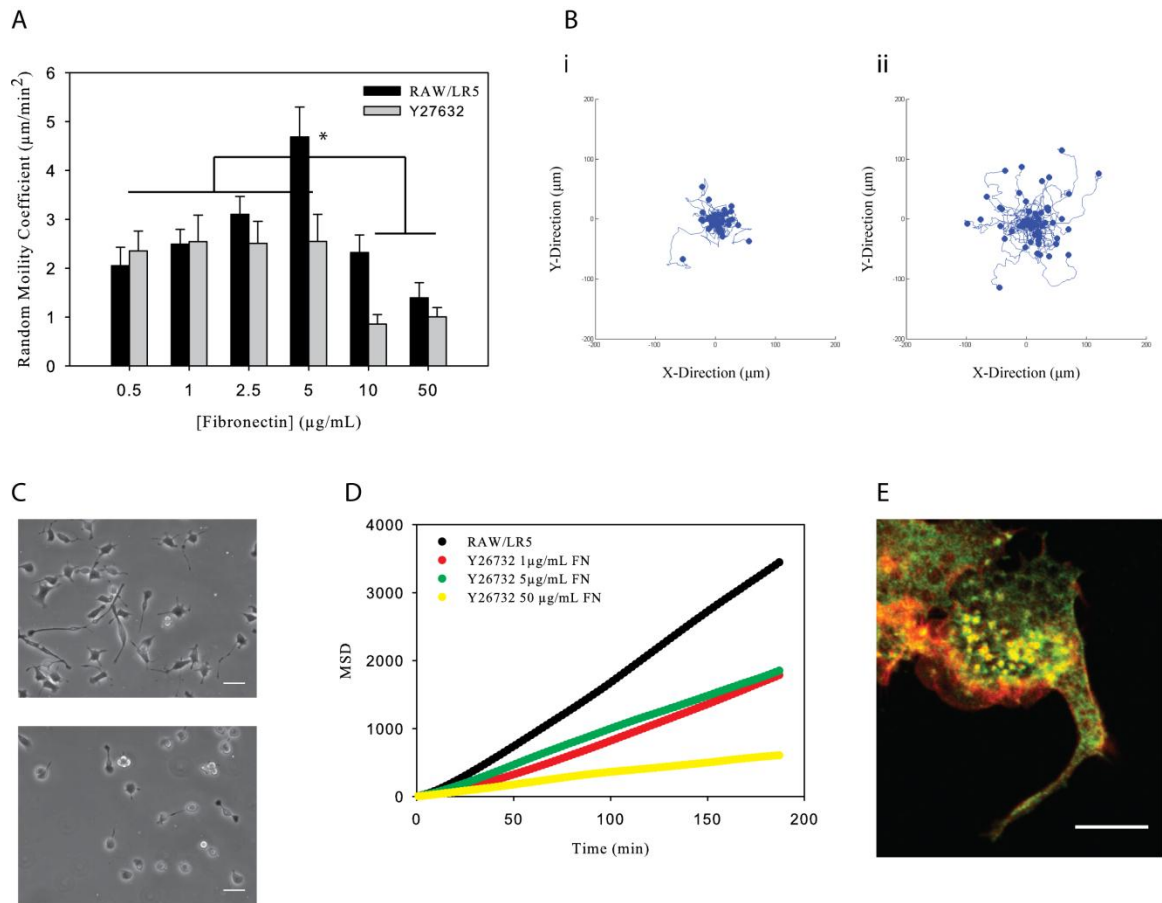


Figure 3.7. Migration of RAW/LR5 macrophages with inhibited ROCK signaling. (A) Random motility coefficient of RAW/LR5 macrophages and macrophages inhibited with 10 μM Y27632 as a function of fibronectin concentration. (n = 9 experiments; an average of 501 ± 28 cells per condition). (B) Dispersion plots for RAW/LR5 macrophages plated on (i) 50 μg/mL fibronectin and (ii) 2.5 μg/mL fibronectin and inhibited with Y27632. (C) Phase images of RAW/LR5 macrophages plated on 50 μg/mL fibronectin (top) show long unretracted tails and on 1 μg/mL fibronectin (bottom) show rounded morphology. Scale Bar = 100 μm. (D) Mean Squared Displacement versus time for wild type macrophages and macrophages inhibited with Y27632 on 1 μg/mL, 5 μg/mL, and 50 μg/mL fibronectin. (E) Staining of RAW/LR5 macrophage plated on 5 μg/mL

fibronectin and inhibited with 10 μ M Y27632 show podosomes at the leading edge of the cell; actin (red) and vinculin (green). Error bars are standard error. * indicates $p < 0.05$.

difference in random motility on high versus low fibronectin concentrations can be appreciated qualitatively by examining the dispersion plots for cells migrating on a high concentration and a low concentration of fibronectin (Figure 3.7B). The random motion of ROCK inhibited RAW/LR5 cells migrating on 50 μ g/mL fibronectin show far less dispersion and overall movement than the cells migrating on 2.5 μ g/mL fibronectin. The change in random motility was accompanied by a change in cell morphology between low and high fibronectin concentrations (Figure 3.7C). On high concentrations of fibronectin, RAW/LR5 cells were unable to contract their trailing edges; this caused the cells to have long unretracted tails during migration (Figure 3.7C, top). In contrast, on low concentrations of fibronectin, RAW/LR5 cells showed a much more rounded morphology and showed long uropods that after sufficient migration would release and “snap” back to the cell body (Figure 3.7C). The reduced migration of ROCK inhibited RAW/LR5s on high concentrations of fibronectin is also illustrated in the plot of mean squared displacement versus time (Figure 3.7D). The cells on high concentrations of fibronectin have a far lower overall displacement over time. Finally, cells were stained to determine the effect of ROCK inhibition on the assembly of podosomes. ROCK-inhibited macrophages showed typical podosome structures (Figure 3.7E) with actin bundles surrounded by clear vinculin rings. These cells also show active actin-rich lamellipodia and display a long trailing tail which contains both actin and vinculin. Other researchers have found that stabilization of the actin cytoskeleton and integrin activation are tightly correlated with ROCK activity in monocytic cells [22] which complements our finding that fibronectin signaling levels alter the motile behavior of ROCK-inhibited RAW/LR5 cells. Overall, our data suggests that ROCK activity is not necessary for

macrophage motility but plays an important role in organizing the response to fibronectin. Different levels of fibronectin lead to the activation of different signaling pathways or different levels of response to ROCK; this then leads to changes in the morphology and motility of RAW/LR5 macrophages.

RAW/LR5 Speed and Persistence Times in Motile Conditions

One major advantage of imaging cells and analyzing their motility in two dimensions is the ability to quantitatively compare cells moving under different conditions. We measured the values of speed and persistence time for the motile RAW/LR5 cells investigated in this chapter and determined what specific relationships could be determined by comparing cells with inactive ROCK or reduced endogenous levels of Cdc42 to wild-type RAW/LR5 macrophages. When the persistence time of the cells was plotted versus their speed, we saw an inverse relationship for all motile cells (Figure 3.8A). This inverse relationship between speed and persistence time is seen in many motile cell types [23] and often lends insight into the type of migration a cell is undergoing and its physiological role. For example, endothelial cells, which must move in a directed path during tissue development or wound repair, move slowly but with high persistence [24], whereas neutrophils and other immune cells, which must constantly be scavenging for pathogens and areas of inflammation, move with high speed but low persistence [11, 20, 25]. The persistence time of migrating macrophages was found to be biphasic as a function of fibronectin concentration for all motile cells (Figure 3.8B). The fibronectin concentration at which the maximum persistence time occurred for cells with reduced endogenous levels of Cdc42 was slightly lower compared to wild type cells. The

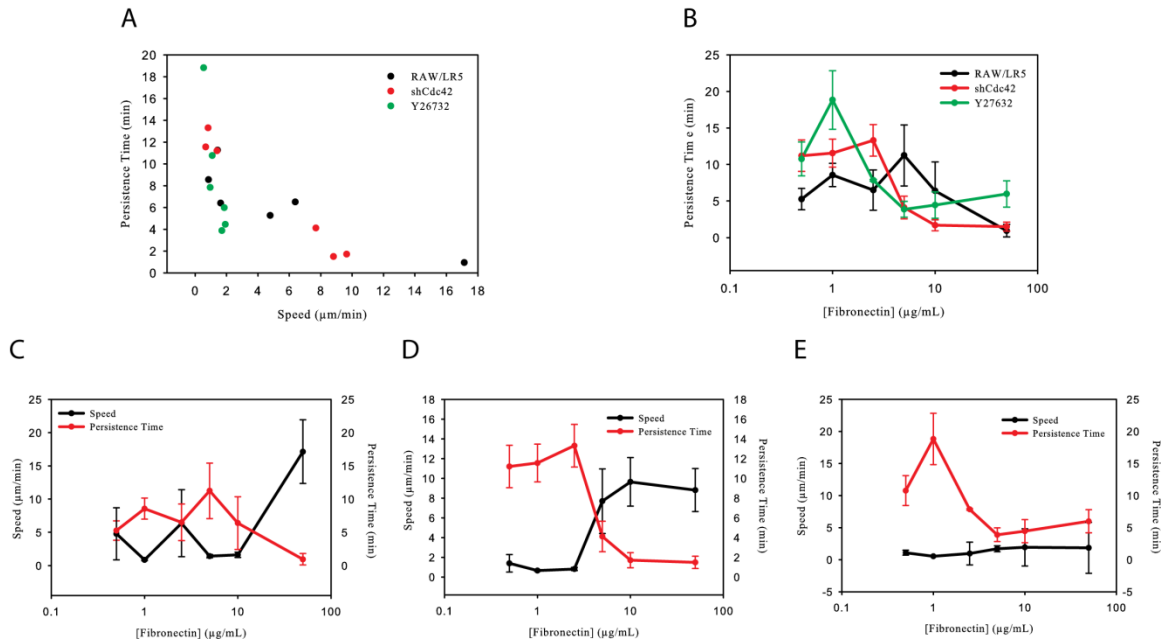


Figure 3.8. Quantitative analysis of RAW/LR5 migration. (A) Persistence versus speed shows inverse relationship for all motile conditions: RAW/LR5, shCdc42s, and RAW/LR5 macrophages inhibited with Y27632. (B) Persistence time versus fibronectin concentration for all motile conditions. (C) Speed and persistence time versus fibronectin concentration for wild type RAW/LR5 macrophages. (D) Speed and persistence time versus fibronectin concentration for shCdc42 macrophages shows that at low fibronectin concentrations motility is dominated by persistence time and at high fibronectin concentrations cell motility is dominated by speed. (E) Speed and persistence time versus fibronectin concentration for RAW/LR5 macrophages inhibited with Y27632 shows motility is dominated by persistence time. Error bars are standard error.

fibronectin concentration required for maximum persistence time was even lower for cells with inhibited ROCK signaling. For all conditions, the maximal persistence time corresponded to the fibronectin concentration with the highest random motility coefficient, indicating that RAW/LR5 migration is driven by persistence even though the random motility coefficient only depends mathematically first order on persistence and second order on speed. Physiologically, it is important for cells to have some persistent motion because without persistent motion cells do not explore a wide enough territory to fully take advantage of the persistent random walk for investigating their surroundings.

The speed and persistence time of individual cell migration were compared to determine which parameter dominated the motility. The speed and persistence time of migrating wild type RAW/LR5 cells show no real trend on increasing concentrations of fibronectin other than an increased dependence of speed on fibronectin concentration at high fibronectin concentrations (Figure 3.8C). We used cells with reduced endogenous levels of Cdc42 and cells with inhibited ROCK signaling to clarify the roles of specific proteins on the speed and persistence of migrating RAW/LR5. We found that the motility of RAW/LR5 cells with reduced endogenous levels of Cdc42 is dominated by persistence time at low concentrations of fibronectin but is dominated by speed at high concentrations of fibronectin (Figure 3.8D). This indicates that Cdc42 is involved in signaling pathways downstream of integrins binding to fibronectin, and the slight inhibition of this pathway leads to changes in the persistence of the cells. Macrophages with inhibited ROCK activity show a constant speed of about 2 $\mu\text{m}/\text{min}$ across all fibronectin concentrations (Figure 3.8E). It is possible that this occurs because cells without myosin II contraction are unable to significantly modulate their speed in response

to variable integrin signaling. This data confirms the proposal that ROCK signaling is important in stabilizing the actin cytoskeleton during spreading and migration [22]. Changes in the random motility coefficient for the ROCK inhibited macrophages, therefore, arise from differences in their persistence time. This data also indicates that ROCK signaling is important for modulating the speed of macrophages on differing fibronectin concentrations.

DISCUSSION

The importance of properly regulated macrophage migration in maintaining biological homeostasis is well documented and, in the future, macrophages could be used as therapeutic targets because of their role in the progression of various diseases [1-3, 26]. Before we can properly target these cells, however, we must have a better understanding of the signaling pathways that control macrophage migration. In the past, the signaling pathways involved in macrophage migration have been studied with and without the contribution of extracellular matrix proteins [4-6, 27]. We have extended this work by investigating the roles of Cdc42, ROCK, and PI3K in RAW/LR5 motility on a well-defined surface. Visualizing cell migration in two-dimensions using time-lapse imaging is a useful quantitative tool for understanding the way in which changes in signaling affect cell motility [11]. Changes in the speed or persistence time of cells cannot be easily detected using methods such as transwell assays. A small difference in a cell's ability to persist or a small change in its velocity can significantly alter the cell's ability to use a persistent random migration to efficiently monitor surrounding tissues [28]. We have shown that surfaces microcontact-printed with fibronectin and blocked with Pluronic-F127 are ideal for studying macrophage migration in response to changes in fibronectin concentration. Microcontact-printing allowed us to visualize macrophage migration in two dimensions and determine the migration parameters of macrophages moving on various fibronectin concentrations. The functional blocking employed by this technique prevents any cell attachment to non-ligand bound surfaces, ensuring all cell motility is a direct result of fibronectin-integrin binding without confounding cell-surface

interactions. The completeness of our blocking is striking in contrast to traditional blocking moieties such as bovine serum albumin (BSA) to which macrophages can attach and migrate. BSA has been demonstrated to be a ligand to beta-2 integrins, which may explain the residual adhesion of macrophages to BSA [11].

Macrophages do not form classical focal adhesions or stress fibers like mesenchymal cells; instead, they form small punctate complexes known as podosomes. These podosomes consist of an actin core surrounded by a ring of proteins typically found in mesenchymal focal adhesions such as talin, vinculin, and paxillin [8, 29]. We stained RAW/LR5 macrophages seeded on microcontact-printed surfaces for actin and vinculin and found small punctate actin cores surrounded by vinculin rings under the leading edge of polarized RAW/LR5 macrophages. This result indicated that the ability of macrophages to form podosomes was intact on our microcontact printed surfaces.

Extracellular matrix proteins, such as fibronectin, are found in all tissues in the body where macrophages reside; however, the specific role that integrin-fibronectin binding plays in macrophage migration is still not well known. By varying the concentration of fibronectin stamped onto our surface, we were able to determine that RAW/LR5 macrophages display biphasic motility with increasing ligand concentration. This result is further illustrated by the dispersion of cells on differing fibronectin concentrations. On the intermediate concentration that gave rise to the optimal motility, the cells are able to explore a much wider area than on high and low concentrations of fibronectin. This type of motility profile is common among cells that rely on integrin-ligand binding and un-binding for migration [19]. This may be important in diseases where high levels of fibronectin are pathological, such as atherosclerosis, and changes in

fibronectin concentration could contribute to increased macrophage recruitment [30]. We were able to show that all motile macrophages are displaying uncorrelated random walks with normal diffusion.

We were also able to show the importance of CSF-1 signaling on macrophage migration by varying the soluble CSF-1 concentration. The motility was again biphasic with increasing CSF-1 concentration at a fixed concentration of fibronectin. This indicates that at low concentrations of CSF-1 the cell is not completely stimulated, and at very high concentrations the cell is desensitized, perhaps by receptor down regulation; both conditions lead to sub-optimal motility. The maximum in the random motility coefficient for alveolar macrophages with chemokine concentration was shown previously [31] and is consistent with our results. The limited motility at high CSF-1 concentrations is likely because the CSF-1 receptor is internalized quickly after stimulation and is not recycled back to the membrane [26], leading to reduced CSF-1 signaling after the initial stimulation.

Several Rho GTPases are thought to contribute to macrophage motility downstream of both integrin-binding and CSF-1R signaling. Cdc42 has been implicated in directional sensing of macrophages to a gradient of CSF-1 but has not been found to be necessary for random migration [4, 5]. We found that reduction of Cdc42 did not significantly change the random motility of cells except at the fibronectin concentration of 5 μ g/mL that was optimal for wild-type motility. These results suggest that the reduction of Cdc42 activity is mostly compensated for by other signaling molecules. We also saw slight morphological changes in migrating cells with reduced Cdc42 levels, indicating a link between Cdc42 signaling and the cytoskeletal network in macrophages.

We found that these cells had broader lamellipodia and reduced uropods compared to wild-type RAW/LR5 macrophages. Their lamellipodia also showed increased ruffling. Similar morphological changes have previously been seen in Bac1.2F5 macrophages expressing a dominant negative Cdc42 [5]. Staining of RAW/LR5 macrophages with reduced Cdc42 levels on fibronectin printed surfaces revealed a lack of podosome formation. Both actin and vinculin were found throughout the cell but were not organized into structures, consistent with the theory that Cdc42 regulates actin organization into podosomes [4, 6]. It is still unclear what role podosomes have in macrophage migration, but our data with these macrophages suggests that podosomes are not required for random migration on fibronectin. It has been previously postulated that Cdc42 restricts the speed of migration in macrophages because expression of dominant negative Cdc42 in Bac1.2F5 cells leads to an increase in speed on glass surfaces [5]. We found that on high concentrations of fibronectin, the speed of RAW/LR5 macrophages with reduced endogenous levels of Cdc42 was significantly higher than their speeds on low concentrations of fibronectin, indicating that this restraint might be dependent on integrin-ligand binding. It is possible that an incomplete knockdown of Cdc42 in the cells left sufficient Cdc42 for motility signaling. However, the observation that these cells no longer form podosomes and the previous result showing decreased migration to the chemokine CX3CL1 [10] indicate that motility and cytoskeletal signaling pathways are altered by the reduction in Cdc42.

Phosphoinositide 3-kinase (PI3K) becomes activated by both integrins and the CSF-1R at the plasma membrane of macrophages [6]. PI3K has been shown to be upstream of many signaling pathways in macrophages and is important for macrophage

migration [27, 32, 33]. Therefore, it is not surprising that we found no motility in RAW/LR5 cells inhibited with either LY29004 or Wortmannin, two PI3K inhibitors. Cells inhibited with either chemical inhibitor showed no polarization or ability to migrate on fibronectin printed surfaces, and PI3K-inhibited cells showed no actin or vinculin organization. A requirement for PI3K signaling in macrophage migration has also been shown with Bac1.2F5 macrophages and primary murine macrophages [27, 33].

Our ability to visualize macrophages migrating in two-dimensions over time allowed us to discover a unique property of ROCK-inhibited macrophages migrating on fibronectin surfaces. We found that in the presence of the ROCK inhibitor Y-27632, RAW/LR5 macrophages showed a switch-like change in motility with increasing fibronectin concentration. Under ROCK inhibition, macrophages had significantly lower motility on high concentrations of fibronectin (10 μ g/mL or higher) than on low concentrations of fibronectin (5 μ g/mL or lower), but the random motility coefficient was constant within each regime. This sensitivity to fibronectin concentration was also accompanied by a change in morphology for migrating macrophages. On high concentrations of fibronectin, the cells showed a defect in contractility, leaving long un-retracted tails behind them. This accumulation of un-retracted tails has also been seen in THP-1 monocytes inhibited with Y-27632 [22]. On low concentrations of fibronectin, however, ROCK-inhibited RAW/LR5 cells showed a much more rounded morphology with small but broad lamellipodia and almost no tails. Others have shown that loss of one ROCK isotype, ROCK1, leads to a significant increase in adhesion to the fibronectin fragment CH296 [34]. It has also been previously found in THP-1 monocytes that inhibition of ROCK leads to increased spreading and membrane activity on fibronectin

[22]. Therefore, it is reasonable to assume that the RAW/LR5 macrophages have reduced migration on high concentrations of fibronectin because of increased attachment to the surface compared to wild-type cells. Even with this increased attachment, however, the ROCK-inhibited cells show efficient motility on all concentrations of fibronectin, consistent with previous findings that RhoA is not required for forward migration, only efficient tail-retraction [35]. We were able to show that podosome assembly still occurs in the absence of ROCK activity, consistent with the finding that ROCK inhibition leads to increased integrin-dependent phosphotyrosine signaling to podosome-associated proteins such as cofilin [22]. We were able to discover this switch in random motility coefficient accompanied by a change in morphology for ROCK-inhibited RAW/LR5 cells on high versus low concentrations of fibronectin because of our unique ability to study motility in two dimensions.

CONCLUSIONS

We have shown that microcontact printed PDMS surfaces serve as an ideal platform for studying macrophage migration in two-dimensions. We have shown that we can functionally block our surfaces, guaranteeing that all the macrophage motility seen in our experiments is specifically due to cell interactions with fibronectin. Using these surfaces, we were able to show that RAW/LR5 macrophages exhibit biphasic motility with increasing fibronectin or CSF-1 concentrations. We were also able to show that PI3K signaling, but not Cdc42 or ROCK activity, is required for migration of macrophages. This system for studying two-dimensional migration has allowed us to discover unique migratory morphologies for ROCK-inhibited cells on varying fibronectin concentrations. It has also allowed us to quantitatively compare the migration of macrophages under various signaling-impaired conditions. In the future, this surface preparation can serve as a tool for studying highly adhesive cells such as macrophages in two-dimensions and directly relate their migration to integrin-binding interactions without confounding surface effects.

REFERENCES

1. Pollard, J.W., *Trophic macrophages in development and disease*. Nat Rev Immunol, 2009. **9**(4): p. 259-70.
2. Pixley, F.J., *Macrophage Migration and Its Regulation by CSF-1*. Int J Cell Biol, 2012. **2012**: p. 501962.
3. Hamilton, J.A., *CSF-1 signal transduction*. J Leukoc Biol, 1997. **62**(2): p. 145-55.
4. Allen, W.E., et al., *Rho, Rac and Cdc42 regulate actin organization and cell adhesion in macrophages*. J Cell Sci, 1997. **110** (Pt 6): p. 707-20.
5. Allen, W.E., et al., *A role for Cdc42 in macrophage chemotaxis*. J Cell Biol, 1998. **141**(5): p. 1147-57.
6. Jones, G.E., *Cellular signaling in macrophage migration and chemotaxis*. J Leukoc Biol, 2000. **68**(5): p. 593-602.
7. Mantovani, A. and A. Sica, *Macrophages, innate immunity and cancer: balance, tolerance, and diversity*. Curr Opin Immunol, 2010. **22**(2): p. 231-7.
8. Calle, Y., et al., *The leukocyte podosome*. Eur J Cell Biol, 2006. **85**(3-4): p. 151-7.
9. Dovas, A., et al., *Regulation of podosome dynamics by WASp phosphorylation: implication in matrix degradation and chemotaxis in macrophages*. J Cell Sci, 2009. **122**(Pt 21): p. 3873-82.
10. Park, H. and D. Cox, *Syk regulates multiple signaling pathways leading to CX3CL1 chemotaxis in macrophages*. J Biol Chem, 2010. **286**(17): p. 14762-9.
11. Henry, S.J., J.C. Crocker, and D.A. Hammer, *Ligand density elicits a phenotypic switch in human neutrophils*. Integr Biol (Camb), 2014.

12. Cox, D., et al., *Requirements for both Rac1 and Cdc42 in membrane ruffling and phagocytosis in leukocytes*. J Exp Med, 1997. **186**(9): p. 1487-94.
13. Park, H. and D. Cox, *Cdc42 regulates Fc gamma receptor-mediated phagocytosis through the activation and phosphorylation of Wiskott-Aldrich syndrome protein (WASP) and neural-WASP*. Mol Biol Cell, 2009. **20**(21): p. 4500-8.
14. Peltier, J. and D.V. Schaffer, *Viral packaging and transduction of adult hippocampal neural progenitors*. Methods Mol Biol, 2010. **621**: p. 103-16.
15. Desai, R.A., et al., *Subcellular spatial segregation of integrin subtypes by patterned multicomponent surfaces*. Integr Biol (Camb), 2011. **3**(5): p. 560-7.
16. Dunn, G.A., *Characterising a kinesis response: time averaged measures of cell speed and directional persistence*. Agents Actions Suppl, 1983. **12**: p. 14-33.
17. Ye, H., Z. Gu, and D.H. Gracias, *Kinetics of ultraviolet and plasma surface modification of poly(dimethylsiloxane) probed by sum frequency vibrational spectroscopy*. Langmuir, 2006. **22**(4): p. 1863-8.
18. Yang, M.T., et al., *Assaying stem cell mechanobiology on microfabricated elastomeric substrates with geometrically modulated rigidity*. Nat Protoc, 2011. **6**(2): p. 187-213.
19. Palecek, S.P., et al., *Integrin-ligand binding properties govern cell migration speed through cell-substratum adhesiveness*. Nature, 1997. **385**(6616): p. 537-40.
20. Ricart, B.G., et al., *Dendritic cells distinguish individual chemokine signals through CCR7 and CXCR4*. J Immunol, 2011. **186**(1): p. 53-61.
21. Smith, L.A., et al., *Neutrophil traction stresses are concentrated in the uropod during migration*. Biophys J, 2007. **92**(7): p. L58-60.

22. Worthylake, R.A. and K. Burridge, *RhoA and ROCK promote migration by limiting membrane protrusions*. J Biol Chem, 2003. **278**(15): p. 13578-84.
23. Lauffenberger, D.A. and J.J. Linderman, *Receptors: Models for Binding, Trafficking, and Signaling*. 1993: Oxford University Press.
24. Stokes, C.L. and D.A. Lauffenburger, *Analysis of the roles of microvessel endothelial cell random motility and chemotaxis in angiogenesis*. J Theor Biol, 1991. **152**(3): p. 377-403.
25. Jannat, R.A., et al., *Neutrophil adhesion and chemotaxis depend on substrate mechanics*. J Phys Condens Matter, 2010. **22**(19): p. 194117.
26. Pixley, F.J. and E.R. Stanley, *CSF-1 regulation of the wandering macrophage: complexity in action*. Trends Cell Biol, 2004. **14**(11): p. 628-38.
27. Munugalavadla, V., et al., *p85alpha subunit of class IA PI-3 kinase is crucial for macrophage growth and migration*. Blood, 2005. **106**(1): p. 103-9.
28. Nishimura, S.I., M. Ueda, and M. Sasai, *Non-Brownian dynamics and strategy of amoeboid cell locomotion*. Phys Rev E Stat Nonlin Soft Matter Phys, 2012. **85**(4 Pt 1): p. 041909.
29. Dovas, A. and D. Cox, *Signaling networks regulating leukocyte podosome dynamics and function*. Cell Signal, 2011. **23**(8): p. 1225-34.
30. Libby, P., *Molecular and cellular mechanisms of the thrombotic complications of atherosclerosis*. J Lipid Res, 2009. **50 Suppl**: p. S352-7.
31. Farrell, B.E., R.P. Daniele, and D.A. Lauffenburger, *Quantitative relationships between single-cell and cell-population model parameters for chemosensory*

- migration responses of alveolar macrophages to C5a*. Cell Motil Cytoskeleton, 1990. **16**(4): p. 279-93.
32. Papakonstanti, E.A., et al., *Distinct roles of class IA PI3K isoforms in primary and immortalised macrophages*. J Cell Sci, 2008. **121**(Pt 24): p. 4124-33.
33. Vanhaesebroeck, B., et al., *Distinct PI(3)Ks mediate mitogenic signalling and cell migration in macrophages*. Nat Cell Biol, 1999. **1**(1): p. 69-71.
34. Vemula, S., et al., *ROCK1 functions as a suppressor of inflammatory cell migration by regulating PTEN phosphorylation and stability*. Blood, 2010. **115**(9): p. 1785-96.
35. Worthylake, R.A., et al., *RhoA is required for monocyte tail retraction during transendothelial migration*. J Cell Biol, 2001. **154**(1): p. 147-60.

CHAPTER 4: FORCE GENERATION BY MOTILE PRIMARY HUMAN MACROPHAGES

Adapted from: Hind LE, Dembo M, and Hammer DA “Macrophages Generate Strong Traction Forces at their Leading Edge in a Stiffness-Dependent Manner.” *Integrative Biology*. Reproduced by permission of The Royal Society of Chemistry.

ABSTRACT

The ability of macrophages to properly migrate is crucial to their success as early responders during the innate immune response. Furthermore, improper regulation of macrophage migration is known to contribute to several pathologies. The signaling mechanisms underlying macrophage migration have been previously studied, but to date no one has investigated the mechanical mechanism of macrophage migration. In this study, we have created the first traction maps of motile primary human macrophages by observing their migration on compliant polyacrylamide gels. We find that the force generated by migrating macrophages is concentrated in the leading edge of the cell and that the magnitude of this force is dependent on the stiffness of the underlying matrix. With the aid of chemical inhibitors, we showed that signaling through the RhoA kinase ROCK, myosin II, and PI3K is essential for proper macrophage force generation. Finally, we showed that Rac activation by its GEF Vav1 is crucial for macrophage force generation while activation through its GEF Tiam1 is unnecessary.

INTRODUCTION

Macrophages play an important role in the innate immune response by clearing pathogens through phagocytosis and activating the adaptive immune response through cytokine production and antigen-presentation. In order to perform these functions, macrophages must be able to efficiently migrate to sites of infection. Improper regulation of macrophage function has been linked to several diseases including atherosclerosis, rheumatoid arthritis, and cancer [1]; therefore, it is crucial that we develop a better understanding of the mechanisms underlying macrophage migration. Previous work on macrophage migration has investigated the role of signaling molecules on chemokinesis and chemotaxis, [2] but to our knowledge no group has studied the spatio-temporal regulation of forces during macrophage migration.

Cellular traction forces have been shown to be important for cell adhesion [3, 4], spreading [5], motility [3, 6], and extra-cellular matrix remodeling [7]. To effectively migrate on and through tissues, anchorage-dependent cells must attach to their underlying substrate and generate traction against that substrate. In the towing model of cell motility the cell extends a lamellipodia and attaches to the underlying substrate through integrin binding to the extra cellular matrix. The cell then contracts, which exerts traction on its underlying substrate and generates strong cellular forces at the leading edge of the cell. This contraction allows for the release of the cell's uropod and the forward motility of the cell [8]. This towing model has been shown to broadly apply to large contractile cells such as endothelial cells and fibroblasts. The spatial distribution of forces of mesenchymal cells migrating on compliant surfaces has been studied in depth [3, 5, 6];

but despite the importance of immune cell motility, relatively little work has been done to characterize the mechanical mechanisms behind the motility of immune cells.

Leukocyte motility differs from mesenchymal cell motility in several ways. Leukocytes are fast moving cells that migrate with low persistence. In order to achieve their high speed, leukocytes form weak, short-lived adhesions to their substratum. This is in contrast to mesenchymal cells which form strong focal adhesions to their surface and contain stress fibers that allow for large cellular contractions [8]. Our laboratory has embarked on an effort to categorize the spatio-temporal distribution of forces in all the motile cells of the immune system. Previously, we showed that neutrophils achieve motility through an alternative mode of migration termed tail-contraction or rearward-squeezing [9, 10]. In this mode of motility, the traction forces are concentrated in the cell uropod and the cell is pushed forward through a “squeezing” mechanism that is dependent on myosin activity. The traction stresses generated by neutrophils were found to be small compared to those generated by mesenchymal cells, which is consistent with their need to move quickly toward targets. Further work by our lab went on to show that this mode of motility is not shared by all leukocytes. Dendritic cells, which are of the monocytic lineage, display maximal stresses at the leading edge of cell, indicating they use the towing model of migration. The forces displayed during dendritic cell migration were even weaker than those generated by neutrophils [11]. The contrast among the behaviors of leukocytes illustrated the importance of studying the force generation of each cell type individually since no one mode of motility is shared by all leukocytes.

The use of polyacrylamide gels coupled with traction force microscopy offers many advantages over the technologies that have been utilized to quantify cellular

traction forces in the past [3, 6]. Polyacrylamide hydrogels are optically clear and non-toxic which allows for easy cell culture and imaging. Furthermore, they are elastic and can be easily tuned to a variety of stiffnesses, allowing quantification of forces across many magnitudes. In TFM, polyacrylamide gels are fabricated using a specific polymer:crosslinker ratio to obtain gels of the desired stiffness and fluorescent marker beads are embedded within the gel during polymerization. During cell migration, images are taken of the cell and the beads. The cell is then lifted off the gel and an image is taken of the unstressed bead locations. The tractions applied on the gel can then be calculated from the displacement of the beads from the unstressed position. Our lab has used this technology to measure the traction stresses of cells undergoing adhesion and spreading as well as leukocyte migration [5, 9, 10, 12, 13].

In this study we have used traction force microscopy (TFM) to determine the force generation profile of macrophages migrating on compliant surfaces. To our knowledge, this is the first measurement of force generation for motile macrophages. We sought to determine the type of motility employed by macrophages and which signaling molecules are most important for macrophage force generation. Our results indicate that macrophages use a towing mode of motility with the strongest forces concentrated at the leading edge of migrating cells. We have also shown that the magnitude of force generation is dependent on the stiffness of the underlying substrate. Furthermore, we have determined using a range of chemical inhibitors that the force generated by macrophages, like other leukocytes, is dependent on signaling through PI3K, RhoA, and myosin II. Finally, we have shown that Rac signaling is critical for force generation

when Rac is activated by Vav1 but not when Rac is activated by Tiam1; these results illustrate the complexity of signaling that occurs upstream of force generation.

MATERIALS AND METHODS

Reagents

Bovine fibronectin and recombinant human M-CSF were obtained from Sigma (St. Louis, MO). We used the inhibitors Y27632 [14] at 10 μ M from Millipore (Billerica, MA), Blebbistatin [15] at 20 μ M from Sigma (St. Louis, MO), LY294002 [16] at 50 μ M from Cell Signaling (Boston, MA), NSC23766 [17] at 50 μ M from Millipore (San Diego, CA), 6-thio-GTP [18] at 10 μ M from Jena Bioscience (Jena, Germany).

Isolation of Monocytes

Whole blood was obtained from healthy human donors by venipuncture and collected in BD Vacutainer tubes containing sodium heparin as an anticoagulant (BD Biosciences, San Jose, CA). Samples were collected with University of Pennsylvania Institutional Review Board approval from consenting adult volunteers. Blood samples were layered in a 1:1 ratio of whole blood to the density gradient 1-Step Polymorphprep (Axis-Shield, Oslo, Norway). Vials were centrifuged at 1500 rpm for 40 minutes and the mononuclear band was collected into a fresh vial.

Differentiation and Cell Culture of Macrophages

Cells were allowed to adhere to sterile non-tissue culture treated dishes in RPMI-1640 supplemented with 10% heat-inactivated FBS overnight. Non-adhered cells were removed and washed with PBS. Adherent monocytes were then differentiated for 7 days in RMPI-1640 supplemented with 10% heat-inactivated FBS and 2ng/mL M-CSF

(Sigma, St. Louis, MO). Cells were used for experimentation 7-12 days following the start of differentiation.

Surface Preparation

Coverslips (No 1, 45 x 50 mm, Fisher Scientific, Pittsburgh, PA) were chemically activated in preparation for covalent attachment of polyacrylamide gels using a method adapted from the protocol by Pelham and Wang. Briefly, coverslips were washed for 4 hours in 0.2 M hydrogen chloride then rinsed several times with distilled water. They were then neutralized with 0.1 M sodium hydroxide for 30 minutes and rinsed with distilled water. Coverslips were incubated on an orbital shaker in 3-aminopropyl trimethoxysilane 0.5% for 30 minutes and rinsed with distilled water. They were then activated with 0.5% glutaraldehyde for at least 1 hour. The coverslips were then air-dried overnight.

Synthesis of the Bifunctional Linker

N-6-((acryloyl)amino)hexanoic acid (N-6) was synthesized using the method described by Pless et al. The N-6 copolymerizes in the acrylamide to form a reactive polyacrylamide gel. The N-6 contains an *n*-succinimidyl ester that is displaced by a primary amine to link the amine-containing ligand, such as fibronectin, to the polyacrylamide gel.

Gel Synthesis

Acrylamide solutions were prepared containing acrylamide (40% w/v solution), *n,n'*-methylene-bis-acrylamide (2% w/v solution), *n'*-tetramethylethylene di-amine, and ammonium persulfate from Bio-Rad Laboratories (Hercules, CA). Additionally, the gels contained 0.25M HEPES, buffered to pH 8, 5.6mg of N6 dissolved in ethanol, distilled water, and carboxylate-modified fluorescent latex beads (0.5 μ m Fluorospheres, Molecular Probes, Eugene, OR). The concentrations of acrylamide and bis were varied to control the mechanical properties of the hydrogel.

A drop of gel solution was dispensed onto a Rainex-coated 18mm glass coverslip. A second activated rectangular coverslip was placed on top of the gel droplet to flatten the solution; the assembly was polymerized in an inverted position to allow beads to settle to the top surface of the gel. The gels were polymerized under nitrogen for 45 minutes. The top coverslip was gently peeled away leaving a thin gel immobilized on the activated coverslip. Gels were rinsed with distilled water and incubated with 5 μ g/mL fibronectin in 50mM HEPES buffer overnight. Unreacted N-6 was blocked with 1:100 ethanolamine in 50mM HEPES for 30 minutes and stored in 1 x PBS at 4°C for up to 2 weeks.

Traction Force Microscopy of Migrating Macrophages

Traction force microscopy has been described previously [6]. Briefly, traction forces were determined based on deformations in the polyacrylamide substrate relative to the relaxed substrate as detected by movements of 0.5- μ m beads embedded in the gel.

Primary human macrophages were plated on fibronectin-coated polyacrylamide gels at 1×10^4 cells/mL and incubated for 1 hour at 37°C . Unattached cells were washed away and fresh RPMI with 20ng/mL human M-CSF was added to the gel chamber. Phase contrast images of the cell were taken every 10 minutes during cell migration. Directly after a phase image was taken, a corresponding fluorescent image of the beads embedded beneath the cell was taken. Images were taken over a 4 hour period. At the end of migration the cells were removed using 0.5% SDS and an image of the beads in their unstressed state was taken. Using custom-written LIBTRC software, the bead displacements within the gel were calculated, the cell and nucleus were drawn, and a mesh that fits within the outline of the cell was created. Using the bead displacements and the material properties of the gel, the most likely surface traction vectors were calculated using the technique described by Dembo and Wang.

The overall force, $|F|$, exerted by the cell on its substrate, is an integral of the traction field magnitude over the area, $|F| = \int \int \sqrt{(T_x^2(x, y) + T_y^2(x, y))} dx dy$, where $\mathbf{T}(x, y) = [T_x(x, y), T_y(x, y)]$ is the continuous field of traction vectors defined at any spatial position (x, y) within the cell.

Inhibition of Macrophages

All experiments in which macrophages were treated with a chemical inhibitor followed the same protocol. Briefly, macrophages were seeded on 10,400Pa gels functionalized with $5 \mu\text{g/mL}$ fibronectin and allowed to adhere for one hour. The cells were then washed, and fresh media containing the correct concentration of inhibitor was

applied. The macrophages were incubated for 1 hour to allow complete inhibition. M-CSF was then added directly prior to traction force measurements being taken. All traction force measurements were taken in the continued presence of the chemical inhibitor. The forces exerted by inhibited macrophages were compared to the previously measured forces of uninhibited macrophages on 10,400Pa gels.

RESULTS

Macrophage Force Generation is Concentrated at the Leading Edge of Migrating Cells and is Dependent on Substrate Stiffness

Substrate stiffness has been shown to affect a variety of cellular behaviors including differentiation, adhesion, and migration. We therefore hypothesized that changing the substrate elasticity would cause changes in macrophage force generation. Traction force microscopy was used to determine force generated by macrophages on substrates of increasing stiffness. Polyacrylamide gels were fabricated over a range of elastic moduli from 2.5 kPa to 15.6 kPa. This range of moduli encompasses the physiological range of tissue stiffnesses macrophages are exposed to *in vivo* including both healthy and diseased tissue [19, 20]. We used M-CSF to stimulate polarization and motility in our experiments; however macrophages require the chemokine M-CSF to differentiate and proliferate. Therefore, macrophages were differentiated and maintained in M-CSF but the M-CSF was removed for 18 hours prior to experimentation. The cells were then stimulated with 20ng/mL M-CSF immediately before force measurements began. The force generated by macrophages was measured on polyacrylamide hydrogels of increasing stiffness. We found that the force exerted by macrophages increases with increasing substrate stiffness (Figure 4.1A). The area of the macrophages analyzed was also determined and found to be biphasic with respect to substrate stiffness Figure 4.1B. This result indicates that the increasing force seen on substrates of increasing stiffness is directly correlated to the stiffness of the substrate and not an artifact of increased spreading of the macrophage.

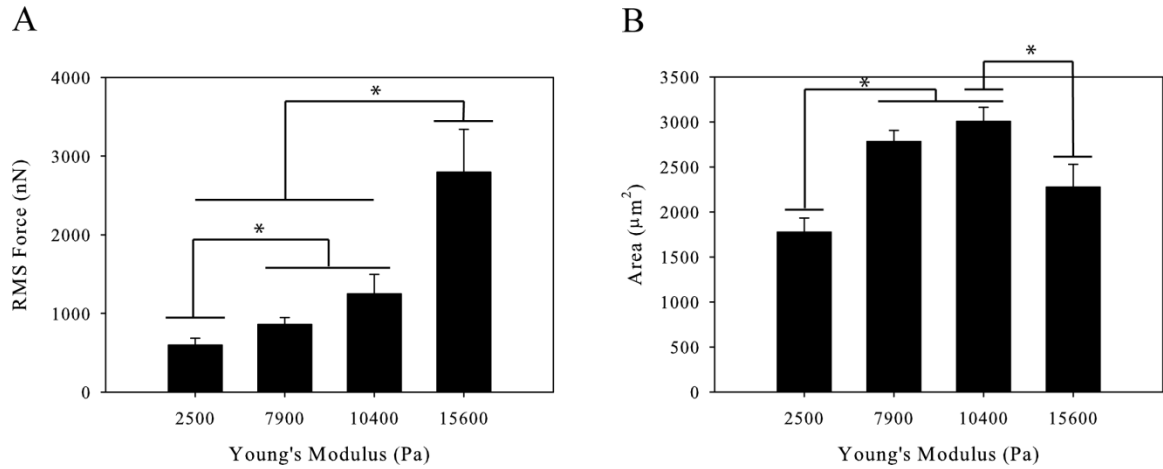


Figure 4.1. Primary human macrophages on polyacrylamide gels of increasing stiffness.

(A) Root-mean-squared force of primary human macrophages increases as a function of gel stiffness. (B) Spread area of primary human macrophages is biphasic with gel stiffness. ($n > 46$ cells per condition). Error bars are standard error,

* indicates $p < 0.05$.

Different patterns of force organization have been seen in various motile leukocytes. Our lab has previously shown that neutrophils have high forces in the rear of the cells relative to motion, indicating a rearward-squeezing mode of motility [9, 10]. Conversely, dendritic cells show high forces at the front of the cells relative to motion, indicating a forward towing mechanism [11]. Therefore, we next wanted to determine the distribution of forces in a motile macrophage to better understand the type of motility macrophages employ. Using traction maps of highly motile cells, we found that macrophages generate the strongest forces in the front of the cell relative to motion. A representative cell illustrating this result is shown in Figure 4.2A. These figures illustrate cell tractions using heat maps to show the areas of greatest traction and arrows to indicate the direction of cell motion between the current position and the next frame. An illustration of the cell migration track for the representative cell is shown in Figure 4.2B. This type of force pattern suggests that macrophages use a towing mechanism of motility in which cells extend a pseudopod and attach to the substrate, generate cellular contraction through their actomyosin cytoskeleton which exerts tension on the substrate, and then release the uropod.

Macrophage Force Generation Requires Myosin Contraction through ROCK Signaling

Actin-myosin activity within the cell is important for cellular contraction and tail retraction during motility. This contractility depends on RhoA signaling to myosin II through its kinase ROCK. To determine the contribution of RhoA signaling on

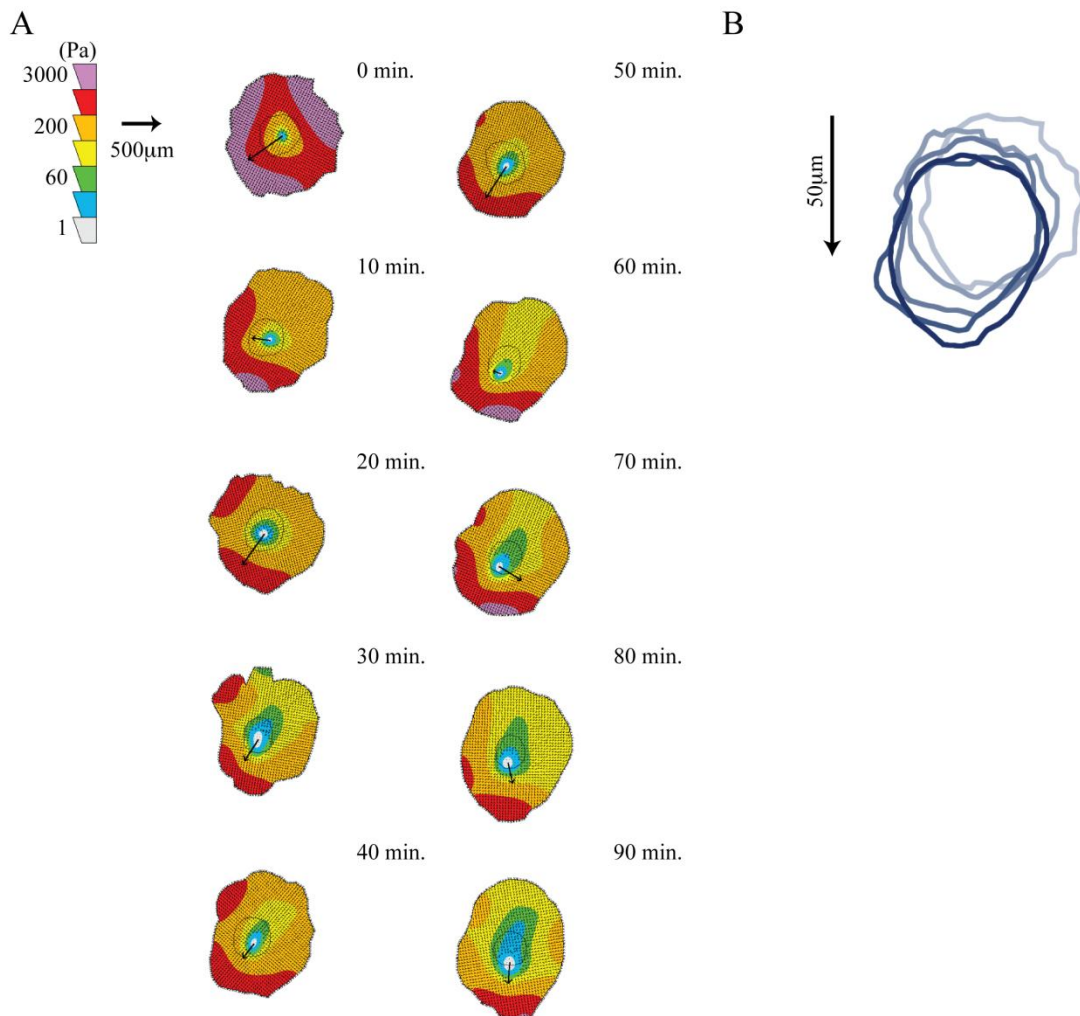


Figure 4.2. Traction contour maps of a migrating macrophage. (A) Contour plots shows traction stresses and arrows indicate the direction of motion between the indicated timepoint and the next timepoint of a representative macrophage on a 10,400Pa gel. (B) Outlines of cell position every 20 minutes to illustrate cell migration.

macrophage force generation we used two chemical inhibitors: Y27632 to block ROCK signaling and Blebbistatin to block myosin II signaling. Both inhibitions were performed separately following the protocol described in the materials and methods section. We found that treatment of the cells with either Y27632 or Blebbistatin lead to a significant reduction in force generation (Figure 4.3A). As has been previously seen, cells inhibited with Y27632 displayed long, unretracted tails and little force generation (Figure 4.3B). Cells treated with Blebbistatin showed no polarization or significant force generation (Figure 4.3C).

Macrophage Force Generation is Dependent on PI3K Signaling and Rac Signaling Downstream of Vav1 but not Tiam1

Phosphoinositide 3-kinase (PI3K) is a membrane-bound signaling protein that interacts with both integrin receptors as well as the M-CSF receptor [21]. Upon stimulation, PI3K signals downstream to several pathways inducing membrane ruffling, cell polarization, and motility [22-24]. We investigated the role of PI3K activity in macrophage force generation by inhibiting cells with 50 μ M LY294002. Cells were inhibited using the same protocol outlined in materials and methods. We found that inhibition of PI3K caused a significant decrease in macrophage force generation (Figure 4.4A); a representative traction map of an LY294002 inhibited cell is shown in Figure 4.4B.

Rac, a GTPase downstream of PI3K signaling, is known to be involved in lamellipodial protrusion at the leading edge of migrating macrophages [25]. We hypothesized that Rac would be important for macrophage force generation because of its

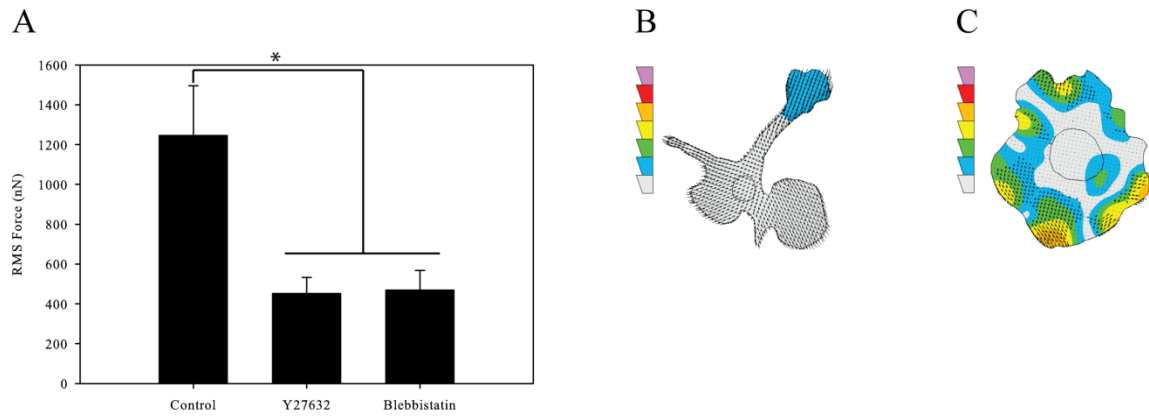


Figure 4.3. Macrophage force generation with rear contraction inhibition. (A) Root-mean-squared forces of uninhibited macrophages, macrophages inhibited with 10 μ M Y27632 to reduce ROCK signaling, and macrophages inhibited with 20 μ M Blebbistatin to reduce myosin II activity. (B) Traction contour plot of a representative cell inhibited with Y27632 imaged at 10 minutes. (C) Traction contour plot of a representative cell inhibited with Blebbistatin imaged at 340 minutes. The traction contours are plotted using the same force scale as in Figure 2A. All results from macrophages plated on 10,400Pa gels with 5 μ g/mL fibronectin. (n > 44 for each condition). Error bars are standard error. * indicates p < 0.05.

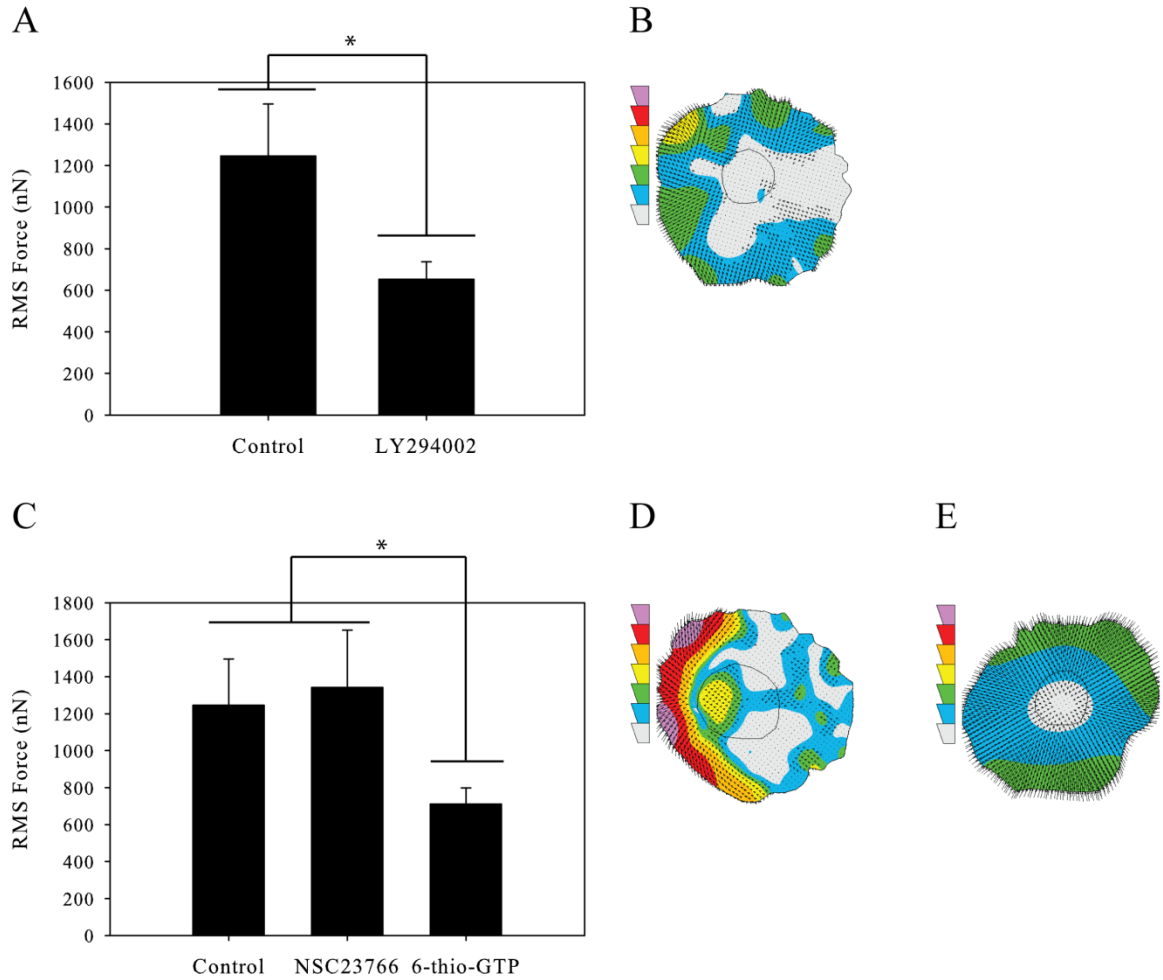


Figure 4.4. Macrophage force generation with leading edge inhibition. (A) Root-mean-squared force of uninhibited macrophages and macrophages inhibited with 50 μ M LY294002 to reduce PI3K signaling. (B) Traction contour plot of a representative cell inhibited with LY294002 imaged at 230 minutes. (C) Root-mean-squared force of uninhibited macrophages, macrophages inhibited with 50 μ M NSC23766 to reduce Rac-Tiam1 binding, and macrophages inhibited with 10 μ M 6-thio-GTP to block Rac-Vav1 binding. (D) Traction contour plot of a representative cell inhibited with NSC23766 imaged at 320 minutes. (E) Traction contour plot of a representative cell inhibited with 6-thio-GTP imaged at 240 minutes. The traction contours are plotted using the same

force scale as in Figure 2A. All results from macrophages plated on 10,400Pa gels with 5 μ g/mL fibronectin. (n > 58 for each condition). Error bars are standard error.

* indicates p < 0.05.

role in motility at the leading edge of cells and our previous finding that macrophage forces during motility are the strongest at the front of the cell. We first inhibited cells with 50 μ M NSC23766, a chemical inhibitor that primarily prevents activation of Rac by blocking the interaction of Rac and Tiam1, a Rac GEF. We found that this inhibition caused no significant change in the ability of macrophages to generate force (Figure 4.4C and D). However, others have previously found that the specific GEF involved in Rac activation can determine Rac's downstream function [26]. We therefore sought to inhibit Rac through a GEF known to be important in cell motility. Macrophages were treated with 10 μ M 6-thio-GTP which prevents Rac binding to its GEF Vav1. Contrary to our results with NSC23766, this inhibition of Rac lead to a significant reduction in the force produced (Figure 4.4C and E). This result suggests that the activation of Rac for force generation is, at least to some degree, GEF-specific.

DISCUSSION

Previous work has shown that matrix stiffness has a significant effect on force-mediated cell behaviors including cell adhesion [3, 4], spreading [5], and migration [3, 6]. We have shown that in primary human macrophages, force generation is a stiffness-dependent process with increasing stiffness of the underlying matrix resulting in increased force generation. This trend has been seen in other cell types including leukocytes [9]. This result is important physiologically because macrophages must migrate through tissues of different densities in the body. In addition, many of the diseases associated with macrophage migration are accompanied by changes in the stiffness of native tissues such as hardening of the arteries in atherosclerosis and development of solid tumors in cancer [1, 20, 27, 28]. We have shown that macrophages are able to sense the stiffness of the underlying tissue and modulate their mechanobehavior accordingly. They are able to generate very large traction stresses in response to stiff substrates which may be necessary for migration through tissues in the body.

We were also able to show that the increase in force seen on substrates of increasing stiffness was not solely due to an increase in cell area because cell spread area was found to be biphasic with increasing matrix stiffness. Although many cells increase their cell area as a function of matrix stiffness, others have found a similar biphasic relationship of area with increasing stiffness [29]. This could be explained by the recent result indicating that an increase in substrate stiffness leads to an increase in integrin

clustering [30]. This clustering could prevent the cells from spreading over a large area on stiff substrates.

We have created the first traction maps of migrating macrophages and have shown that the highest areas of traction stress are at the leading edge of a migrating macrophage. This result indicates that macrophages utilize a forward towing mechanism of motility. Our lab has previously shown that this type of force distribution is seen in dendritic cells, another monocytic cell lineage [11]. The forces exerted by dendritic cells are much smaller than those exerted by macrophages, although a direct comparison of the magnitude of the forces is impossible because these forces were measured using a micropost array. This distribution of forces among leukocytes of monocytic lineage is in contrast to the distribution seen in neutrophils [9] suggesting that leukocyte motility is diverse and the mechanisms used by cells undergoing amoeboid motility are not uniform.

We next sought to investigate the signaling involved in the generation of traction force by macrophages. We have previously shown that inhibition of the RhoA kinase ROCK in a macrophage cell line does not significantly decrease the cell's motility but it has a strong effect on cell morphology. Others have also shown that ROCK is important for the generation of cellular traction forces [9]. Therefore, we used the chemical inhibitor Y27632 to investigate the effect of ROCK signaling on macrophage force generation. We found that cells inhibited with Y27632 show long unretracted tails due to a defect in myosin contraction. These cells also exhibited little to no force (Figure 4.3A and B). Therefore, RhoA signaling through ROCK is clearly necessary for macrophage force generation. These results support previous findings that ROCK activity is strongly correlated with the stabilization of the actin cytoskeleton and integrin activation in

monocytic cells [31, 32]. We also found that the myosin II inhibitor, Blebbistatin, lead to a significant reduction in traction force (Figure 4.3A and C). As expected, this result indicated that myosin II is necessary for proper cytoskeletal contraction and force generation.

Several signaling pathways localized in the front of migrating cells have been shown to be important for macrophage migration. Phosphoinositide 3-kinase (PI3K) is activated at the cell membrane and has been shown to be upstream of many signaling pathways involved in macrophage migration [22-24]. We found that in addition to macrophage migration, PI3K signaling is also important for macrophage force generation. Inhibition of macrophages with the chemical inhibitor LY294002 led to a significant decrease in force generation (Figure 4.4A and B).

One GTPase known to be activated downstream of PI3K is Rac. Rac has been previously shown to be important for macrophage ruffling and motility. Like other GTPases, Rac is activated by several guanine nucleotide exchange factors or GEFs. These GEFs exchange a GDP bound to the GTPase for a GTP, thereby activating the GTPase. We have shown that inhibition of Rac through NSC23766, which blocks Rac binding to the GEF Tiam1, leads to no change in force generation but inhibition of Rac through 6-thio-GTP, which blocking binding between Rac and Vav1, leads to a significant reduction in force. This result indicates that Rac's downstream activity is affected by which GEF activated it. Others have previously shown that in chronic lymphocytic leukemia cells, Rac activated through Tiam1 was not necessary for cell motility but was important for proliferation [33]. Furthermore, it has been shown that in neutrophils Vav1 is essential for motility and the mechanosensing under flow [34]. Vav1

has also been shown to be important in F-actin reorganization in macrophages [35]. These previous results along with the results presented in this study indicate that Rac activation by Vav1 is crucial for macrophage force generation, potentially due to Vav1's role in mediating signals from integrins to Rac and its ability to reorganize the cytoskeleton. Rac activation by Tiam1, however, leads to signaling events that are not necessary for macrophage force generation.

We have shown that macrophages are mechanoresponsive cells capable of exerting large forces on their underlying substrate. This ability may offer an advantage to macrophages which spend large amounts of time navigating through tissues of different densities. We have also shown that macrophages concentrate their forces at the leading edge of migrating cells and that signaling events that occur at the front of migrating cells are critical for macrophage force generation. PI3K is known to translocate to the leading edge of polarized cells [24], and it has been shown that Vav1 is a PI3K-dependent activator for Rac1 in macrophages stimulated with CSF-1 [36]. Therefore, it is significant to note that inhibition of either PI3K activity or the Vav1-Rac1 interaction leads to a significant reduction in force generation by macrophages. It is plausible that the signaling activity through PI3K and Rac1 has a significant influence on the frontal-towing mechanism of migrating macrophages.

CONCLUSIONS

We have been able to show that macrophages produce large forces during migration on compliant surfaces. These traction maps indicate that macrophages use a pulling mechanism of motility with large forces in the front of migrating cells. We have found some of the molecules responsible for this force and have shown that the activation path for GTPases is important when considering their downstream effector functions. To our knowledge, this is the first demonstration of force generation during macrophage migration. In the future, studies like this will be crucial in understanding the role of mechanosensing in macrophage migration and the signaling events involved in motility.

REFERENCES

1. Pollard, J.W., *Trophic macrophages in development and disease*. Nat Rev Immunol, 2009. **9**(4): p. 259-70.
2. Ridley, A.J., *Rho proteins, PI 3-kinases, and monocyte/macrophage motility*. FEBS Lett, 2001. **498**(2-3): p. 168-71.
3. Pelham, R.J., Jr. and Y. Wang, *Cell locomotion and focal adhesions are regulated by substrate flexibility*. Proc Natl Acad Sci U S A, 1997. **94**(25): p. 13661-5.
4. Reinhart-King, C.A., *Endothelial cell adhesion and migration*. Methods Enzymol, 2008. **443**: p. 45-64.
5. Reinhart-King, C.A., M. Dembo, and D.A. Hammer, *The dynamics and mechanics of endothelial cell spreading*. Biophys J, 2005. **89**(1): p. 676-89.
6. Dembo, M. and Y.L. Wang, *Stresses at the cell-to-substrate interface during locomotion of fibroblasts*. Biophys J, 1999. **76**(4): p. 2307-16.
7. Lemmon, C.A., C.S. Chen, and L.H. Romer, *Cell traction forces direct fibronectin matrix assembly*. Biophys J, 2009. **96**(2): p. 729-38.
8. Lauffenberger, D.A. and J.J. Linderman, *Receptors: Models for Binding, Trafficking, and Signaling*. 1993: Oxford University Press.
9. Jannat, R.A., M. Dembo, and D.A. Hammer, *Traction forces of neutrophils migrating on compliant substrates*. Biophys J, 2011. **101**(3): p. 575-84.
10. Smith, L.A., et al., *Neutrophil traction stresses are concentrated in the uropod during migration*. Biophys J, 2007. **92**(7): p. L58-60.

11. Ricart, B.G., et al., *Measuring traction forces of motile dendritic cells on micropost arrays*. Biophys J, 2011. **101**(11): p. 2620-8.
12. Jannat, R.A., et al., *Neutrophil adhesion and chemotaxis depend on substrate mechanics*. J Phys Condens Matter, 2010. **22**(19): p. 194117.
13. Reinhart-King, C.A., M. Dembo, and D.A. Hammer, *Cell-cell mechanical communication through compliant substrates*. Biophys J, 2008. **95**(12): p. 6044-51.
14. Ishizaki, T., et al., *Pharmacological properties of Y-27632, a specific inhibitor of rho-associated kinases*. Mol Pharmacol, 2000. **57**(5): p. 976-83.
15. Kovacs, M., et al., *Mechanism of blebbistatin inhibition of myosin II*. J Biol Chem, 2004. **279**(34): p. 35557-63.
16. Vlahos, C.J., et al., *A specific inhibitor of phosphatidylinositol 3-kinase, 2-(4-morpholinyl)-8-phenyl-4H-1-benzopyran-4-one (LY294002)*. J Biol Chem, 1994. **269**(7): p. 5241-8.
17. Gao, Y., et al., *Rational design and characterization of a Rac GTPase-specific small molecule inhibitor*. Proc Natl Acad Sci U S A, 2004. **101**(20): p. 7618-23.
18. Poppe, D., et al., *Azathioprine suppresses ezrin-radixin-moesin-dependent T cell-APC conjugation through inhibition of Vav guanosine exchange activity on Rac proteins*. J Immunol, 2006. **176**(1): p. 640-51.
19. Engler, A.J., et al., *Matrix elasticity directs stem cell lineage specification*. Cell, 2006. **126**(4): p. 677-89.
20. Paszek, M.J., et al., *Tensional homeostasis and the malignant phenotype*. Cancer Cell, 2005. **8**(3): p. 241-54.

21. Jones, G.E., et al., *Requirement for PI 3-kinase gamma in macrophage migration to MCP-1 and CSF-1*. *Exp Cell Res*, 2003. **290**(1): p. 120-31.
22. Munugalavadla, V., et al., *p85alpha subunit of class IA PI-3 kinase is crucial for macrophage growth and migration*. *Blood*, 2005. **106**(1): p. 103-9.
23. Papakonstanti, E.A., et al., *Distinct roles of class IA PI3K isoforms in primary and immortalised macrophages*. *J Cell Sci*, 2008. **121**(Pt 24): p. 4124-33.
24. Vanhaesebroeck, B., et al., *Distinct PI(3)Ks mediate mitogenic signalling and cell migration in macrophages*. *Nat Cell Biol*, 1999. **1**(1): p. 69-71.
25. Pixley, F.J., *Macrophage Migration and Its Regulation by CSF-1*. *Int J Cell Biol*, 2012. **2012**: p. 501962.
26. Park, Y.M., et al., *Oxidized LDL/CD36 interaction induces loss of cell polarity and inhibits macrophage locomotion*. *Mol Biol Cell*, 2012. **23**(16): p. 3057-68.
27. Bussy, C., et al., *Intrinsic stiffness of the carotid arterial wall material in essential hypertensives*. *Hypertension*, 2000. **35**(5): p. 1049-54.
28. Kothapalli, D., et al., *Cardiovascular protection by ApoE and ApoE-HDL linked to suppression of ECM gene expression and arterial stiffening*. *Cell Rep*, 2012. **2**(5): p. 1259-71.
29. Kraning-Rush, C.M., J.P. Califano, and C.A. Reinhart-King, *Cellular traction stresses increase with increasing metastatic potential*. *PLoS One*, 2012. **7**(2): p. e32572.
30. Paszek, M.J., et al., *Integrin clustering is driven by mechanical resistance from the glycocalyx and the substrate*. *PLoS Comput Biol*, 2009. **5**(12): p. e1000604.

31. Worthylake, R.A. and K. Burridge, *RhoA and ROCK promote migration by limiting membrane protrusions*. J Biol Chem, 2003. **278**(15): p. 13578-84.
32. Worthylake, R.A., et al., *RhoA is required for monocyte tail retraction during transendothelial migration*. J Cell Biol, 2001. **154**(1): p. 147-60.
33. Hofbauer, S.W., et al., *Tiam1/Rac1 signals contribute to the proliferation and chemoresistance, but not motility, of chronic lymphocytic leukemia cells*. Blood, 2014. **123**(14): p. 2181-8.
34. Phillipson, M., et al., *Vav1 is essential for mechanotactic crawling and migration of neutrophils out of the inflamed microvasculature*. J Immunol, 2009. **182**(11): p. 6870-8.
35. Bhavsar, P.J., et al., *Vav GEFs regulate macrophage morphology and adhesion-induced Rac and Rho activation*. Exp Cell Res, 2009. **315**(19): p. 3345-58.
36. Vedham, V., H. Phee, and K.M. Coggeshall, *Vav activation and function as a rac guanine nucleotide exchange factor in macrophage colony-stimulating factor-induced macrophage chemotaxis*. Mol Cell Biol, 2005. **25**(10): p. 4211-20.

CHAPTER 5: MOTILITY AND FORCE

GENERATION OF M1 AND M2 POLARIZED MACROPHAGES

ABSTRACT

Macrophages become polarized by cues in their environment and this polarization causes a change in the function of the macrophages as well as their cytokine release and cell surface receptor profiles. Two main subsets of macrophages have been described; M1 or “classically activated” macrophages are pro-inflammatory and M2 or “alternatively activated” macrophages are anti-inflammatory. In addition to chemical changes, polarization has been shown to change the morphology of macrophages and it has further been reported that changes in shape can alter the polarization state of macrophages in the absence of chemical cues. In this study, we investigated the migration and force generation of primary human macrophages polarized down the M1 and M2 pathways. We found that M1 macrophages are significantly less motile and M2 macrophages are significantly more motile than unpolarized, M0, macrophages. We also showed that M1 macrophages generate significantly less force than M0 or M2 macrophages. Finally, using the chemical inhibitor Y27632 we found that M0 and M2 but not M1 force generation is dependent on myosin II contraction through ROCK. This

study represents the first investigation of the changes that occur in the mechanical mechanisms underlying macrophage motility after polarization.

INTRODUCTION

Macrophages are a highly heterogeneous and plastic group of cells that reside in differing tissues throughout the body and perform diverse functions. Originating from circulating monocytes, macrophages differentiate upon entering tissues and can become further activated by cues in their environment [1]. It has been shown that a variety of soluble cues can drive this activation as well as mechanical changes such as cell shape [2, 3]. In general, macrophages are categorized into two main ‘activation’ states.

Macrophages can be ‘classically activated’ along a pro-inflammatory or M1 pathway by microbial stimuli such as $\text{INF}\gamma$ and lipopolysaccharide (LPS) [4]. M1 macrophages are found in active inflammation and secrete high amounts of cytokines such as $\text{TNF}\alpha$, IL-12, and IL-23 that lead to an adaptive immune response [2]. In contrast, macrophages can also be ‘alternatively activated’ along an anti-inflammatory or M2 pathway by IL-4 or IL-10 [2]. M2 macrophages are seen in the resolution phase of inflammation and secrete anti-inflammatory cytokines such as CCL17 and CCL22 [1]. Macrophage activation also leads to changes in the morphology and mRNA profiles of these cells [5].

Polarization of macrophages has also been shown to change the motility of the cells; M1 macrophages have lower overall motility and M2 macrophages have increased motility in both random and chemotactic environments [6, 7]. Furthermore, differentially polarized macrophages have been associated with the progression of certain disease states. In type II diabetes, chronic inflammation in adipose tissue is caused by the enhanced recruitment of pro-inflammatory (M1) macrophages [8]. In contrast, anti-inflammatory M2 macrophages facilitate tumor progression and invasion in cancer by

suppressing the immune response as well as promoting angiogenesis and metastasis [9, 10]. Macrophages have also been seen migrating with tumor cells away from solid tumors and into the vasculature [11].

Mechanical stimuli have also been shown to contribute to macrophage polarization. Macrophage polarization has been shown to alter cell morphology. M2 polarized macrophages are much more elongated and M1 macrophages are circular [5]. It has been shown that elongation of macrophages can cause an M2 phenotype in the absence of chemical cues and protect against M1 polarization in the presence of LPS and $\text{INF}\gamma$. Furthermore, restriction of cellular morphology to prevent cell elongation reduced the M2 phenotype characteristics [2]. These results indicate that there is a physical and mechanical basis for macrophage polarization. We therefore hypothesized that there will be a change in the mechanical properties of macrophages polarized down M1 and M2 pathways.

In this study we have used traction force microscopy and a chemokinesis assay to evaluate the motility and force generation of polarized macrophages on compliant polyacrylamide gels. Primary human macrophages were polarized on 10,400Pa gels functionalized with fibronectin into an M1 or M2 phenotype using $\text{INF}\gamma$ and LPS or IL-4 respectively, and untreated (M0) macrophages were used as a control. The motility or force generation of the polarized cells was then measured after 24 hours. We found that M1 macrophages have significantly reduced motility and M2 macrophages have significantly higher motility than unpolarized macrophages. We have also discovered that M1 macrophages generate significantly less force than both M0 and M2

macrophages, but there is no significant change in force associated with M2 polarization. Finally, we have shown that inhibition of ROCK activity using a chemical inhibitor reduces the force generation by M0 and M2 macrophages but does not alter the force generation of M1 macrophages, indicating that the forces produced by M1 macrophages are not dependent on myosin II contraction downstream of ROCK signaling. These results show that in addition to changes in cellular signaling and cytokine production, polarization changes the mechanical phenotype of macrophages.

MATERIALS AND METHODS

Reagents

Bovine fibronectin, recombinant human M-CSF, and E. Coli LPS (lipopolysaccharide) were obtained from Sigma (St. Louis, MO). Recombinant human IFN γ (interferon- γ) and recombinant human IL-4 were obtained from Peprotech (Rocky Hill, NJ). We used the inhibitor Y27632 at 10 μ M from Millipore (Billerica, MA).

Isolation of Monocytes

Whole blood was obtained from healthy human donors by venipuncture and collected in BD Vacutainer tubes containing sodium heparin as an anticoagulant (BD Biosciences, San Jose, CA). Samples were collected with University of Pennsylvania Institutional Review Board approval from consenting adult volunteers. Blood samples were layered in a 1:1 ratio of whole blood to the density gradient 1-Step Polymorphprep (Axis-Shield, Oslo, Norway). Vials were centrifuged at 1500 rpm for 40 minutes and the mononuclear band was collected into a fresh vial.

Differentiation and Cell Culture of Macrophages

Cells were allowed to adhere to sterile non-tissue culture treated dishes in AimV media overnight. Non-adhered cells were removed and washed with PBS. Adherent monocytes were then differentiated for seven days in AimV supplemented with 2ng/mL M-CSF (Sigma, St. Louis, MO). Cells were used for experimentation 7-12 days following the start of differentiation.

Polarization of Macrophages

Macrophages were plated on polyacrylamide gels in AimV media supplemented with 2ng/mL M-CSF and 1% penicillin-streptomycin and incubated for 1 hour. Non-adherent cells were washed away and attached cells were polarized for 24 hours in AimV supplemented with 2ng/mL, penicillin-streptomycin, and specific polarization factors. M1 macrophages were polarized with 20ng/mL IFN γ and 100ng/mL LPS. M2 macrophages were polarized with 20ng/mL IL-4. M0 macrophages were plated without polarization factors and incubated on the gels for the same amount of time as the polarized cells.

Surface Preparation

Coverslips (No 1, 45 x 50 mm, Fisher Scientific, Pittsburgh, PA) were chemically activated in preparation for covalent attachment of polyacrylamide gels using a method adapted from the protocol by Pelham and Wang. Briefly, coverslips were washed for 4 hours in 0.2 M hydrogen chloride then rinsed several times with distilled water. They were then neutralized with 0.1 M sodium hydroxide for 30 minutes and rinsed with distilled water. Coverslips were incubated on an orbital shaker in 3-aminopropyl trimethoxysilane 0.5% for 30 minutes and rinsed with distilled water. They were then activated with 0.5% glutaraldehyde for at least 1 hour. The coverslips were then air-dried overnight.

Synthesis of the Bifunctional Linker

N-6-((acryloyl)amino)hexanoic acid (N-6) was synthesized using the method described by Pless et al. The N-6 copolymerizes in the acrylamide to form a reactive polyacrylamide gel. The N-6 contains an *n*-succinimidyl ester that is displaced by a primary amine to link the amine-containing ligand, such as fibronectin, to the polyacrylamide gel.

Gel Synthesis

Acrylamide solutions were prepared containing acrylamide (40% w/v solution), *n,n'*-methylene-bis-acrylamide (2% w/v solution), *n'*-tetramethylethylene di-amine, and ammonium persulfate from Bio-Rad Laboratories (Hercules, CA). Additionally, the gels contained 0.25M HEPES, buffered to pH 8, 5.6mg of N6 dissolved in ethanol, distilled water, and carboxylate-modified fluorescent latex beads (0.5 μ m Fluorospheres, Molecular Probes, Eugene, OR). The concentrations of acrylamide and bis were varied to control the mechanical properties of the hydrogel.

A drop of gel solution was dispensed onto a Rainex-coated 18mm glass coverslip. A second activated rectangular coverslip was placed on top of the gel droplet to flatten the solution; the assembly was polymerized in an inverted position to allow beads to settle to the top surface of the gel. The gels were polymerized under nitrogen for 45 minutes. The top coverslip was gently peeled away leaving a thin gel immobilized on the activated coverslip. Gels were rinsed with distilled water and incubated with 5 μ g/mL fibronectin in 50mM HEPES buffer overnight. Unreacted N-6 was blocked with 1:100

ethanolamine in 50mM HEPES for 30 minutes and stored in 1 x PBS at 4°C for up to 2 weeks.

Chemokinesis Assay

Polyacrylamide gels fabricated on 25mm coverslips were attached to 6-well plates with vacuum grease. Cells were plated in each well at 4.2×10^4 cells/mL and incubated for one hour. After incubation, the cells were washed with AimV to remove any unattached cells. Cells were polarized for 24 hours in AimV supplemented with polarization factors (Sigma, St. Louis, MO and Peprotech, Rocky Hill, NJ) and 1% penicillin-streptomycin. Using a custom-built LabView (Texas Instruments, Austin, TX) software, 15 fields of view per condition were imaged at 10x magnification by phase microscopy on a Nikon Eclipse TE300 (Nikon, Melville, NY). Images were captured every 10 minutes for 24 hours using time-lapse microscopy. Cell trajectories were captured using the ImageJ Manual Tracking plugin. Chemokinesis parameters were calculated using a custom written MATLAB (Mathworks, Natick, MA) script which fits the speed (S) and persistence time (P) to the Dunn Equation:[12] $\langle d^2 \rangle = nS^2 [Pt - P^2(1 - e^{-t/P})]$. The random motility coefficient is a relative diffusion coefficient for the cells in a uniform chemokine field. The random motility coefficient, μ , is calculated using the fit parameters in the following equation: $\mu = \frac{1}{n} S^2 P$.

Traction Force Microscopy of Migrating Macrophages

Traction force microscopy has been described previously [13]. Briefly, traction forces were determined based on deformations in the polyacrylamide substrate relative to the relaxed substrate as detected by movements of 0.5- μm beads embedded in the gel.

Primary human macrophages were plated on fibronectin-coated polyacrylamide gels at 1×10^4 cells/mL and incubated for 1 hour at 37°C. Unattached cells were washed away and fresh AimV with 2ng/mL human M-CSF was added to the gel chamber. The cells were allowed to polarize for 24 hours. Phase contrast images of the cell were taken every 10 minutes during cell migration. Directly after a phase image was taken, a corresponding fluorescent image of the beads embedded beneath the cell was taken. Images were taken over a 4-hour period. At the end of migration, the cells were removed using 0.5% SDS and an image of the beads in their unstressed state was taken. Using custom-written LIBTRC software, the bead displacements within the gel were calculated, the cell and nucleus were drawn, and a mesh that fits within the outline of the cell was created. Using the bead displacements and the material properties of the gel, the most likely surface traction vectors were calculated using the technique described by Dembo and Wang.

The overall force, $|F|$, exerted by the cell on its substrate, is an integral of the traction field magnitude over the area, $|F| = \iint \sqrt{T_x^2(x, y) + T_y^2(x, y)} dx dy$, where $\mathbf{T}(x, y) = [T_x(x, y), T_y(x, y)]$ is the continuous field of traction vectors defined at any spatial position (x, y) within the cell.

Inhibition of Macrophages

Macrophages were seeded on 10,400Pa gels functionalized with 5 μ g/mL fibronectin and allowed to adhere for 1 hour. After incubation, the cells were washed with AimV to remove any unattached cells. Cells were polarized for 24 hours in AimV supplemented with polarization factors (Sigma, St. Louis, MO and Peprotech, Rocky Hill, NJ) and 1% penicillin-streptomycin. After 24 hours, the ROCK inhibitor was added to the wells at 10 μ M. The macrophages were incubated for 1 hour to allow complete inhibition. All traction force measurements were taken in the continued presence of the chemical inhibitor. The forces exerted by inhibited macrophages were compared to the previously measured forces of uninhibited macrophages on 10,400Pa gels.

RESULTS

Macrophage Polarization Alters Macrophage Motility on Polyacrylamide Gels

We first sought to determine the effect of polarization on macrophage migration on compliant polyacrylamide gels. Other laboratories have studied the migration of M1 and M2 polarized macrophages using transwell chambers and three-dimensional gels, but M1 and M2 macrophage migration has not yet been described on two-dimensional gels. For the chemokinesis experiments, gels were fabricated at 10,400Pa and functionalized with 5 ug/mL fibronectin. Primary human macrophages were seeded on these gels and polarized into an M1 or M2 phenotype overnight. As a control, one well was not treated with any polarization factors and will be referred to as the M0 phenotype. The control M0 macrophages were able to efficiently migrate on the polyacrylamide gels. The random motility coefficient, a relative diffusion coefficient of migrating cells, of M1 polarized macrophages was significantly reduced when compared to the M0 and M2 macrophages (Figure 5.1). Furthermore, the M2 macrophages had a higher random motility coefficient than control M0 macrophages.

M1 Macrophages Generate Significantly Less Force than M0 or M2 Macrophages

Macrophage polarization has previously been shown to lead to a change in cell morphology; however, the mechanical changes accompanying macrophage polarization have not been studied. Unpolarized primary human macrophages have been shown to generate strong forces on compliant polyacrylamide gels. We therefore hypothesized that

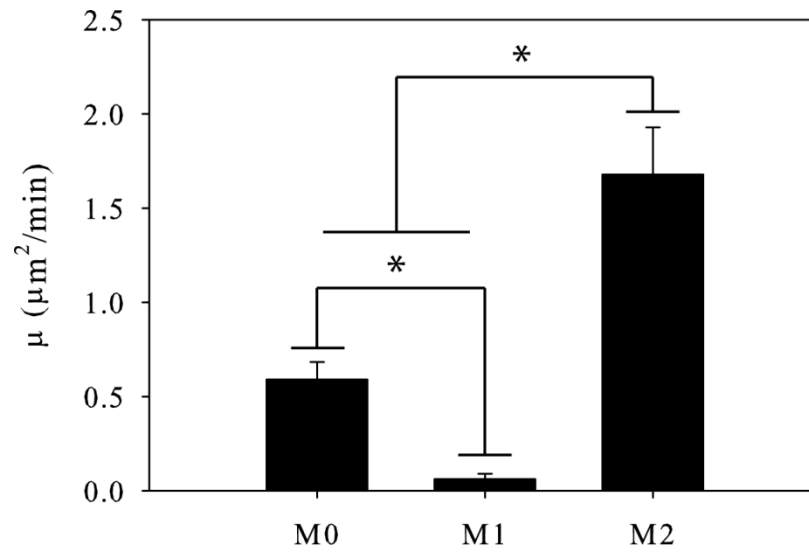


Figure 5.1: Motility of polarized macrophages. Random motility coefficient of M0, M1, and M2 polarized macrophages migrating on 10,400Pa gels coated with 5μg/mL fibronectin. (n > 300 cells per condition) Error bars are standard error. * indicates p < 0.05.

macrophage polarization would lead to a change in the force generation of the cells. We used traction force microscopy to measure the forces generated by M1 and M2 polarized macrophages and compared them to the forces generated by control, unpolarized, M0 macrophages. Macrophages were seeded on 10.4 kPa gels and polarized for 24 hours into the M1 phenotype with $\text{INF}\gamma$ and LPS or the M2 phenotype with IL-4 in AimV supplemented with 2ng/mL M-CSF. M1 polarized macrophages were found to generate significantly less traction force than M0 macrophages or M2 polarized macrophages, but there was no significant difference in the force generated by M0 and M2 macrophages (Figure 5.2A). This reduced force generation by M1 macrophages is due to a significant reduction in traction stress (Figure 5.2B); the M1 and M2 polarized macrophages had a significantly increased spread area on the gels compared to unpolarized M0 macrophages (Figure 5.2C).

Force Generation by M0 and M2 but not M1 Macrophages Requires ROCK Activity

It has been shown that myosin contraction is necessary for force generation in many types of cells [14, 15]. We therefore thought that ROCK signaling upstream of myosin contraction would be necessary for traction force generation in polarized macrophages. We polarized macrophages as described before, and then exposed the polarized cells to the chemical inhibitor Y27632 to block ROCK activity for one hour. We then measured the traction forces of the inhibited cells in the continued presence of the inhibitor. We found that both M0 and M2 polarized macrophages produced

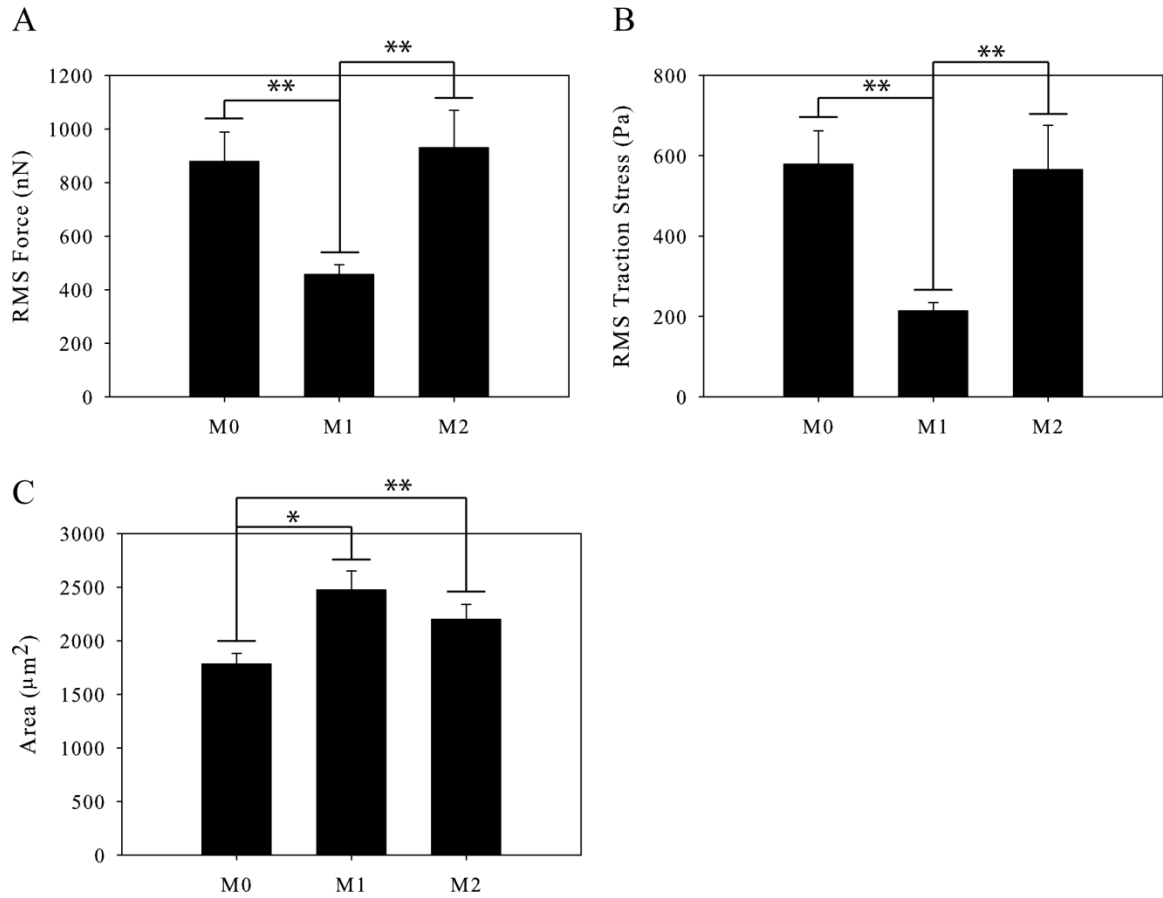


Figure 5.2: Traction force generation by polarized macrophages. (A) Traction force generated by M0, M1, and M2 macrophages on 10,400Pa. (B) Traction stresses generated by M0, M1, and M2 macrophages. (C) Area of M0, M1, and M2 macrophages. ($n > 50$ per condition) Error bars are standard error. * indicates $p < 0.05$ and ** indicates $p < 0.002$.

significantly less force under ROCK inhibition than they did when uninhibited (Figure 5.3A). This reduction in traction stress is due to a significant reduction in traction stress (Figure 5.3B) but was also caused by a reduction in area in M2 macrophages (Figure 5.3C). Interestingly, M1 macrophages had no reduction in force generation, indicating that the small force generated by M1 macrophages are not due to myosin contraction. There was no significant difference seen in the force generation, traction stress, or area between M0, M1, and M2 polarized macrophages when ROCK is inhibited. It is therefore possible that the differences in the mechanical phenotypes between M0-M1 and M1-M2 polarized macrophages are largely due to differences in myosin contraction.

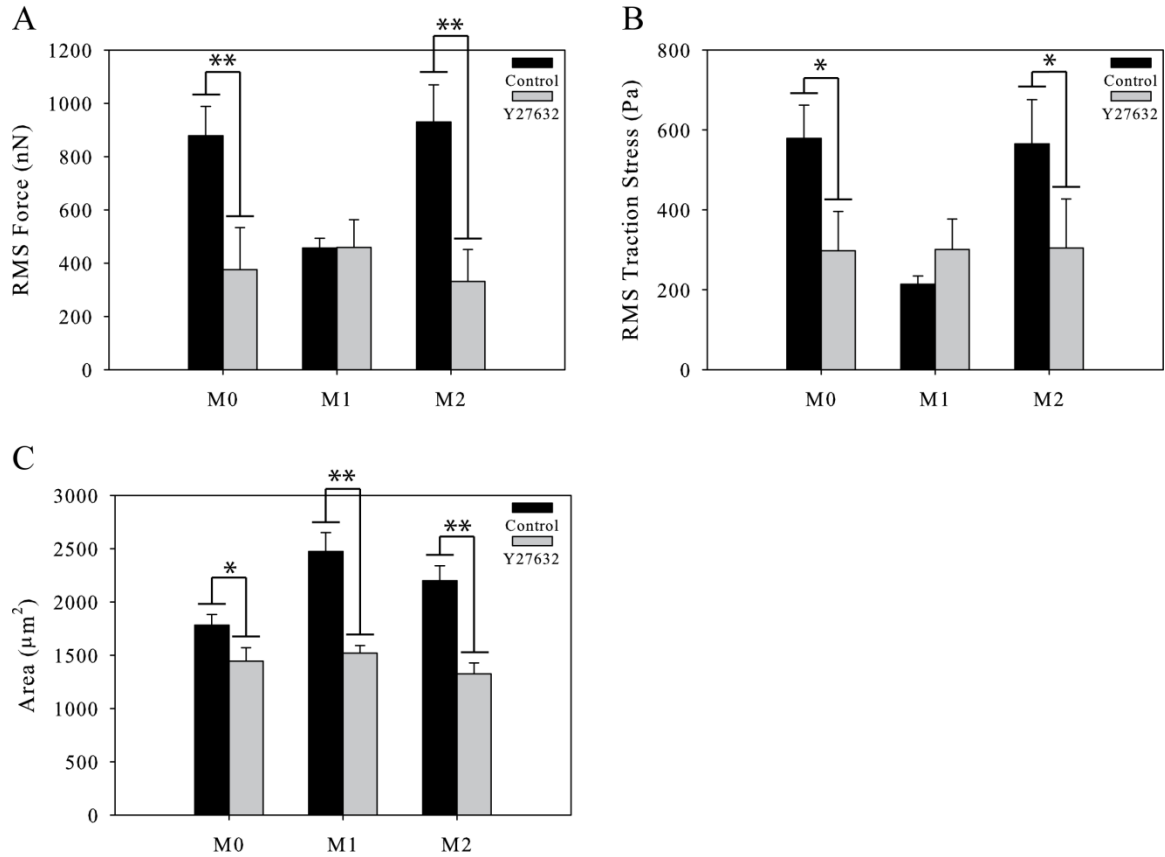


Figure 5.3: Traction force generated by polarized macrophages under ROCK inhibition.

(A) Traction forces of control M0, M1, and M2 macrophages and macrophages under

ROCK inhibition. (B) Traction stresses of polarized macrophages under ROCK

inhibition. (C) Area of control and ROCK inhibited M0, M1, and M2 polarized

macrophages. (n > 20 per condition) Error bars are standard error. * indicates p < 0.05

and ** indicates p < 0.002.

DISCUSSION

Previous studies have shown that macrophages can be activated by cues in their environment and that this activation alters the behavior of these cells in both healthy immune responses and in disease [7, 8, 11]. Furthermore, it has been suggested that mechanical signals such as cell shape can also alter the activation status of macrophages [2]. We have shown that on polyacrylamide gels, M1 polarized macrophages are significantly less motile and M2 polarized macrophages are significantly more motile than unpolarized macrophages. This result agrees with a previous study that found reduced motility in M1 macrophages and increased motility in M2 macrophages in both 3D matrigel and 2D transwell assays [6]. It has also been previously reported that the M2 macrophages migrate and chemotax toward several chemokines more efficiently than M1 macrophages using a TAXIScan assay [7]. The study presented in this chapter is the first to directly quantify the random motility of M0, M1, and M2 polarized macrophages. The finding presented by this study and others that M1 polarized macrophages lose motility and M2 polarized macrophages gain increased motility agrees with the physiological roles of polarized macrophages. M1 macrophages are pro-inflammatory macrophages present at the beginning stages of an active immune response [10]; therefore, it makes sense that upon arriving at the site of inflammation and becoming polarized these cells would no longer need to migrate. Their primary role is to remain at the site of infection, clearing away pathogens and activating the adaptive immune response [1]. In contrast, M2 macrophages are present at the resolution of an immune response and secrete anti-inflammatory cytokines to dampen the adaptive immune response [10]. It is therefore

important that M2 macrophages migrate away from the site of infection. In addition to aiding in the normal function of M2 macrophages in an immune response their increased migration might explain their role in cancer metastasis. The presence of M2 macrophages at the site of a tumor is often associated with increased metastatic potential and a poor patient prognosis [9, 10, 16, 17]. Furthermore, macrophages have been observed co-migrating with tumor cells away from solid tumors and toward the vasculature suggesting that macrophage may aid tumor cell entry into blood vessels [18]. It is possible that this increased migration seen in M2 macrophages could assist in metastasis and may be a potential therapeutic target in the future [19, 20].

In addition to increased migration, it has also been shown that mechanical phenotypes can be altered by macrophage polarization. Specifically, macrophage polarization has been reported to alter the morphology of human macrophages with M2 macrophage becoming far more elongated while M1 macrophages remain rounded [21]. Furthermore, it has been shown that cell shape is sufficient to polarize macrophages in the absence of chemical stimuli, and cell elongation can protect against M1 polarization by chemical stimuli [2]. This result indicated that macrophage polarization has an effect on the mechanical machinery of the cells. We found that M1 polarization led to a significant reduction in force generation by polarized macrophages, but no significant difference was found between M0 and M2 macrophages. It was also shown that this change in force was directly caused by a change in the traction stresses the cells generated on their substrate. These results together indicate that macrophage polarization directly alters the mechanical properties of the cells.

We have previously shown that myosin II contraction through ROCK is important for macrophage force generation, confirming the results of others that myosin II is directly involved in force generation [14]. We therefore sought to determine the role of ROCK signaling in force generation by polarized macrophages. We found that loss of myosin II contraction through the chemical ROCK inhibitor Y27632 led to a significant decrease in the force generated by M0 and M2 macrophages, in agreement with our previous results. Interestingly, the force generated by M1 macrophages was unchanged by ROCK inhibition. The forces generated by M0, M1, and M2 polarized macrophages under ROCK inhibition were not significantly different, indicating that the increased force generated by M0 and M2 macrophages is dependent on myosin II contraction. This also suggests that a second force generating mechanism, not dependent on myosin II contraction, is present in all three polarized macrophage subsets and equally contributes to their force generation.

CONCLUSIONS

We have been able to show that polarization changes the motility and force generation capabilities of macrophages. Specifically, we showed that M1 macrophages have reduced motility and M2 macrophages have increased motility compared to unpolarized macrophages. Furthermore, we found that M1 macrophages generate significantly less force than M0 and M2 macrophages but M2 macrophages have no significant change in force compared to M0 macrophages. Finally, we showed that myosin II contraction through ROCK is important for force generation in M0 and M2 macrophages but not M1 macrophages, indicating a second myosin-independent force generation mechanism. Overall, we have shown that polarization not only changes the chemical makeup of macrophages but can also change their mechanical properties. In the future, the differential force generation and motility mechanisms between M1 and M2 macrophages might serve as therapeutic targets in a number of diseases specifically associated with either M1 or M2 macrophages.

REFERENCES

1. Biswas, S.K., et al., *Macrophage polarization and plasticity in health and disease*. Immunol Res, 2012. **53**(1-3): p. 11-24.
2. McWhorter, F.Y., et al., *Modulation of macrophage phenotype by cell shape*. Proc Natl Acad Sci U S A, 2013. **110**(43): p. 17253-8.
3. Murray, P.J., et al., *Macrophage activation and polarization: nomenclature and experimental guidelines*. Immunity, 2014. **41**(1): p. 14-20.
4. Ambarus, C.A., et al., *Systematic validation of specific phenotypic markers for in vitro polarized human macrophages*. J Immunol Methods, 2012. **375**(1-2): p. 196-206.
5. Vogel, D.Y., et al., *Human macrophage polarization in vitro: maturation and activation methods compared*. Immunobiology, 2014. **219**(9): p. 695-703.
6. Cougoule, C., et al., *Blood leukocytes and macrophages of various phenotypes have distinct abilities to form podosomes and to migrate in 3D environments*. Eur J Cell Biol, 2012. **91**(11-12): p. 938-49.
7. Vogel, D.Y., et al., *Macrophages migrate in an activation-dependent manner to chemokines involved in neuroinflammation*. J Neuroinflammation, 2014. **11**: p. 23.
8. Oh, D.Y., et al., *Increased macrophage migration into adipose tissue in obese mice*. Diabetes, 2012. **61**(2): p. 346-54.
9. Mantovani, A. and A. Sica, *Macrophages, innate immunity and cancer: balance, tolerance, and diversity*. Curr Opin Immunol, 2010. **22**(2): p. 231-7.

10. Mantovani, A., et al., *Macrophage polarization: tumor-associated macrophages as a paradigm for polarized M2 mononuclear phagocytes*. Trends Immunol, 2002. **23**(11): p. 549-55.
11. Condeelis, J. and J.W. Pollard, *Macrophages: obligate partners for tumor cell migration, invasion, and metastasis*. Cell, 2006. **124**(2): p. 263-6.
12. Dunn, G.A., *Characterising a kinesis response: time averaged measures of cell speed and directional persistence*. Agents Actions Suppl, 1983. **12**: p. 14-33.
13. Dembo, M. and Y.L. Wang, *Stresses at the cell-to-substrate interface during locomotion of fibroblasts*. Biophys J, 1999. **76**(4): p. 2307-16.
14. Jannat, R.A., M. Dembo, and D.A. Hammer, *Traction forces of neutrophils migrating on compliant substrates*. Biophys J, 2011. **101**(3): p. 575-84.
15. Worthylake, R.A., et al., *RhoA is required for monocyte tail retraction during transendothelial migration*. J Cell Biol, 2001. **154**(1): p. 147-60.
16. Hao, N.B., et al., *Macrophages in tumor microenvironments and the progression of tumors*. Clin Dev Immunol, 2012. **2012**: p. 948098.
17. Solinas, G., et al., *Tumor-conditioned macrophages secrete migration-stimulating factor: a new marker for M2-polarization, influencing tumor cell motility*. J Immunol, 2010. **185**(1): p. 642-52.
18. Sharma, V.P., et al., *Reconstitution of in vivo macrophage-tumor cell pairing and streaming motility on one-dimensional micro-patterned substrates*. Intravital, 2012. **1**(1): p. 77-85.

19. Biswas, S.K. and A. Mantovani, *Macrophage plasticity and interaction with lymphocyte subsets: cancer as a paradigm*. Nat Immunol, 2010. **11**(10): p. 889-96.
20. Chioda, M., et al., *Myeloid cell diversification and complexity: an old concept with new turns in oncology*. Cancer Metastasis Rev, 2011. **30**(1): p. 27-43.
21. Waldo, S.W., et al., *Heterogeneity of human macrophages in culture and in atherosclerotic plaques*. Am J Pathol, 2008. **172**(4): p. 1112-26.

CHAPTER 6: CONCLUSIONS AND FUTURE WORK

SPECIFIC AIMS

The research presented in this thesis shows that we were able to use engineered substrates to investigate the signaling proteins and mechanical mechanisms involved in macrophage migration. The specific aims of this work were as follows:

Aim 1: Macrophage Chemokinesis on Microcontact Printed PDMS Substrates.

Aim 2: Traction Force Generation by Primary Human Macrophages.

Aim 3: M1 and M2 Polarized Primary Human Macrophage Motility and Force Generation.

SPECIFIC FINDINGS

Macrophage Chemokinesis on Microcontact Printed PDMS Substrates

We first investigated the chemokinetic migration of RAW/LR5 murine macrophages on PDMS substrates microcontact printed with the extracellular matrix

protein fibronectin. We hypothesized that these substrates would be ideal for observing the migration of macrophages, which are inherently highly adhesive cells, because of their ability to be functionally blocked with pluronics, eliminating any cell-surface interactions [1]. Furthermore, it has been shown that leukocytes can bind to the common blocking agent BSA through their β_2 integrin [2]; therefore, the functional blocking capabilities eliminate any confounding integrin-binding interactions. We showed that macrophages could efficiently migrate and form typical podosome adhesion structures on these microcontact printed surfaces. We found that the random migration of these cells was biphasic with increasing concentration of the printed fibronectin ligand or the soluble chemokine CSF-1. Through chemical inhibition we showed that PI3K signaling is necessary for the polarization and migration of these cells. We also showed that the loss of Cdc42 activity by protein knockdown lead to complete loss of podosome formation and a non-significant reduction in motility. Finally, we inhibited ROCK activity with chemical inhibition and found a new phenotypic switch between cells on low and high concentrations of fibronectin. Macrophages migrating on 10 $\mu\text{g/mL}$ or higher concentrations of fibronectin had a low but constant random migration and were unable to retract their trailing edge, leaving behind long tails. In contrast, macrophages on 5 $\mu\text{g/mL}$ or lower concentrations of fibronectin had a much higher and constant rate of migration and morphologically were rounded with short tails that snapped back to the cell body during migration. We were successfully able to show that microcontact printed surfaces are an optimal platform for studying the migration of macrophages and the influence of integrin binding on migration without confounding cell-surface or cell-

blocking agent interactions. In the future, these surfaces can serve as a better tool for studying the migration of any cell and the effect of surface ligand-cell interactions.

Force Generation by Primary Human Macrophages

The signaling mechanisms underlying macrophage migration have been well studied [3-5], but the mechanical mechanisms underlying macrophage migration have not previously been studied. We used traction force microscopy to show that macrophages generate strong forces at the leading edge of migrating cells. Substrate stiffness has been shown to regulate a number of cellular processes including cell adhesion [6], spreading [7], differentiation [8], and migration [9, 10]. We have now shown that force generation by primary human macrophages is also a stiffness-dependent process, with cells on stiffer gels producing larger forces than those on soft gels. This increased force generation was caused by an increase in traction stress as the spread area of the cells actually showed a biphasic behavior in relation to substrate stiffness. Chemical inhibition of either ROCK activity with Y27632 or myosin II activity with Blebbistatin lead to a significant decrease in force, indicating that myosin contraction is required for proper force production by macrophages. PI3K activity was also found to be necessary for force generation as inhibition with the inhibitor LY294002 caused a significant reduction in macrophage force. Finally, an investigation of the role of Rac signaling in force generation showed that Rac signaling is important, but only when activated by certain Rac GEFs. The chemical inhibitor NSC23766, which blocks Rac activation by Tiam1, did not cause any change in force generation. In contrast, the inhibitor 6-thio-GTP, which blocks Rac activation by Vav1, caused a significant decrease in force generation. These results

suggest that Rac activation is GEF-specific and signaling downstream of Rac is dependent on the Rac activation reaction. This study represents the first major investigation of macrophage force generation and the signaling mechanisms involved in the mechanical processes driving macrophage migration.

M1 and M2 Polarized Macrophage Motility and Force Generation

Macrophages are a heterogeneous population of cells capable of many functions and they can be activated down different pathways by soluble factors in their environment [11]. This activation, or polarization, can lead to a change in the transcription profile, surface receptor expression, and functional phenotype of the macrophage [12]. It has been previously reported that M1 and M2 polarized macrophages display significant differences in morphology and migration [11, 13]. Furthermore, it has been shown that the activation status of macrophages can be altered by cell shape [14], indicating that mechanics is involved in macrophage polarization. We have now shown that macrophage polarization has a significant effect on their migration and force generation on compliant polyacrylamide gels. We found that macrophages polarized into the M2 phenotype were significantly more motile than unpolarized (M0) macrophages or M1 macrophages as illustrated by the random motility coefficient. M1 macrophages showed a significant reduction in motility compared to both M0 and M2 macrophages. We also found that M1 polarized macrophages generated significantly less traction force than M0 macrophages or M2 polarized macrophages, but there was no significant difference in the force generated by M0 and M2 macrophages. This reduced force generation by M1 macrophages was due to a significant reduction in traction stress;

the M1 and M2 polarized macrophages had a significantly increased spread area on the gels compared to unpolarized M0 macrophages. The discovery that polarized macrophages have different mechanical outputs in addition to differing chemical signals could prove important in diseases such as cancer, where one type of polarized macrophage is commonly found in much higher numbers than another [15].

FUTURE WORK

Chemotaxis of Macrophages on Motility and Force Generation

In the body, macrophages must move up and down gradients of signaling proteins to efficiently reach sites of infection and inflammation. This process of directional migration is known as chemotaxis. It has been well documented that the mechanisms and cellular signaling necessary for chemokinesis and chemotaxis are not always the same [4, 16, 17]. For example in macrophages, it has been previously reported that Cdc42 is not necessary for random migration but rather acts as a directional sensor and is critical for chemotaxis [4]. It would therefore be instructional to determine which signaling molecules are necessary for macrophage chemotaxis on different concentrations of microcontact printed fibronectin. The mechanical mechanisms driving cell migration can also differ between cells in a uniform field versus a gradient of chemokine. It has been shown that neutrophils generate stronger traction stresses when chemotaxing than they do when undergoing random migration and that these tractions are more organized[10]. It would be interesting to see if the forces generated by macrophages would change in magnitude or location during chemotaxis. Finally, it would be interesting to determine if

the signaling proteins necessary for force generation in a gradient are different than those in a uniform field of chemokine. Our lab has previously used a “Christmas Tree” microfluidic device to investigate cells undergoing chemotaxis [10, 18]. This device is compatible with both the microcontact printed PDMS surfaces and the gels used in traction force microscopy. Unfortunately, many attempts to look at macrophage chemotaxis using this device failed because of the flow necessary to maintain the gradient (data not shown). Without flow, macrophages migrated normally, but when flow was introduced, the cells stopped migrating, firmly adhered to the substrate, and eventually died. A point-source experiment was also attempted, but the inability to reproduce the experimental setup and long migration times necessary for efficient macrophage migration caused problems with this assay as well. In the future, a flow-free system that allows for a stable gradient to be formed over long periods of time could be integrated with the substrates used in this thesis to study macrophage chemotaxis.

Stiffness Effect on Cellular Signaling

We were able to show that the force a macrophage generates is dependent on the stiffness of its underlying matrix. We have also shown that this force generation is dependent on myosin contraction as well as PI3K and Rac signaling. We did not, however, explore the possibility that the signaling by these molecules is also stiffness-dependent. It has been previously shown that cells can produce different signals on soft substrates versus stiff substrates, but the exact mechanism by which cells sense the stiffness of their matrix and respond is still unknown [8]. It would be interesting to

determine if some signaling proteins are more or less important for force generation on different stiffness matrixes.

Correlation between Podosome Dynamics and Force Generation

It has previously been shown that macrophage podosomes are necessary for macrophage chemotaxis and matrix degradation, but no direct link between podosomes and motility has been shown [19, 20]. In fact, known regulators of podosome formation such as WASp and Cdc42 are not necessary for random migration in macrophages [20]. We have been able to visualize the podosome dynamics as indicated by formation of small punctate actin structures using a LifeAct-GFP construct (Figure 6.1). It would be possible to simultaneously image the podosome dynamics and the fluorescent beads necessary for traction force measurements using two fluorescent channels on a spinning disk confocal microscope. The podosome formation could then be overlaid with the traction maps to determine if the assembly or disassembly of podosome is correlated to the presence or absence of new traction forces at the leading edge of the cell. Furthermore, chemical inhibitors that block signaling proteins necessary for the formation of podosomes, such as the ML 141 that specifically blocks Cdc42 activity, could be used to determine the necessity of podosomes for efficient force generation.

Force Generation by Tumor Conditioned Macrophages

Macrophages, specifically tumor-associated macrophages, or TAMs, are associated with poor prognosis in most types of cancer [15]. Recently, the activation state of these macrophages has been determined to resemble that of an M2 polarized

macrophage [21]. Furthermore, M2 polarized macrophages and TAMs have been shown to upregulate their migration and the migration of tumor cells [22]. It would therefore be interesting to determine how exposure to tumor-conditioned media or co-culture with tumor cells changes the migration and force profiles of primary human macrophages. Macrophages could be differentiated or stimulated with tumor-conditioned media prior to traction force measurements being taken. Alternatively, macrophages and tumor cells could be labeled and co-cultured prior to force generation measurements. It is possible that the force generation profiles of both the conditioned macrophages and the tumor cells would change as a result of their exposure to the other cell type. Finally, it would be interesting to determine if the force profiles of tumor conditioned macrophages matched that of M2 polarized macrophages since they have been shown to have similar signaling markers.

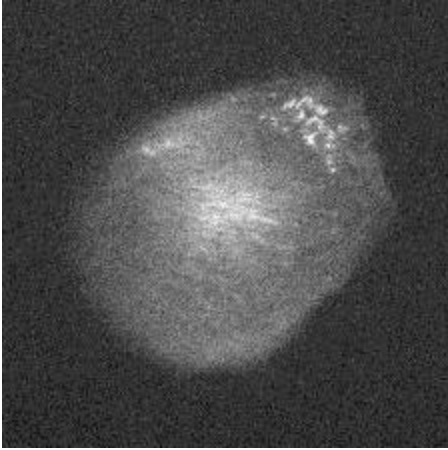


Figure 6.1: Primary human macrophage transfected with LifeAct-GFP. Small punctate actin structures indicate the presence of podosomes.

FINAL THOUGHTS

The importance of macrophage migration, in both maintaining homeostasis and in disease pathogenesis, cannot be overstated. Without macrophage migration the body is unable to defend itself against pathogens and improper regulation of this migration can contribute to disease progression. Because of their role as master regulators during the immune response and their role in disease, macrophages are also an attractive therapeutic target in a number of disease models. It is therefore critical that we completely understand the signaling and mechanical mechanisms that drive macrophage motility. In this thesis, we have successfully used engineered substrates to uncover unique aspects of macrophage migration and hope that in the future this work will continue to inspire the development and use of new tools to study macrophage migration.

ACKNOWLEDGEMENTS

Thanks to Eric Johnston for technical support as well as all members of the Hammer lab for their support and helpful discussions. We also acknowledge financial support from the NSF Graduate Research Fellowship and the National Institute of Health Grant HL18208.

REFERENCES

1. Desai, R.A., et al., *Subcellular spatial segregation of integrin subtypes by patterned multicomponent surfaces*. *Integr Biol (Camb)*, 2011. **3**(5): p. 560-7.
2. Henry, S.J., J.C. Crocker, and D.A. Hammer, *Ligand density elicits a phenotypic switch in human neutrophils*. *Integr Biol (Camb)*, 2014.
3. Abou-Kheir, W., et al., *A WAVE2-Abi1 complex mediates CSF-1-induced F-actin-rich membrane protrusions and migration in macrophages*. *J Cell Sci*, 2005. **118**(Pt 22): p. 5369-79.
4. Allen, W.E., et al., *A role for Cdc42 in macrophage chemotaxis*. *J Cell Biol*, 1998. **141**(5): p. 1147-57.
5. Pixley, F.J. and E.R. Stanley, *CSF-1 regulation of the wandering macrophage: complexity in action*. *Trends Cell Biol*, 2004. **14**(11): p. 628-38.
6. Pelham, R.J., Jr. and Y. Wang, *Cell locomotion and focal adhesions are regulated by substrate flexibility*. *Proc Natl Acad Sci U S A*, 1997. **94**(25): p. 13661-5.
7. Engler, A.J., et al., *Surface probe measurements of the elasticity of sectioned tissue, thin gels and polyelectrolyte multilayer films: Correlations between substrate stiffness and cell adhesion*. *Surface Science*, 2004. **570**(1-2): p. 142-154.
8. Engler, A.J., et al., *Matrix elasticity directs stem cell lineage specification*. *Cell*, 2006. **126**(4): p. 677-89.
9. Jannat, R.A., M. Dembo, and D.A. Hammer, *Traction forces of neutrophils migrating on compliant substrates*. *Biophys J*, 2011. **101**(3): p. 575-84.

10. Jannat, R.A., et al., *Neutrophil adhesion and chemotaxis depend on substrate mechanics*. J Phys Condens Matter, 2010. **22**(19): p. 194117.
11. Vogel, D.Y., et al., *Human macrophage polarization in vitro: maturation and activation methods compared*. Immunobiology, 2014. **219**(9): p. 695-703.
12. Murray, P.J., et al., *Macrophage activation and polarization: nomenclature and experimental guidelines*. Immunity, 2014. **41**(1): p. 14-20.
13. Hofbauer, S.W., et al., *Tiam1/Rac1 signals contribute to the proliferation and chemoresistance, but not motility, of chronic lymphocytic leukemia cells*. Blood, 2014. **123**(14): p. 2181-8.
14. McWhorter, F.Y., et al., *Modulation of macrophage phenotype by cell shape*. Proc Natl Acad Sci U S A, 2013. **110**(43): p. 17253-8.
15. Mantovani, A., et al., *Macrophage polarization: tumor-associated macrophages as a paradigm for polarized M2 mononuclear phagocytes*. Trends Immunol, 2002. **23**(11): p. 549-55.
16. Cammer, M., et al., *The mechanism of CSF-1-induced Wiskott-Aldrich syndrome protein activation in vivo: a role for phosphatidylinositol 3-kinase and Cdc42*. J Biol Chem, 2009. **284**(35): p. 23302-11.
17. Dovas, A., et al., *Regulation of podosome dynamics by WASp phosphorylation: implication in matrix degradation and chemotaxis in macrophages*. J Cell Sci, 2009. **122**(Pt 21): p. 3873-82.
18. Ricart, B.G., et al., *Measuring traction forces of motile dendritic cells on micropost arrays*. Biophys J, 2011. **101**(11): p. 2620-8.

19. Abou-Kheir, W., et al., *Membrane targeting of WAVE2 is not sufficient for WAVE2-dependent actin polymerization: a role for IRSp53 in mediating the interaction between Rac and WAVE2*. J Cell Sci, 2008. **121**(Pt 3): p. 379-90.
20. Monypenny, J., et al., *Role of WASP in cell polarity and podosome dynamics of myeloid cells*. Eur J Cell Biol, 2010. **90**(2-3): p. 198-204.
21. Biswas, S.K., et al., *Macrophage polarization and plasticity in health and disease*. Immunol Res, 2012. **53**(1-3): p. 11-24.
22. Solinas, G., et al., *Tumor-conditioned macrophages secrete migration-stimulating factor: a new marker for M2-polarization, influencing tumor cell motility*. J Immunol, 2010. **185**(1): p. 642-52.